DEVELOPMENT OF NECTIN-4-TARGETING ONCOLYTIC MEASLES VIROTHERAPY FOR THE TREATMENT OF BREAST AND LIVER CANCERS

by

Ching-Hsuan Liu

Submitted in partial fulfilment of the requirements
for the degree of Doctor of Philosophy

at

Dalhousie University
Halifax, Nova Scotia
July 2021

TABLE OF CONTENTS

LIST OF FIGURES

ABSTRACT

Oncolytic viruses (OVs) are a rapidly emerging treatment platform for various types of cancer that offers several advantages over conventional anticancer therapeutics, including selectivity, potency, and targeted cell death. Recent studies have revealed that measles virus (MV), a member of the *Paramyxoviridae* family, possesses the ability to selectively target carcinomas by recognizing the tumor cell marker nectin-4, which is highly expressed in many types of cancer. Specifically, wild-type MV targets nectin-4 on the tumor cells and does not engage CD46, which is an additional receptor expressed on all nucleated cells and employed by vaccine strains of MV for infection. The use of MV-based vectors with wild-type glycoproteins is thus justified as candidate for potential development as an oncolytic agent targeting nectin-4. The results in this thesis present as proof-of-concept, the use of a recombinant wild-type MV as an oncolytic agent to effectively target nectin-4-marked cancers, and demonstrate its ability to induce oncolysis of nectin-4-expressing breast and hepatocellular carcinoma (HCC) tumor cells. Specifically, it was observed that MV could dose-dependently and efficiently target and induce cytotoxicity in both cancer models. In addition, the data also demonstrate the feasibility to use a combination of chemotherapeutic agents or anticancer nanoparticles as a chemovirotherapeutic approach to enhance MV's oncolytic efficacy, while reducing the doses of treatment required and potentially increasing its safety. Results from this study underpin the oncolytic potential of recombinant MV and support the future development of oncolytic virotherapy using MV-based vectors for the management of nectin-4-expressing cancers.

LIST OF ABBREVIATIONS USED

5-FC	5-fluorocytosine
5-FU	5-fluorouracil
ADC	antibody-drug conjugate
ADV	adenovirus
ANXA1	annexin A1
APC	allophycocyanin
APCs	antigen-presenting cells
ANOVA	analysis of variance
ATP	adenosine triphosphate
AU	arbitrary unit
BAF	bafilomycin A1
BBB	blood-brain barrier
BCA	bicinchoninic acid
BCLC	Barcelona Clinic Liver Cancer
CC_{50}	50 % cytotoxic concentration
CD40L	CD40 ligand
CI	combination index
CPA	cyclophosphamide
CPE	cytopathic effect
CPT	camptothecin
CRT	calreticulin
CVB1	coxsackievirus B1
DAA	direct-acting antiviral
DAMP	damage-associated molecular pattern
DMEM	Dulbecco's Modified Eagle's medium
DMSO	dimethyl sulfoxide
dpi	days post infection
dsRNA	double-stranded RNA
EGFP	enhanced green fluorescent protein
ELISA	enzyme-linked immunosorbent assay
ER	estrogen receptor

EV71	enterovirus 71
F	fusion protein
FBS	fetal bovine serum
FDA	Food and Drug Administration
FESEM	field emission scanning electron microscopy
H	hemagglutinin protein
HBV	hepatitis B virus
HCC	hepatocellular carcinoma
HCV	hepatitis C virus
HDAC	histone deacetylases
HER2	human epidermal growth factor receptor 2
HIV	human immunodeficiency virus
HMGB1	high mobility group protein B1
HPLC	high-performance liquid chromatography
HRP	horseradish peroxidase
HSP	heat shock protein
HSV-1	herpes simplex virus type 1
ICD	immunogenic cell death
IFN	interferon
Ig	immunoglobulin
IHC	immunohistochemistry
IL	interleukin
IL1-R	interleukin-1 receptor
IU	international units
i.v.	intravenous
i.t.	intratumoral
kDa	kiloDalton
L	large protein
LC3	microtubule-associated proteins 1A/1B-light chain 3
LDH	lactate dehydrogenase
M	matrix protein
MAVS	mitochondrial antiviral signaling
MePdR	6-methylpurine-2’-deoxyriboside
MLKL	mixed lineage kinase domain-like

MMAE	monomethyl auristatin E
MMR	measles, mumps and rubella
MMRV	measles, mumps, rubella, and varicella
MOI	multiplicity of infection
MTT	3-(4,5-dimethylthiazol-2-yl)-2,5-diphenyltetrazolium bromide
MV	measles virus
MV-Edm	MV Edmonston-B attenuated vaccine strain
MV-IC323	MV wild-type Ichinose-B 323 strain
MV-NIS	MV encoding thyroidal sodium iodide symporter
MV-PNP	MV encoding purine nucleoside phosphorylase
MV-SCD	MV encoding super cytosine deaminase
N	nucleocapsid
nAb	neutralizing antibodies
NDV	Newcastle disease virus
NS	non-structural
NT	non-tumor
OD	optical densities
ORR	objective response rate
OV	oncolytic virus
P	phosphoprotein
PAMP	pathogen-associated molecular pattern
PARP	poly (ADP-ribose) polymerase
PBS	phosphate-buffered saline
PCS	photon correlation spectroscopy
PD-1	programmed cell death protein 1
PE	phycoerythrin
PFA	paraformaldehyde
PI3K	phosphatidylinositol 3-kinase
poly I:C	polyinosinic:polycytidylic acid
PR	progesterone receptor
PUG	punicalagin
PVP	polyvinylpyrrolidone
PVRL4	poliovirus receptor-related 4
RANTES	regulated upon activation, normal T cell expressed and secreted

RdRp	RNA-dependent RNA polymerase
RIPA	radioimmunoprecipitation assay buffer
RLU	relative light unit
RNP	ribonucleoprotein
RV	reovirus
NOD/SCID	Nonobese diabetic/severe combined immunodeficiency
SD	standard deviation
SEM	standard error of the mean
SLAM	signaling lymphocytic activation molecule
SN-38	7-ethyl-10-hydroxycamptothecin
SN-38G	SN-38 glucuronide
ssRNA	single-stranded RNA
STAT1	signal transducer and activator of transcription 1
T	tumor
$TCID_{50}$	50 % tissue culture infective dose
TIR	Toll/IL-1R homology
TLR	Toll-like receptor
TME	tumor microenvironment
TMZ	temozolomide
TNBC	triple-negative breast cancer
TNF-α	tumor necrosis factor-α
TNM	Tumor, Node, Metastasis
Topo I	topoisomerase I
TRIF	TIR-domain containing adaptor inducing IFN-β
UA	ursolic acid
UA-NP	UA nanoparticle
UA-PM	UA-PVP physical mixture
VACV	vaccinia virus
VSV	vesicular stomatitis virus
XRD	X-ray diffraction

ACKNOWLEDGEMENTS

First, I would like to express my deepest appreciation to my supervisors. Dr. Liang-Tzung Lin, thank you for the years of guidance, training, and mentorship; my research development and this journey would not have been possible without your unwavering support and nurturing. Dr. Christopher Richardson, thank you for giving me the opportunity and honor to work under your guidance and to learn from your invaluable knowledge and expertise. I am also very grateful to my supervisory committee, Dr. Roy Duncan, Dr. Shashi Gujar, and Dr. Lisa Barrett, for their constructive advice that helped improve my study. Special thanks to the Lin lab members (Rita, Wen-Chan, Ben, Shu Hui, Derek) and the Richardson lab members (Ryan, Sebastien, Gary, Angel), for experimental assistance and previous efforts put into the projects. Last but not the least, to my parents and brother, thank you for your unconditional love and support.

CHAPTER 1 INTRODUCTION

1.1. The Measles Virus

1.1.1. General background

Measles virus (MV) is the etiologic agent that causes the measles disease which is a highly contagious respiratory infection that typically affects children. Despite the availability of effective vaccines for over 60 years [1], MV still caused about 869,770 infections in 2019 resulting in over 200,000 deaths worldwide [2], making it an important public health concern with humans as the only known reservoir. Recent decline in vaccination coverage due to vaccine hesitancy has consequently led to decreased herd immunity, resulting in a re-emergence of measles outbreaks [3, 4]. Notably, in 2019, the USA and France reported a 300 % hike in clinical MV cases that were reported compared to 2018 [5]. Measles is also the most contagious virus known with an R_0 of 12 to 18 [6], in other words, an infected person within a susceptible population will transmit the viral infection to about 12 – 18 people on average. Populations with impaired or compromised immunity may see a further increased transmission rate of infection [7]. MV is spread by infectious respiratory aerosols and droplets from one person to the next and precedes the appearance of exanthem (skin rash) which may limit the timely identification and containment of the disease [7]. Typical symptoms of measles include fever, cough, runny nose, conjunctivitis, pathognomonic Koplik spots on the oral mucosa, and erythematous maculopapular rash, but more severe complications such as pneumonia and encephalitis can occur which can be fatal [8]. Without immunization, children are the primary targets of MV, but the virus can affect people of any age including adults [7]. Given the recent

dramatic increase in measles cases, MV remains a global major cause of morbidity and mortality, especially in poor developing countries, with an estimated mortality rate of 3 – 6 % [2, 9].

1.1.2. Management

There are no specific antiviral drugs to treat measles, and current treatment includes supportive therapy to prevent dehydration and treat malnutrition, as well as early detection and treatment of secondary bacterial infections, such as pneumonia and otitis media [10]. Early vitamin A supplementation in children with moderate to severe measles, especially in those with vitamin A deficiency, can also reduce individual mortality by 50 % and prevent or reduce the risk of severity and complications [11].

A safe and highly effective live-attenuated vaccine is available to prevent outbreaks of measles. However, despite routine immunization, MV infection remains endemic globally due to suboptimal vaccination coverage and inadequate population immunity. Any population with less than 95 % herd immunity is at risk of measles outbreak [12]. Different MV strains are used in vaccines, but all vaccine strains belong to MV genotype A [13]. Immunization against measles is usually given in combination with other childhood viral disease vaccines, including the measles, mumps, and rubella (MMR) vaccine or the measles, mumps, rubella, and varicella (MMRV) vaccine. The measles vaccine consists of live-attenuated MV, and the MMR vaccine is given in two doses, the first dose when the child is 12 to 15 months old and the second dose 4 to 6 years of age [14].

In general, immunization provides robust humoral and cellular immunity, and the administration with the two doses vaccine typically generates protective measles antibodies

in at least 90 % of the immunized individuals [15]. With > 100 million doses administered worldwide yearly since 2000, MV-containing vaccines have an excellent safety record [10]. Serious adverse reactions are rarely observed and substantially much less risky than symptoms from a natural MV infection, including anaphylaxis (2 – 14 cases/million doses), febrile seizures (1 case/3000 doses), and measles inclusion body encephalitis in persons with documented immunodeficiency [16, 17]. This suggests that MV-based vaccines are safe and sets precedent for consideration in the development of this virus for other applications including as therapeutic vaccines.

1.1.3. Molecular virology and life cycle

MV is an enveloped virus belonging to the genus *Morbillivirus* within the *Paramyxoviridae* family and *Mononegavirales* order. It possesses a non-segmented single-stranded RNA (ssRNA) genome that is of negative sense, with six genes encoding the viral nucleocapsid (N), phosphoprotein (P), matrix (M) protein, the two viral glycoproteins fusion (F) and hemagglutinin (H), and the viral polymerase (large, L) [8]. The P gene further encodes the virulence factors V and C, which are two non-structural proteins are mainly responsible for altering the host cell innate immunity [18-21].

Wild-type MV clinical isolates infect target cells using signaling lymphocytic activation molecule 1 (SLAMF1/SLAM/CD150) and nectin-4 receptors [22-24], while vaccine strains additionally use the CD46 complement regulatory molecule that is ubiquitously expressed as a cellular receptor [25, 26]. MV cell entry is pH-independent and proceeds by direct fusion of the viral membrane with the plasma membrane through direct protein-protein interactions [27]. However, it is also possible for MV to attain cell entry

via endocytosis and this event is observed to be facilitated in B-lymphoblastoid cells with SLAM expression or A549 cells rendered to overexpress SLAM (A549-SLAM), and alternatively also by means of engaging the nectin-4-induced micropinocytosis pathway in tumor cell lines of the breast (MCF-7) and colon (HTB-20, and DLD-1) [28, 29]. Certain MV strains, such as the Edmonston or Hallé strains, may also utilize a micropinocytosis-like mechanism involving SLAM and CD46 to infect non-lymphoid and lymphocytic cells, although it is still not well understood [30, 31].

MV infection of the target cell begins when the MV H protein binds to the entry receptor on the cell surface and induces a conformational change in the F protein, allowing the hydrophobic fusion peptide to insert into the plasma membrane of the target cell [32, 33].The structural rearrangement of the F protein into a metastable conformation (from pre-fusion to post-fusion form) brings the viral envelope and host cell membrane into close proximity and destabilizes them, causing fusion of the two lipid bilayers and subsequent release of the viral genome into the cytoplasm [34-36]. Besides the initial function of the MV F protein to induce virus-cell fusion during virus entry, F also causes the infected cells to fuse with neighboring cells leading to the formation of syncytia (giant multinucleated giant cells) at later stages of the infection which is typical of MV's cytopathic effect (CPE) [8]. Transcription starts from a single promoter and is performed by the viral RNA-dependent RNA polymerase (RdRp), leading to a transcriptional gradient with mRNA transcripts encoding N as most abundant to the least abundant mRNA transcripts expressing L, thus allowing an efficient viral life cycle [37]. After translation, N and P proteins' accumulation induces replication of the viral genome to produce positive-strand of the RNA antigenome, resulting in subsequent synthesis of the negative-strand RNA that

is then encapsidated by the *de novo* produced N, P, and L proteins [38]. The MV N protein encapsidates the RNA genome to form a helical nucleocapsid [39], while the proteins L and P make up the MV RdRp [37]. The viral ribonucleoprotein (RNP) is therefore composed of the MV N, P, and L proteins [37]. The MV M protein interacts directly with protein N to regulate RNA synthesis and assembly [8], ensuring the integrity of viral particles [1] and facilitating the formation of new virions [8]. The assembly of viral proteins occurs at the plasma membrane, where new viruses can be released by budding, or surface glycoproteins can be transported to the plasma membrane, allowing intercellular transmission [1].

1.2. Oncolytic Virotherapy

Oncolytic virotherapy is a rapidly emerging anticancer strategy that offers several advantages over conventional treatments, including selectivity, potency, and mechanism of cell kill [40]. Importantly, it is delivered as a therapeutic vaccine by intratumoral (*i.t.*) or intravenous (*i.v.*) injection, low invasiveness, high cost-effective ratio, and good maintenance of patient's quality of life. This therapy, which employs an oncolytic virus (OV), is based on the observations that some viruses have natural tendencies to infect and lyse cancer cells without harming normal cells. Today, viral oncolytics is an exploding field with many natural/mutant forms or engineered viral strains explored for clinical use [41]. One of the first products, the adenovirus (ADV) H101 (Shanghai Sunway Biotech), was licensed in China in 2007 as a therapy for head and neck cancer [42]. More recently in 2015, the U.S. Food and Drug Administration (FDA) approved its first intralesional oncolytic virotherapy, the talimogene laherparepvec/T-VEC (Imlygic®; Amgen Inc.),

which is a herpesvirus-based vector against melanoma [43]. Authorization from Europe and Australia followed, marking the international licensing of a first-in-class oncolytic viral vector for the treatment of cancers. Several other viral platforms including Newcastle disease virus (NDV), reovirus (RV), vaccinia virus (VACV), vesicular stomatitis virus (VSV), and MV are being explored in advanced clinical trials worldwide [44-46].

Multiple factors are considered for the selection of OV vectors. These include viral genome, virus size, tropism, pathogenicity, immunogenicity, and stability [47, 48]. Generally, DNA viruses are easier to genetically modify, whereas RNA viruses replicate more efficiently. Viruses with a large genome have high transgene capacity, such as ADV and HSV, which have been developed into transgene-encoding vectors for clinical trials [49, 50]. In contrast, small viruses may penetrate tumors better and cross the blood-brain barrier (BBB); of which, parvovirus [51] and RV [52] have demonstrated clinically their ability to transverse the BBB to infect intracranial tumors when administered intravenously. Viruses with known receptors, existing antiviral drugs, attenuation (less virulence), or do not cause significant diseases in humans are preferred for biosafety considerations. Examples include VACV and attenuated MV which have been delivered as vaccines, and ADV and VSV which do not typically cause serious human illness. On the other hand, viral immunogenicity determines the strength of immune response and may affect how the vector is delivered (intralesional or systemic). Finally, the stability of viral particles during production, purification, storage, and delivery, as well as the achievable titer, are also crucial to clinical applicability of the viral vector [47, 48].

1.2.1. Engineered Paramyxovirus as an oncolytic agent

Paramyxoviruses are negative-stranded viruses that recently garnered attention as oncolytic agents, including Sendai virus [53], mumps virus [54], parainfluenza virus 5 [55, 56], NDV [57], and MV. Recombinant MV has been explored against non-small-cell lung carcinoma [58], glioblastoma [59], ovarian cancer [60], osteosarcoma [61], acute myeloid leukemia [62], among others, thus demonstrating its potential as a future cancer treatment. The wild-type virus is enveloped and infects primates (Figure 1A) [8]. As aforementioned, the two viral glycoproteins, the H receptor binding protein and the F membrane fusion protein play critical roles in mediating MV cell entry, including cell recognition and binding followed by the F protein-mediate fusion. The syncytia induced by the F protein (Figure 1B) marks MV's CPE in the target host cells and eventually leads to apoptotic death of the infected cells [8]. MV utilizes three receptors to target the host cells, including CD46 [26], SLAM/CD150 [22], and the more recently identified tumor marker nectin-4 [23, 24]. Nectin-4, also known as poliovirus receptor-related 4 or PVRL4, serves as an adhesion receptor and is found in the cell adherens junctions [63]. Nectin-4 is also an embryonic protein that has been identified as a tumor marker for several cancer types including lung, breast, ovarian, pancreatic, and bladder carcinomas [64-68] and also late stage liver cancer [69]. In humans, it is typically not expressed in normal tissues, but found in abundance in the placenta and also with some small levels in the respiratory epithelium [63], suggesting that nectin-4 could serve as a novel prognostic biomarker and a potential target for therapy in several types of cancers. These evidences point to using MV oncolytics to target and treat nectin-4-positive cancers, particularly using a nectin-4-selective MV vector as OV. Finally, the MV genome is genetically modifiable, and reverse-genetics technology [70] has allowed engineering of MV genome possible, permitting inclusion of

genes for tracking the infection (e.g. EGFP or luciferase) and also editing the receptor recognition genes to enhance targeting specificity.

1.2.2. Precision medicine, combinatorial treatment, and viro-immunotherapy

Precision medicine is becoming an essential part of modern-day medical practices by identifying the most effective approach for patients based on genetic, environmental, and lifestyle factors [71, 72]. In viral oncolytics, the expression of the proper receptor in the tumor is crucial to the targeting of the oncolytic vector. In such a way, diagnostic test of biomarker expression should be incorporated to determine the patient's eligibility for oncolytic virotherapy. Some challenges to viral oncolytics are: **1.** Residual innate immunity in the tumor cells as an initial infection barrier; **2.** Immune checkpoints that limit the potentiation of anti-tumor immunity following tumor infection; and **3.** Optimizing viral dose efficacy without compromising safety. As such, the killing mediated by the oncolytic vectors alone may be insufficient to eradicate all tumor cells and augmenting the viral dose is often limited by the tolerable safe dosage. Combining oncolytic vectors with existing therapeutics or immunomodifiers is an emerging trend that can overcome these challenges [73, 74]. For instance, induction of residual innate immunity interferons (IFNs) in the tumor cells may counter the oncolytic virus initially [40]. However, at later stages of the infection, the immune system is pivotal in mounting an anti-tumor response that facilitates clearance of the cancer cells. Specifically, the tumor immunogenic cell death (ICD) and the pro-inflammatory signals generated by the virus-induced CPE can help attract and activate immune cells to the tumor site, process neo-antigens, and switching the originally immune-cold tumors to an immune-hot scenario [75-78]. A potential limiting factor to this

ICD-induced anti-tumor response is the immune checkpoint blockade, and an example is the programmed cell death protein 1 (PD-1) system, whose ligand is often upregulated in the tumor microenvironment to promote immune escape [79]. Thus, inhibition of these immune checkpoints is considered useful to potentiate the anti-tumor response following oncolytic viral infection [80]. In this regard, increasing tumor-killing efficiency with anticancer drugs, augmenting viral infection through cell innate immunity inhibitors, and potentiating the oncolytic activity with immune modulators are modalities to help optimize/tailor oncolytic viro-immunotherapy [81]. Such strategies can yield synergistic treatment effects and reduce the viral dose needed, which in turn enhances safety. Recent examples include tailoring viral vectors with chemotherapeutic paclitaxel [82], histone deacetylases (HDAC) inhibitors [83], molecular sensitizers [84], and immune checkpoint inhibitors including PD-1 antibody [81].

1.2.3. Evidence of the clinical applicability of OVs— novel strategies to overcoming pre-existing immunity and incentive for therapeutic product development

Being exclusively cancer-specific and capable of inducing systemic and immunostimulatory activities, oncolytic virotherapy encompasses the key qualities to a successful oncotherapy that can safely achieve cancer clearance and further protect against cancer recurrence. Specifically, it has been proposed that OVs induces a three-fold anticancer effect: **first** is the direct infection of cancer cells leading to oncolysis; **second** is the triggering of immune response that leads to immune cell infiltration and processing of cancer neo-antigens released from the oncolysis, which in turn culminates to invasion of cancer-targeted cytotoxic T cells and anti-tumor immunity; **third,** this anti-tumor

immunity maintains durable immunological memory that has been experimentally shown to prevent cancer recurrence [47, 81, 85, 86]. Recent success of Dr. Stephen Russell and Dr. Kah Whye Peng at the Mayo Clinic in curing a patient with multiple myeloma through use of the Edmonston MV [87] indicates that it is clinically feasible to employ MV-based oncolytics to treat cancers.

Although pre-existing humoral immunity against MV in a vaccinated individual could potentially limit the virus' clinical applicability, it has been demonstrated that prior immunization with MV does not decrease the oncolytic potential of recombinant virus bearing MV components, especially when large quantities of the virus are being administered to a localized area [88]. This concept has been proven in immunocompetent NDV mouse model [89] and ADV hamster model [90], where the antitumor activities of intratumorally administered oncolytic vectors were not compromised in immunized animals with pre-existing neutralizing antibodies (nAbs). The presence of prior immunity may even enhance the immune filtration in recurrent and distant tumors which in turn assists in tumor suppression [89]. More importantly, this has been validated clinically with the recently FDA-approved herpes simplex virus type 1 (HSV-1)-based T-VEC [91], which has a complete clinical response rate up to 61.5 % [92] despite high seroprevalence of nAbs in the global population [93]. The therapeutic effect of T-VEC intratumoral injection appeared similar in both HSV-1 seronegative and seropositive patients, and tumor regression was also observed in the uninjected lesions due to activated T cell response [94]. These studies indicate that potential factors accounting for the feasibility of employing oncolytic vectors under circumstances of pre-existing immunity include: **1)** intratumoral/intralesional injection which bypasses pre-existing humoral immunity but

triggers cellular immunity; and **2)** the fusogenic ability of certain oncolytic viruses which permits direct cell-to-cell spread without exposure to extracellular nAbs [95].

However, the practicality of intratumoral/intralesional administration should be considered, as not all tumors are accessible through this route. To enable the more practical systemic/intravenous delivery of the oncolytic vector, various novel strategies have obtained breakthroughs to protect MV vectors against the pre-existing nAbs induced by vaccination. Specifically, the concept of bypassing potential neutralization by antibodies through vector "stealth" has now become an important aspect of the next-generation oncolytic virotherapy development. This includes chemical shielding of the viral particles through polymer coating [96] and the use of mesenchymal stem cells as carriers [97, 98], which for their success, are now being evaluated preclinically in non-human primates in Japan (http://mhlw-grants.niph.go.jp/niph/search/NIDD00.do?resrchNum=201307017A) and in U.S. clinical trial (e.g. NCT02068794), respectively. The above underscores the promising avenue of utilizing MV-based oncolytic vectors for the treatment of cancers.

In addition, the ease of cancer treatment with oncolytic virotherapy will be revolutionarily simplified to injection shots, which will redefine cancer treatment as outpatient therapy with significant socioeconomic benefits for both healthcare providers and patients. With these important edges over current first line cancer therapies (surgery, chemotherapy and radiotherapy), oncolytic virotherapy is extensively pursued as a valuable anti-cancer strategy. The clinically applicability and development of oncolytic virotherapy as a future arm of anticancer treatment are attested by the sheer number of registered clinical trials worldwide (> 148 registered trials over the past 15 years for > 61 potential therapies, mainly dominated by the USA and Europe) [99] and growing global

market (predicted by 2026 to reach 700 million USD) which will continue to expand as part of the next decade precision medicine.

1.3. Breast Cancer

Worldwide, female breast cancer accounts for 2.3 million new cases in 2020 and has surpassed lung cancer to become the most commonly diagnosed cancer and the leading cause of cancer death among all cancers [100]. Almost all breast cancers originate in the epithelial lining of the milk ducts or in the lobules that supply milk to the ducts, and these cancers can be classified as either ductal or lobular cancers. Presence or absence of the growth hormone receptors in the breast tumors including estrogen receptor (ER), progesterone receptor (PR), and the human epidermal growth factor receptor 2 (HER2) dictates the classification of the breast cancer type as well as the treatment strategy and prognosis [101]. Breast cancer cells without ER, PR, or HER2, are called basal-like or classified as triple negative breast cancer (TNBC). Breast cancer causes more than 508,000 deaths each year and is at present a top killer of the female population [93]. As breast cancer continues to be the top most occurring cancer in women and ranking second in terms of leading cause of cancer-associated death globally [102], it remains an important global health threat for which improved management is necessary. Treatment strategies of breast cancer include surgery, radiotherapy, hormonal therapy (e.g. tamoxifen, aromatase inhibitors) for ER+/PR+ breast cancers, chemotherapy for triple negative and HER2+ breast cancers, targeted therapy (e.g. HER2 monoclonal antibody Trastuzumab; CDK4/6, PARP, and PIK3 inhibitors), and the emerging immunotherapy (e.g. immune checkpoint inhibitors) [101]. However, while early-stage breast cancers tend to have a favorable

prognosis, advanced stage breast cancers including metastatic breast cancers are very difficult to treat and are even frequently incurable [103]. Chemotherapy is a major treatment option in the clinical management of breast cancer for treating patients with larger tumor burdens, lymph node invasion, or recurrent/metastatic breast cancer [104]. The most frequently observed chemotherapies in clinical setting for the treatment of breast cancer include a variety of anthracyclines and taxanes, which are associated with adverse side-effects and can include neurotoxicity, alopecia [105], cardiotoxicity [106], and bone marrow suppression [105, 106]. Therefore, there is an urgent need to develop new treatment modalities to reduce toxicity and improve efficacy, especially for advanced and metastatic breast cancer.

1.4. Liver Cancer and Hepatitis C Virus-Induced Hepatocellular Carcinoma

Hepatocellular carcinoma (HCC) is a major killer worldwide, and can be caused by infections from hepatitis B virus (HBV) and hepatitis C virus (HCV) [107]. Specifically, chronic HCV infection is responsible for about 30 % – 50 % of all HCC cases in North America, and in most cases, this cancer of the liver is diagnosed very late in the course of the diseases owing to the lack of symptoms during the early phases [108]. Without a preventive vaccine, HCV will become the future major viral etiologic agent for virus-induced HCC due to the continuous phasing out of hepatitis B population resulting from effective anti-HBV antivirals and vaccines. While novel direct acting antivirals (DAAs) offer potential cures for hepatitis C, the lack of vaccine predisposes about 170 – 300 million carriers globally to risks of HCV-induced HCC. Furthermore, options for the treatment of late-stage liver cancer resulting from HCV infection are limited [109]. Although potentially

curative approaches for HCC treatments including transplantation, local ablation, and liver resection have improved to a 5-year survival rate for up to 75 %, recurrence remains the foremost issue with the intrahepatic spread of primary HCC or the precancerous lesions in the residual liver; less than 20 % of HCC patients are suitable for such treatments due to the advanced tumor stages, liver dysfunction, or lack of donor livers [110]. These issues underscore the need for the development of novel therapies against HCC, including in the scenario of HCV-associated hepatoma.

1.5. Hypothesis and General Research Objectives

With the advent of OVs and recombinant DNA technology, oncolytic virotherapy has emerged as a novel treatment option for cancers, with its ability to preferentially target and kill the cancer cells. MV is one of the OVs that is currently being actively researched on as an oncolytic agent for the treatment of many cancer types. In particular, recent discovery of the tumor marker nectin-4 as the epithelial receptor for MV provides impetus to explore MV as an oncolytic agent targeting this tumor marker, since nectin-4 is highly expressed in various cancer types including breast adenocarcinomas and HCC. The vaccine strains of MV can recognize both CD46 and nectin-4 as receptors, whereas the wild-type strains of MV employ nectin-4 but do not engage CD46 [111]. Since CD46 is expressed on all human nucleated cells [112], the use of MV vectors with wild-type glycoproteins is thus justified for oncolytic development targeting nectin-4 [111]. Currently, breast cancer remains a top killer of woman in the world, and HCC, which includes HCV-associated HCC, is also a top killer globally. More importantly, both cancer types have poor prognosis in advanced stages of the disease with little treatment options available. Fortuitously, both

breast adenocarcinomas and HCC have elevated levels of nectin-4, suggesting the feasibility to target this tumor marker as a therapeutic intervention strategy, including using MV with wild-type glycoproteins. This thesis therefore explores as proof-of-concept the anticancer effect and treatment modalities including chemovirotherapies of recombinant wild-type MV as an oncolytic agent against breast and liver cancers using *in vitro* and *in vivo* models.

1.6. Figures, Tables, and Legends

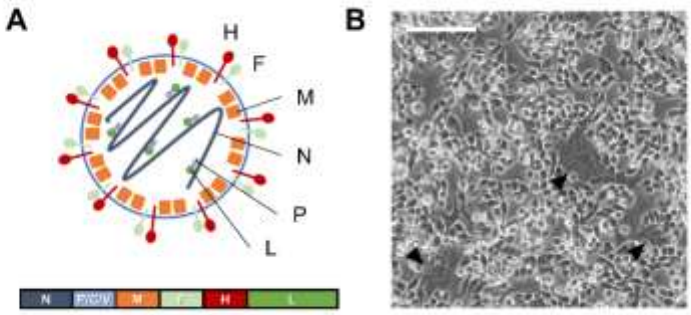

Figure 1. Schematics of measles virus (MV).
A. Schematic diagram of MV and genome organization. MV harbors (-) ssRNA genome that encodes nucleocapsid protein (N), a phosphoprotein (P), virulence factors (C and V), matrix protein (M), membrane fusion protein (F), the hemagglutinin/receptor binding protein (H), and an RNA polymerase (L). Adapted from Tai et al. Sci Rep. 2019 May 1;9(1):6767. **B.** Syncytia formation (indicated by black arrowheads) in MV-infected B95a cells. Scale bar = 100 μm.

CHAPTER 2 MATERIALS AND METHODS

2.1. Cell Culture, Virus, and Reagents

Human breast adenocarcinoma cell lines MCF-7 (kindly provided by Dr. Ming-Sound Tsao; Ontario Cancer Institute, Toronto, Canada), BT-474 (ATCC HTB-20; American Type Culture Collection, Rockville, MD, USA), MDA-MB-468 (ATCC HTB-132; ATCC), human hepatoma cell lines Huh-7 (kindly provided by Dr. Stanley M. Lemon, University of North Carolina at Chapel Hill, Chapel Hill, NC, USA), HepG2 (ATCC HB-8065; ATCC), Hep3B (ATCC HB-8064; ATCC), PLC/PRF/5 (ATCC CRL-8024; ATCC), immortalized human hepatocyte PH5CH8 (kindly provided by Dr. Stanley M. Lemon, University of North Carolina at Chapel Hill), monkey kidney cell line Vero (ATCC CCL-81; ATCC), murine breast adenocarcinoma cell lines 4T1 (ATCC CRL-2539; ATCC) and E0771 (ATCC CRL-3461) were maintained in Dulbecco's Modified Eagle's medium (DMEM; GIBCO-Invitrogen; Carlsbad, CA, USA), supplemented with 10 % fetal bovine serum (FBS; GIBCO-Invitrogen), 100 U/ml of penicillin G, 100 µg/ml of streptomycin, and 0.25 µg/ml of amphotericin B (GIBCO-Invitrogen), in a 5 % CO_2 humidified incubator at 37 °C. HCV subgenomic replicon cells AB12-A2 [113] and sbJFH1-B2 [114], and E0771 cells overexpressing human Nectin-4 (E0771.hNectin-4) were cultured with G418-containing media. 4T1 cells overexpressing human Nectin-4 (4T1.hNectin-4) cells were cultured with Hygromycin B selection. The A2.IFNα-Cured and B2.IFNα-Cured cells were generated by curing the AB12-A2 and sbJFH1-B2 cells of their subgenomic replicons by continuous culture in media containing IFN-α (200 IU/ml; Sigma) for 2 weeks prior to confirmation of the absence of viral protein expression through immunoprobing for NS5A.

For establishment of the A2.DAC-Cured and B2.DAC-Cured cells, AB12-A2 and sbJFH1-B2 cells were cured of the replicating HCV subgenomes by treatment with fresh media containing 1 nM daclatasvir (Toronto Research Chemicals; North York, ON, Canada) every 72 h for 21 days before verification through determination of NS5A expression.

The recombinant Ichinose-B 323 wild-type measles virus (MV-IC323) tagged with enhanced green fluorescent protein ('MV-EGFP', a.k.a. MV.IC323-EGFP; obtained from Dr. Roberto Cattaneo, Mayo Clinic, Rochester, MN, USA) or firefly luciferase ('MV-FLuc', a.k.a. MV.IC323-Fluc) [29] were and propagated in marmoset B lymphoblastoid cells (B95a) as previously described [24]. The 50 % tissue culture infective dose ($TCID_{50}$) assay was used to determine the viral titer, and virus concentrations were represented by multiplicity of infection (MOI). Camptothecin (CPT), ursolic acid (UA), and polyvinylpyrrolidone (PVP) were purchased from Sigma-Aldrich Chemicals Co. (St. Louis, MO, USA). All other experimental reagents were of analytical grade. For drug preparation that uses dimethyl sulfoxide (DMSO) solvent, the final DMSO concentrations were all below 0.2 %.

2.2. Cell Viability and Cytotoxicity Assays

The impact of treatment on cancer cell viability was assessed using the 3-(4,5-dimethylthiazol-2-yl)-2,5-diphenyltetrazolium bromide (MTT) cell viability assay kit (Merck-Millipore; Bedford, MA, USA). Briefly, cells seeded in 96-well plate (10^4 cells per well) were treated with various concentrations of test agents for the indicated time period. Cell viability was then determined according to the manufacturer's protocol, and optical densities (OD) were recorded at 550 nm using a microplate reader and calculated as follows:

Cell viability (%) = (Absorbance $_{\text{test compound}}$ / Absorbance $_{\text{control}}$) × 100 %. The 50 % cytotoxic concentration (CC_{50}) value was then calculated using the GraphPad Prism 7 software (San Diego, CA, USA). For analysis using lactate dehydrogenase (LDH)-based cytotoxicity test, seeded cells were treated with test agents for the indicated time period and analyzed with LDH cytotoxicity detection kit (Takara Bio; Kusatsu, Shiga, Japan) following the manufacturer's instructions. Briefly, supernatant from each well was transferred to 96-well plates, mixed with reaction substrates, and incubated at 37 °C for 30 min before the absorbance was measured at 490 nm using a microplate reader.

2.3. Synergistic Effect of MV-Drug Combinations

Cells seeded in 96-well plates (10^4 cells per well) were studied in three different experiments of MV-drug combinations. (i) Drug sensitization – drug was added to the cells at different concentrations for 2 days, prior to the infection of cells with MV for 3 days. (ii) Viral sensitization – cells were first infected with MV for 2 days, followed by drug treatment at varying concentrations for 3 days. (iii) Co-treatment – cells were infected with MV and at the same time, treated with varying concentrations of drug for a total of 5 days. For all experiments, MV infection was performed for 1.5 h at 37 °C and cells were washed with phosphate buffered saline (PBS; Hyclone, GE Healthcare, Chicago, IL, USA) before and after viral challenge. Cell viability was determined via the MTT or LDH assay as described above. The impact of MV-drug cobinations on the cancer cell viability was determined by calculating the combination index (CI) value using the Chou-Talalay method with the equation $CI = (D)_1/(D_x)_1+(D)_2/(D_x)_2$, where $(D_x)_1$, $(D_x)_2$ are the respective concentrations of drug 1 and drug 2 used in their single treatments that decrease the cell

viability by x %, and $(D)_1$, $(D)_2$ are the respective concentrations of drug 1 in combination with drug 2 that together decreased the cell viability by x % [115]. Calculation of the CI value is done by using the CompuSyn software developed by T. C. Chou and Nick Martin. The effect was determined as follows: additive (CI = 1), synergistic (CI < 1) or antagonistic (CI > 1) [115].

2.4. Influence of Drug Treatment on Early Viral Entry Steps of MV Infection

The impact of drug treatment on the early MV viral entry steps, including (i) free virus particles, (ii) viral attachment, and (iii) viral penetration was examined as previously described [116] with some modifications. (i) Cell-free MV particles were first incubated with varying concentrations of drug for 3 h at 37 °C. The virus-drug mixture was then diluted 20-fold with DMEM containing 2 % FBS to ineffective concentrations of drug and a final MV MOI of 0.1, before addition to cells seeded in 96-well plate (10^4 cells per well) for 1.5 h. Cells were then washed with PBS and incubated in fresh 2 % FBS DMEM for 3 days at 37 °C. (ii) The virus-drug inocula containing MV (MOI 0.1) and varying concentrations of drug were prepared and added to pre-chilled (at 4 °C) cells seeded in 96-well plate (10^4 cells per well) for 1.5 h at 4 °C, before removing the virus-drug inocula, washing with PBS, and further incubating for 3 days at 37 °C in fresh 2 % FBS DMEM. (iii) Cells seeded in 96-well plate (10^4 cells per well) were first pre-bound with MV (MOI 0.1) at 4 °C for 1.5 h, which allows for virus binding but precludes internalization [117]. This was then followed by removal of viral inoculum and washing with PBS before shifting the temperature to 37 °C to facilitate viral penetration and treating the cells with varying concentrations of drug for 1.5 h. The supernatant was subsequently removed and the wells

were washed with PBS before incubation for 3 days at 37 °C in fresh 2 % FBS DMEM. In all the above, after the 3-day incubation, fluorescence signals from the reporter-tagged virus were scanned using the Typhoon 9410 variable mode imager (Amersham Biosciences; Baie d'Urfe, QC, Canada) and quantified using Image Quant TL software (Amersham Biosciences) to assess the viral infectivity.

2.5. Time-of-Drug-Addition Assays

Drug addition at different time-points (denoted as 'pre-treatment', 'co-addition', and 'post-infection') were performed as previously described [117] to investigate potential antiviral effect of drugs on oncolytic MV infection. In pre-treatment analysis, cells (10^4 cells per well of 96-well plate) were pre-treated with drugs for 24 h after which the supernatants were removed and cells were challenged with MV (MOI 0.1) for 1.5 h at 37 °C. Viral inocula were later removed and replaced with fresh 2 % FBS DMEM for 3 days' incubation at 37 °C. In co-addition analysis, MV (MOI 0.1) and drugs were concurrently added to the cells for 1.5 h before the virus-drug inocula were discarded and replaced with fresh 2 % FBS DMEM for 3 days' incubation at 37 °C. In post-infection analysis, cells were infected with MV (MOI 0.1) for 1.5 h, followed by removal of viral inocula before incubating the cells with 2 % FBS DMEM containing drugs for 3 days at 37 °C. For all assays, the viral reporter fluorescence signals were analyzed at the end of the 3-day incubation as described above.

2.6. Cell Cycle Analysis

Cells (3 x 10^5 cells per well of 6-well plate) were treated with MV (MOI 0.01 or 0.1) and the drug, individually or concurrently, for 1.5 h at 37 °C. The supernatants were subsequently removed and the treated cells were refreshed with 2 % FBS DMEM with or without the drug for 5 days' incubation at 37 °C. The cells were then trypsinized, collected into 15 ml tubes, washed twice with ice-cold PBS by centrifugation, and finally fixed with 70 % ethanol overnight at 4 °C. After fixation, the cells were washed twice with PBS by centrifugation prior to 30 min incubation in PBS solution containing 10 mg/ml ribonuclease A from bovine pancreas (RNase A; Sigma-Aldrich) at 37 °C. Propidium iodide (PI; 40 µg/ml; Sigma-Aldrich) was subsequently added to the cells for 15 min incubation in the dark at 37 °C before subjecting to flow cytometric cell cycle analysis using the Beckman Coulter FC500 flow cytometer (Beckman Coulter Inc.; Brea, CA, USA).

2.7. Apoptosis Analysis by Annexin V/Propidium Iodide Double Staining

Cells (3 x 10^5 cells per well) seeded in 6-well plate were treated with MV (MOI 0.01 or 0.1) and the drug, individually or concurrently, for 1.5 h at 37 °C. The supernatants were then removed before refreshing the cells with 2 % FBS DMEM with or without the drug for further incubation (5 days) at 37 °C. At the end of the incubation, the cells were subsequently trypsinized for collection into 15 ml tubes, ice-cold PBS-washed twice by centrifugation, and finally resuspended in binding buffer containing 1 µl/ml PI and 1 µl/ml allophycocyanin (APC)-conjugated Annexin V (Enzo Life Sciences, Inc; East Farmingdale, NY, USA). Apoptosis detection via flow cytometry was then analyzed on a flow cytometer (Beckman Coulter FC500 apparatus; Beckman Coulter Inc.).

2.8. Nectin-4 Surface Staining Analysis

Cells (10^6 cells per well) were seeded in 6-well plate overnight. The next day cells were dissociated by dissociation buffer (C5789; Sigma), centrifuged and re-suspend with PBS containing 1 % FBS. Cells were then incubated with 5 µl of either phycoerythrin (PE)-conjugated anti-nectin-4 antibody (FAB2659P; R&D Systems, Minneapolis, MN, USA) or PE-conjugated mouse IgG2B isotype control (IC0041P; R&D Systems) for 45 min on ice. Cells were washed twice in PBS containing 1 % FBS and fixed by 1 % paraformaldehyde (PFA). Samples were analyzed using the Beckman Coulter FC500 apparatus (Beckman Coulter Inc.) or BD FACSCelesta (BD Biosciences, Franklin Lakes, NJ, USA).

2.9. Western Blot Analysis

For western blot analysis, cells (3 x 10^5 cells per well) seeded in 6-well plate was treated with MV (MOI 0.01 or 0.1) and the drug, individually or concurrently, for 1.5 h at 37 °C. The virus-drug inocula were then discarded and the cells were refreshed with 2 % FBS DMEM with or without the drug for a 5-day incubation at 37 °C. The cells were subsequently lysed with radioimmunoprecipitation assay buffer (RIPA) buffer (Sigma-Aldrich) containing protease inhibitor (Roche Molecular Biochemicals; Indianapolis, IN, USA), and protein concentrations were measured by bicinchoninic acid (BCA) protein assay kit (Thermo Fisher Scientific Inc.; San Jose, CA, USA). Protein samples were then subjected to standard western blot analysis and proteins were probed using primary antibodies for poly (ADP-ribose) polymerase (PARP) (1:1000; Cell Signaling Technology, Inc., Danvers, MA, USA) and β-actin (1:10000; Cell Signaling Technology, Inc.) followed by anti-rabbit and anti-mouse horseradish peroxidase (HRP)-conjugated secondary

antibodies (1:1000 and 1:10000; Cell Signaling Technology, Inc.). For autophagy analysis, cells seeded in 12-well plate (2.5 x 10^5 cells per well) were treated with drug, MV (MOI 0.1), or concurrently treated with both agents for 48 h before being harvested and analyzed for microtubule-associated proteins 1A/1B-light chain 3 (LC3; 1:1000; Thermo Fisher Scientific), p62 (1:1000; GeneTex, Irvine, CA, USA), and β-actin (1:10000; Cell Signaling Technology) expression using western blotting. Bafilomycin A1 (BAF, 100 nM; Sigma-Aldrich) was added to the indicated groups 4 h before harvesting the cells. MV H protein was probed to indicate MV infection using a rabbit anti-MV H serum H606 [118] (1:1000; kindly provided by Dr. Christian Buchholz; Paul-Ehrlich-Institut, Langen, Germany). Detection was performed using the Immobilon™ Western Chemiluminescent HRP substrate (Merck Millipore), followed by chemiluminescence imaging using the UVP BioSpectrum 500 imaging system (UVP; Upland, CA, USA). Protein band intensities were quantitatively evaluated and compared against the β-actin loading control via densitometry analysis.

2.10. Preparation of UA Nanoparticles (UA-NPs)

The UA-loaded nanoparticles or UA-NPs were prepared using the emulsion-solvent diffusion technique as previously described [119]. UA was first dissolved in ethanol to obtain an organic phase (UA concentration = 3 mg/ml), which was then mixed with the aqueous PVP (prepared in water) at 1:1, 1:3, or 1:6 UA to PVP weight ratios. Subsequently, the solutions were homogenized by sonication at 20 kHz for 10 min in cold-water bath. Next, the organic ethanol solvent was removed using a rotary vacuum evaporator with water bath at 40 °C. The residue was passed through qualitative filter paper (Advantec®

No. 1, Toyo Roshi Kaisha, Ltd., Tokyo, Japan) to remove aggregates. The filtrate containing UA-NP was collected and stored at 4 °C for immediate use, or lyophilized and then stored at -20 °C in a moisture-proof container for longer period storage.

2.11. UA-NPs Particle Size Analysis by Photon Correlation Spectroscopy (PCS)

Mean size of UA-NPs was measured by the Malvern Zetasizer (Malvern Instruments Ltd., Worcestershire, United Kingdom). The temperature was maintained at 25 °C and the test sample was diluted 50-fold using deionized water before measurement. Each determination was performed in triplicate.

2.12. High-Performance Liquid Chromatography (HPLC) Analysis of UA and UA-NPs

HPLC was performed using the Hitachi D-7000 HPLC system (Hitachi, Ltd.; Tokyo, Japan) with a reverse-phase C18 column (LichroCART® Purospher® STAR; Merck KGaA; Darmstadt, Germany). The mobile phase consisted of acetonitrile and 0.1 % phosphoric acid (85:15, v/v). The analytical process was carried out under a flow rate of 1 ml/min for 15 min with UV detection at 210 nm. The calibration curve was linear over the concentration range of 0.45 – 90 μg/ml with a coefficient estimate of 0.999.

2.13. UA-NPs Yield Quantification

The yield of UA nanoformulation was determined by HPLC analysis using a previously described method [119]:

$$\text{Yield (\%)} = [C_{UA}\ (\mu g/ml) \times V_{UA\text{-}NP}\ (ml) / W_{UA}\ (\mu g)] \times 100$$

C_{UA} (μg/ml): concentration of UA detected in UA-NPs

$V_{UA\text{-}NP}$ (ml): final volume of UA-NPs

W_{UA} (μg): quantity of UA used in the preparation for nanoformulation

2.14. Field Emission Scanning Electron Microscopy (FESEM)

The morphological characteristics of the UA-NPs were imaged using FESEM as previously reported [119]. UA-NP samples were sputter-coated with gold in low energy input (E-1045 ion sputter; Hitachi, Ltd.) and then viewed under the Hitachi SU8010 SEM with an accelerating voltage of 5 kV.

2.15. X-Ray Diffraction (XRD)

An X-ray diffractometer with Cu-Kα radiation and Ni filter (Siemens D5000; Siemens AG; Munich, Germany) was used to examine the crystalline properties of UA, PVP, UA-PVP physical mixture (UA-PM), and lyophilized UA-NP powder. UA-PM was prepared by thoroughly mixing UA and PVP with a mortar in the same composition ratio as for UA-NP, which was 1:1 in weight. Prior to XRD analysis, all samples were dried overnight to remove moisture. XRD patterns were obtained at 40 kV and 25 mA, with a scanning rate of 4°/min, over the diffraction angle (2θ) range of 2° to 50°.

2.16. Dissolution Test

The dissolution test was performed based on USP apparatus II (paddle) method [119] in accordance to the United States Pharmacopeia XXIX [120]. To achieve better discriminating dissolution profiles for the poorly soluble crude drug and its

nanoformulation, non-sink condition was applied for the analysis [121, 122]. Briefly, UA or UA-NP sampling powders were prepared by placing 4.68 mg equivalent of UA in 100 ml of pH 7.4 phosphate buffer with continuous stirring by paddle at 100 rpm and temperature maintained at 37 ± 0.5 °C (n = 6). During the experiment, 1 ml of sample was withdrawn at successive time intervals (0, 1, 10, 20, 30, 60, 90, and 120 min). The concentration of UA was analyzed by HPLC and the data acquired were calculated and converted into 'percent of dissolved amount' to represent the drug dissolution property.

2.17. HCV NS5A Immunofluorescence Staining

Cells seeded in 96-well plate (1 x 10^4 cells per well) were fixed with 4 % PFA for 30 min at room temperature. After that, cells were washed twice with PBS and permeabilized with 0.3 % Triton X-100 for 30 min at room temperature. Cells were then blocked with 3 % BSA for 30 min at room temperature before incubated with 9E10 antibody (1:5000; purchased from Cell Essentials, Inc., Boston, MA, USA with permission from Dr. Charles M. Rice) at room temperature for 1 h. After two washed with PBS, Alexa fluor 488-conjugated anti-mouse IgG (1:1000; Invitrogen) were added to the cells for 30-min incubation in the dark at room temperature. Finally, cells were wash three times with PBS and the nuclei were stained with 4',6-Diamidino-2-Phenylindole, Dihydrochloride (DAPI; Invitrogen) before imaging with a fluorescence microscope.

2.18. IFN-β Reporter Assay

Cells were seeded 96-well plate (1 x 10^4 cells per well) and transfected with 5 ng of pRL-TK LUC and 200 ng of IFNβ-pGL3 LUC [123] (kindly provided by Dr. John Hiscott,

Laboratorio Pasteur Istituto Pasteur Italia, Fondazione Cenci Bolognetti, Rome, Italy). The next day, supernatant was removed and replaced with DMEM containing 2 % FBS. Cells were then transfected with 200 ng of polyinosinic:polycytidylic acid (poly I:C; Sigma) or infected with MV-EGFP at MOI 1. After 20 h, firefly luciferase and *Renilla* luciferase activities were measured using Dual-Luciferase® Reporter Assay System (Promega; Madison, WI, USA) following the manufacturer's instructions.

2.19. MV Infection of Huh-7 Cells Transiently Expressing HCV NS3/4A by Adenoviral Vector Transduction

Huh-7 cells seeded in 96-well plate (1 x 10^4 cells per well) were infected with various MOI of the GFP-tagged ADV control (ADV-Cntrl) or GFP-tagged ADV encoding the HCV NS3/4A from the genotype 1a strain H77 (ADV-NS3/4A(H77)), which were generated using the AdEasy Adenoviral Vector System (Agilent Technologies, Inc.; Santa Clara, CA, USA). The infected cells were incubated for 24 h to allow gene expression and then infected with MV-FLuc (MOI 0.1) before incubating for another 48 h. Luciferase activity produced by MV-FLuc was then measured with the Luciferase Assay System following the manufacturer's instructions (Promega).

2.20. MV Infection of Tumor Spheres

Cells were seeded 10-cm dishes (1 x 10^5 cells per dish) coated with 1 % agarose and cultured in 15 ml of DMEM containing 10 % FBS for 7 days to form tumor spheres before MV infection. Approximately 120 spheres were transferred to a 5 ml tube and infected with MV-EGFP (10^5 $TCID_{50}$) for 2 h at 37 °C, then the virus was removed and spheres were

resuspended in DMEM containing 10 % FBS and cultured in ultra-low attachment 6-well plate. Spheres were observed using a fluorescence microscope. For confocal microscopy, samples were prepared using previously described method [124]. Briefly, spheres were fixed in 4 % PFA for 3 h at 4 °C, washed and blocked in PBS containing 2 % FBS for 15 min at room temperature, and incubated in fructose–glycerol clearing solution for 20 min at room temperature. Cleared spheres were mounted onto 1mm microscopy slides and stored at -20 °C before imaging.

2.21. Animal Study

For syngeneic mouse model, 6 to 8-week-old female BALB/c mice or C57BL/6 mice were inoculated with 4T1.hNectin-4 (2 x 10^6 cells per mouse) or E0771.hNectin-4 (5 x 10^6 cells per mouse) murine breast cancer cells, respectively, in the mammary fat pad and allowed to develop the tumor for 10 days. Mice received intratumoral treatment of PBS (control) or MV (2 x 10^6 $TCID_{50}$ per mouse for 4T1.hNectin-4 tumors or 5 x 10^6 $TCID_{50}$ per mouse for E0771.hNectin-4 tumors) at the indicated timepoints. Tumor volume was measured on the treatment days and twice per week afterwards and calculated with the formula: Tumor volume = $(4/3) \times \pi \times (L/2) \times (W/2) \times (D/2)$.

2.22. Statistical Analysis

Unless otherwise stated, all data from the experiments are expressed as means ± the standard deviations (SD) or standard error of means (SEM). Statistical significance was assessed by GraphPad Prism 7 software, using Student's t-test or one-way analysis of

variance (ANOVA) followed by Dunnett's or Sidak's multiple comparisons, with $P < 0.05$ considered as statistically significant.

CHAPTER 3

ONCOLYTIC POTENTIAL OF MEASLES VIRUS FOR THE TREATMENT OF BREAST ADENOCARCINOMA THROUGH THE TARGETING OF NECTIN-4

3.1. Abstract

Breast cancer is among the leading causes of female cancer deaths worldwide and its incidence has increased over the past decade. Oncolytic virotherapy using viruses that preferentially target and kill cancer cells represents a novel therapy for the management of breast cancer. Recent discoveries that attenuated strains of MV possess oncolytic properties and can be used to destroy tumor cells have sparked an interest to employ MV as oncolytic agent. Although earlier attempts have been made to use CD46-preferred vaccine strains of MV to target breast cancer cells, the vector is potentially hazardous and non-specific due to expression of CD46 on most normal nucleated cell types. On the other hand, breast cancer cells, which highly express the tumor marker nectin-4, have recently been observed to be susceptible to infection by wild-type MV strains, which preferentially engage nectin-4 as its epithelial cell entry receptor and does not recognize CD46. This observation suggests that vectors bearing wild-type MV glycoproteins could potentially be further explored as an effective and highly specific oncolytic agent against breast cancer. Taking advantage of this targeting specificity, in this study, as proof-of-concept, the ability of a recombinant wild-type strain of MV to infect and induce breast cancer cell oncolysis was evaluated *in vitro* and *in vivo*. Specifically, various breast cancer cell lines expressed nectin-4 which correlated with the infection and dose-dependent oncolysis induced by MV. Expression of nectin-4 could be observed by immunohistochemistry staining of clinical breast cancer tissue array and was associated with lower survival rate and a higher frequency of recurrence, triple-negative typing, advanced staging, and metastasis, suggesting the clinical utility of targeting nectin-4 as a tumor marker for breast cancer. Intratumoral injection of recombinant MV tagged with luciferase reported in nude mice

demonstrated that the virus could successfully infect and spread within the tumor *in vivo*, although the tumor showed little regression or inhibition in growth suggesting limited efficacy in the absence of the immune system. Using a syngeneic mouse model, we demonstrated that intratumoral MV treatment of mouse breast cancer cells expressing human nectin-4 showed infection by the recombinant wild-type MV and the tumor exhibited an obvious restricted growth resulting in higher animal survival compared to the PBS saline control treatment. This observation suggested the importance of the immune system in MV-associated oncolytic treatment and also its clinical applicability as an oncolytic agent for targeting nectin-4-positive breast cancers. Altogether, results from this study provide a foundation for the development and application of oncolytic vectors with wild-type MV glycoproteins as future virotherapy for the management of breast cancer.

3.2. Rationale and Aim

Globally, breast cancer is among the most common adenocarcinomas [125]. Despite novel advances in treatments including chemotherapy, hormone therapy, radiotherapy, and surgery to improve survival, the disease continues to be a foremost cause of death in women [101]. While early stage-detected breast cancers tend of have a more favorable prognosis, advanced stages including metastatic breast cancers are typically very difficult to treat and are often incurable [101], thus continuous research to develop novel therapies that are more effective is thus warranted. Ongoing research has highlighted oncolytic virotherapy as another uprising treatment option in various stages of pre-clinical and clinical development as monotherapy or combinatorial therapies against numerous cancer types [126]. The oncolytic virotherapy anti-cancer activity is primarily attributed to

the inherent susceptibility of cancer cells to lytic infection by replication-competent wild-type or genetically engineered attenuated viruses, while abortive infection protects normal healthy cells, thus minimizing off-target toxicities and rendering the treatment highly safe and effective [127]. Furthermore, the induction of cancer killing by lytic death of infected cells sustains the added advantages of triggering destruction of tumor vasculature which leads to death of uninfected tumor cells, and importantly, recruitment of tumor-specific adaptive immunity which plays a crucial role in cancer clearance and preventing recurrence [127]. Oncolytic virotherapy is therefore recognized as a valuable treatment strategy that combines key qualities to a successful oncotherapy with its cancer-specific killing, safety, and ability to activate adaptive immunotherapeutic protection. Additionally, oncolytic virotherapy using OVs is potentially an effective therapeutic approach that can enable the detection and elimination of micro- and macrometastases of breast cancers [103].

Of the diverse range of oncolytic viruses that have been studied against breast cancer, including adenoviruses, herpesviruses, poxviruses, reoviruses, paramyxoviruses [126, 127], MV is a commonly and extensively used viral agent due to its excellent safety record with population immunity and generally low pathogenic and mutation risks [128]. As an enveloped particle, MV possesses a single-stranded RNA genome that is negative-sense. The virus is able to target several host receptors, whereby the signaling lymphocyte activation molecule (SLAM/CD150), the complement regulatory protein CD46, and the more recently identified nectin-4 (aka PVRL4) are used by the Edmonton vaccine strain whereas wild-type strains of MV employ only SLAM and nectin-4 for entry [111]. Nectin-4 is an immunoglobulin (Ig) superfamily member of the nectin family which regulates the formation of cell-cell junctions [129]. This adhesion junction protein has three Ig-like

domains in its extracellular portion, including one variable (V) type domain in the outmost section followed by two constant (C) type domains towards the cellular membrane. In the placenta, nectin-4 is highly expressed (hence also an embryonic protein), but modestly expressed in the trachea and skin, and absent in most tissues of the human body. Interestingly, nectin-4 has been identified as a tumor marker of several carcinomas, including lung [66], breast [65], ovarian [64], esophageal [130], gastric [131], pancreatic [67], liver [69], colon [132], and bladder [133] cancers. Given nectin-4's high level of expression and importance as tumor marker in breast adenocarcinomas while being absent in normal breast epithelium [65], this supports particularly the use of MV vector with wild-type glycoproteins as an oncolytic agent with nectin-4 selectivity for breast cancer over the vaccine strain, due to its additional usage of CD46 which is expressed in all nucleated cells [128].

In this study, we explore the oncolytic potential of recombinant wild-type MV for the treatment of breast adenocarcinoma through the targeting of nectin-4 using *in vitro* and *in vivo* models.

3.3. Results

3.3.1. Nectin-4 is expressed in various breast cancer cell lines and is associated with infection susceptibility and dose-dependent oncolysis induced by recombinant wild-type MV infection

Receptor specificity determines the permissiveness of a cell to initial infection by the virus. As wild-type MV can engage nectin-4 [23, 24], the expression of nectin-4 can be used to predict the oncolytic sensitivity of the target cells, including breast cancer cells.

For this purpose, we therefore first examined the expression of nectin-4 in the various breast cancer cell lines. As shown in Figure 2A, nectin-4 expression was detected in MCF-7 and MDA-MB-468 cells, but not in MDA-MB-231 cells. Upon challenge by the recombinant wild-type MV tagged with EGFP, only the nectin-4-expressing cell lines were permissive to the viral infection, as indicated by the presence of fluorescent syncytium (Figure 2B). More importantly, the nectin-4-negative MDA-MB-231 cells, which are refractory to the recombinant wild-type MV infection, can be rendered permissive upon overexpression of nectin-4 (Figure 2 A and B), thus indicating the ability of recombinant wild-type MV to exhibit targeting specificity towards the tumor marker nectin-4 on breast cancer cells. To examine the cytotoxicity of cancer cells induced by the oncolytic properties of MV, the different breast cancer cell types including luminal A (MCF-7 and T47D), luminal B (BT-474), and TNBC (MDA-MB-468) were treated with varying MOI of the EGFP-tagged virus for 5 days, which effectively induced a dose-dependent oncolysis (Figure 3). The median death rate dosage occurs at about MOI 1 for most cell types examined except for the luminal B BT-474 which is approximately at MOI 0.1. These results indicate that recombinant wild-type MV can utilize nectin-4 to target the various clinically relevant breast tumor subtypes and induce a dose-dependent oncolysis.

3.3.2. Immunohistochemistry analysis of nectin-4 expression in breast cancer tissue array correlates with poorer prognosis and advanced stages/malignant phenotypes

To further substantiate and assess the clinical utility of targeting nectin-4 as a marker for breast cancer treatment using oncolytic MV, we examined the expression of nectin-4 in a breast cancer tissue array of 117 patients using immunohistochemistry. As

shown in Supplementary Figure S1A, nectin-4 expression was readily observed in the dissected paraffin-embedded breast tumor biopsies by staining with anti-nectin-4 antibody and the intensity of the staining was used to determine the grading, with 3 being most intense (nectin-4 high) and 0 being the negative (nectin-4 low). Use the pathological grading as reference, the samples were then compared between 'nectin-4 high' (grade 2 – 3) and 'nectin-4 low' (grade 0 – 1). Interestingly, we observed that the 'nectin-4 high' cohort was associated with lower patient survival probability and a lower frequency of recurrence-free survival compared to the 'nectin-4 low' population (Supplementary Figure S1 B and C). In addition, investigation on the association of nectin-4 with breast cancer subtypes and disease progression indicated that 'nectin-4 high' expression had an overall increased frequency in basal-like phenotype (triple-negative typing), advanced tumor grading, and metastasis (Supplementary Figure S1D). Altogether, the above results suggest nectin-4 as a poor prognosis biomarker and an important tumor marker for the difficult-to-treat or advanced stages of breast cancer, and hence a valuable target for therapeutic intervention for nectin-4-targted MV oncolytics.

3.3.3. MV can infect breast cancer xenografts *in vivo* and exhibit oncolytic effect that is dependent on an immune competent host

Based on the above observations that recombinant wild-type MV can utilize nectin-4 to target breast cancer cells and induce oncolysis, we next assessed MV's oncolytic activities *in vivo* in mouse xenograft breast tumor models as proof-of-concept for its potential therapeutic application against breast cancer. Our laboratory previously established MDA-MB-468 xenografts in BALB/c nude mice and treated the tumors with

MV-FLuc via intratumoral (*i.t.*) injection at day 0. As shown in Supplementary Figure S2A, luciferase signals could be readily detected at day 15 post virus injection in the BALB/c nude mice established with MDA-MB-468-derived breast tumor, specifically concentrating on site of the tumor location. In a similar experiment, nonobese diabetic/severe combined immunodeficiency (NOD/SCID) mice bearing TNBC patient-derived xenograft were *i.t.* injected with MV-FLuc, and luciferase activity was monitored over 15 days. As shown in Supplementary Figure S2B, luciferase signals could be detected in the tumors injected with the vector. These results therefore validate MV's targeting ability *in vivo*. However, upon further monitoring and despite MV infection of the nectin-4-positive tumors in the mice, tumor regression was not readily observed. We hypothesized that additional factors or parameters may be necessary for tumor control using the MV treatment, such as using a multiple dose approach, or more importantly, to consider the immune system, which has recently been emphasized as an important arm contributing to the efficacy of oncolytic virotherapy [134]. Furthermore, as tumor regression is best observed under immunocompetent scenario which is more reflective of clinical setting, we then proceeded to evaluate MV's oncolytic potency *in vivo* using syngeneic mouse models.

Syngeneic mouse models have previously been developed in immune competent mice with murine 4T1 [135, 136] and E0771 [137] breast tumors expressing human/foreign proteins. For this purpose, we first established 4T1 and E0771 cells overexpressing human Nectin-4 (4T1.hNectin-4 and E0771.hNectin-4). Both cell lines overexpress nectin-4 on their cell surface (Figure 4A and Figure 5A) and are permissive and susceptible to recombinant wild-type MV-induced infection and oncolysis (Figure 4 B and C, Figure 5 B and C). The 4T1.hNectin-4 and E0771.hNectin-4 cells were then injected subcutaneously

in the mammary fat pad of mice to evaluate MV's oncolytic activity *in vivo*. As shown in Figure 4C, four consecutive doses of MV treatment effectively suppressed 4T1.hNectin-4 tumor growth in the immunocompetent mice compared to the PBS control treatment. Additionally, the MV-treated mice exhibited significantly higher survival compared to mice injected with only PBS control (Figure 4D). Similar results were observed with the E0771.hNectin-4 model, whereby the tumor growth was robustly restricted by six intermittent doses of MV treatment (Figure 5C) and resulted in higher survival compared to the PBS control treatment (Figure 5D). This observation therefore confirms the oncolytic properties of MV in inhibiting tumor growth *in vivo* and suggests the importance of the immune system in MV-associated oncolytic treatment.

Together, these results indicate that recombinant wild-type MV can target to the nectin-4-expressing breast tumor cells *in vitro* and *in vivo* and exhibit oncolytic properties, suggesting MV with wild-type glycoproteins as a potential oncolytic agent for the development of nectin-4-targeting breast cancer treatment.

3.4. Discussion

We have observed and validated that the use of recombinant wild-type MV can efficiently target to the nectin-4 positive breast cancer cells and induce a dose-dependent oncolysis. More specifically, we were able to observe MV infection of the established tumors *in vivo* in both xenografts in immune-deficient and immune-competent mouse models, and additionally, the syngeneic mouse model demonstrated growth inhibition of the breast tumors. Overall, the results presented show a proof-of-concept of using recombinant wild-type MV as an oncolytic agent and its potential clinical applicability for

targeting nectin-4-positive breast cancers. Such analysis provides a foundation for future exploration and development of MV-based oncolytic vectors for virotherapy.

In contrast to the other nectin family members, nectin-4 is mainly found in the placenta with little expression in the airway of normal human tissues [63]. Recent literature suggests that this adhesion molecule plays an important role in cancer progression. The upregulation of nectin-4 was first reported in breast cancer, especially prominent in ductal carcinomas and positively correlates with basal-like markers which often implies poor prognosis [65]. This observation was further supported by a bigger dataset where nectin-4-high triple negative breast cancer patients had shorter metastasis-free survival [138]. Nonetheless, nectin-4 expression is also related to shorter disease-free survival and relapse-free survival in luminal A [139] and luminal B HER2-negative [140] breast cancers, suggesting that nectin-4 could be a prognostic marker and a target for therapeutic intervention of the different breast cancer types. As such, the oncolytic ability of MV described here could serve as a potential future strategy for the treatment of the various types of breast cancers and merits to be further explored in such scenarios.

In summary, the studies presented here establish a foundation for exploring the MV vector as a candidate anticancer therapeutic for targeted treatment against breast cancer. The *in vitro* and *in vivo* evidence for the oncolytic potency of MV vectors against breast adenocarcinoma from this study will also serve as an important basis for preclinical evaluation of such potential therapy.

3.5. Figures, Tables, and Legends

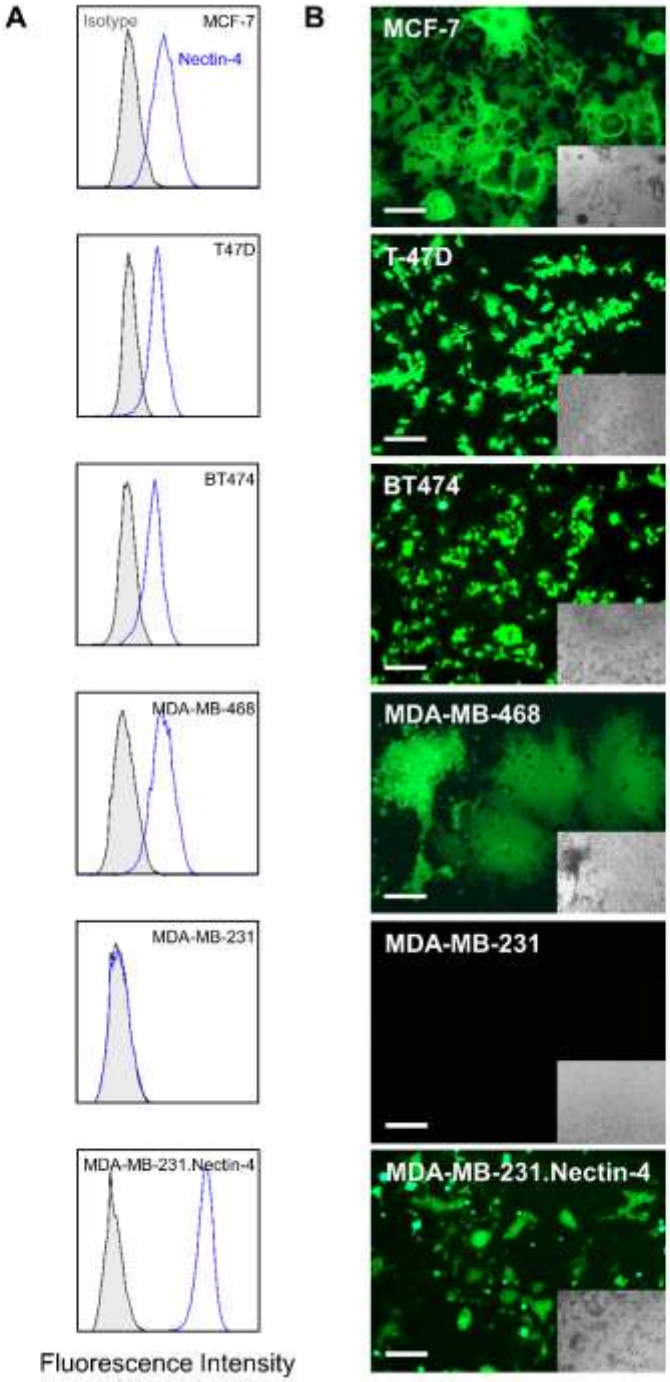

Figure 2. Nectin-4 expression and oncolytic MV infection of human breast cancer cell lines.
A. Flow cytometry analysis of surface nectin-4 expression. Staining with anti-nectin-4 is shown in blue, and isotype control is shown in gray. **B.** Representative micrographs of MV-EGFP infection at 3 dpi (MOI 1). Scale bar = 200 μm. MDA-MB-231 and MDA-MB-231 overexpressing nectin-4 (MDA-MB-231.Nectin-4) serve as negative and positive controls.

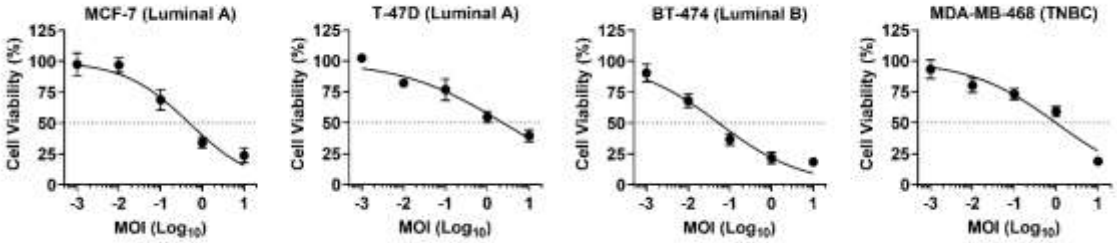

Figure 3. MV infection of breast cancer cell lines.
Oncolytic activity of MV-EGFP (MOI 0.001 – 10) at 5 dpi in luminal A (ER+ PR+ HER2-), luminal B (ER+ PR+ HER2+), and triple negative breast cancer (TNBC; ER- PR- HER2-) cell lines. Data shown are means± SD from three independent experiments.

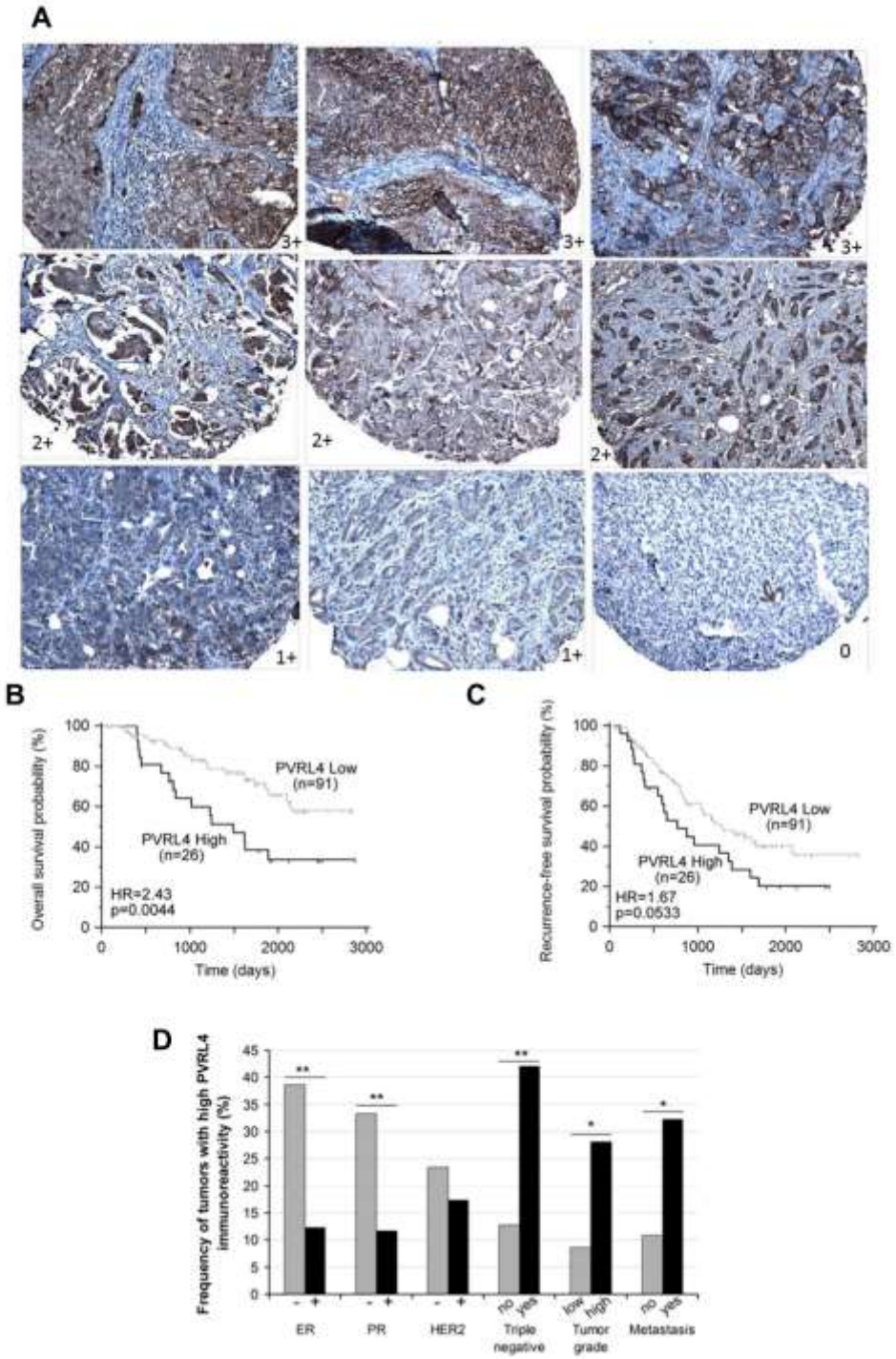

Supplementary Figure S1. Clinical implications of PVRL4/nectin-4 in breast cancer.
A. Representative nectin-4 immunohistochemistry (IHC) staining and grading of breast cancer tissue array. **B.** Overall survival rate and **C.** recurrence-free survival rate of breast cancer patients with high or low PVRL4 expression in the dissected tumor tissues. **D.** Association of PVRL4 with breast cancer subtypes and disease progression. Dataset provided by Drs. Roseline Godbout, John Mackey, and Rong Dong from University of Alberta.

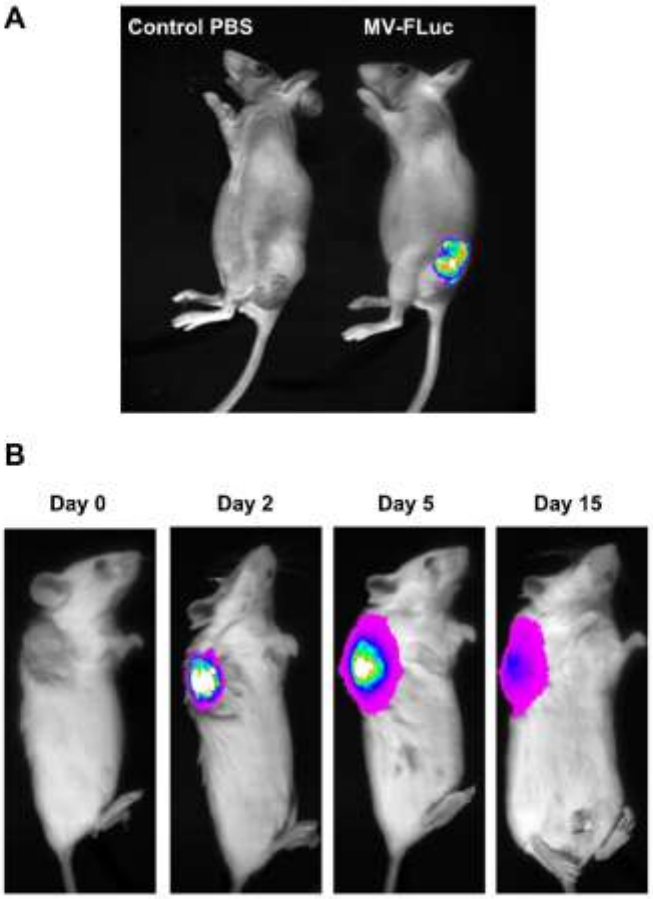

Supplementary Figure S2. MV-FLuc injection in immunodeficient breast tumor models.
A. BALB/c nude mice were injected with MDA-MB-468 cells on the flank, and luciferase-tagged MV vector (MV-FLuc) or PBS control was injected intratumorally. **B.** NOD/SCID mice were injected with patient-derived triple negative on the flank, and MV-FLuc was injected intratumorally. Mice were monitored for luciferase activity at 0, 2, 5, and 15 days post-treatment.

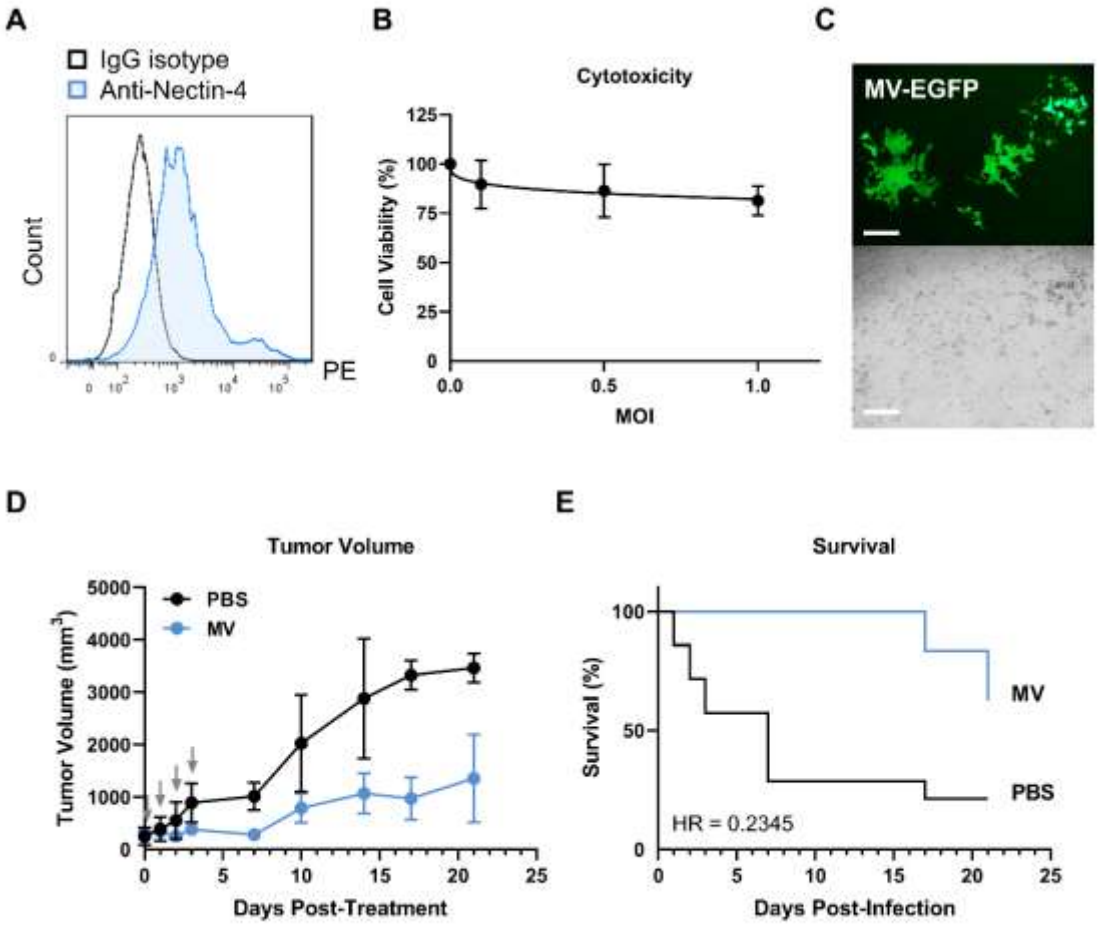

Figure 4. Oncolytic effect of MV in 4T1 syngeneic mouse model.

A. Flow cytometry analysis of surface nectin-4 expression on murine breast cancer cell line 4T1 overexpressing human nectin-4 (4T1.hNectin-4). **B.** Cytotoxicity of MV-EGFP (MOI 0.1, 1, and 5) in 4T1.hNectin-4 at 5 dpi. Data shown are means ± SD from three independent experiments. **C.** Fluorescence microscopy of MV-EGFP infection in 4T1.hNectin-4 cells (MOI 0.5; 2 dpi). **D.** Intratumoral MV treatment of 4T1.hNectin-4 tumors in syngeneic mouse model. Ten days after tumor cell inoculation (2 x 10^6 cells per mouse), mice received intratumoral treatment of PBS (control) or MV (2 x 10^6 $TCID_{50}$ per mouse) for four consecutive days. Tumor volume was measured on the treatment days (indicated by gray arrows) and twice per week afterwards. Tumor volume = (4/3) × π × (L/2) × (W/2) × (D/2). **E.** Kaplan-Meier survival curve. Hazard ratio (HR; MV/PBS) was analyzed by log-rank method.

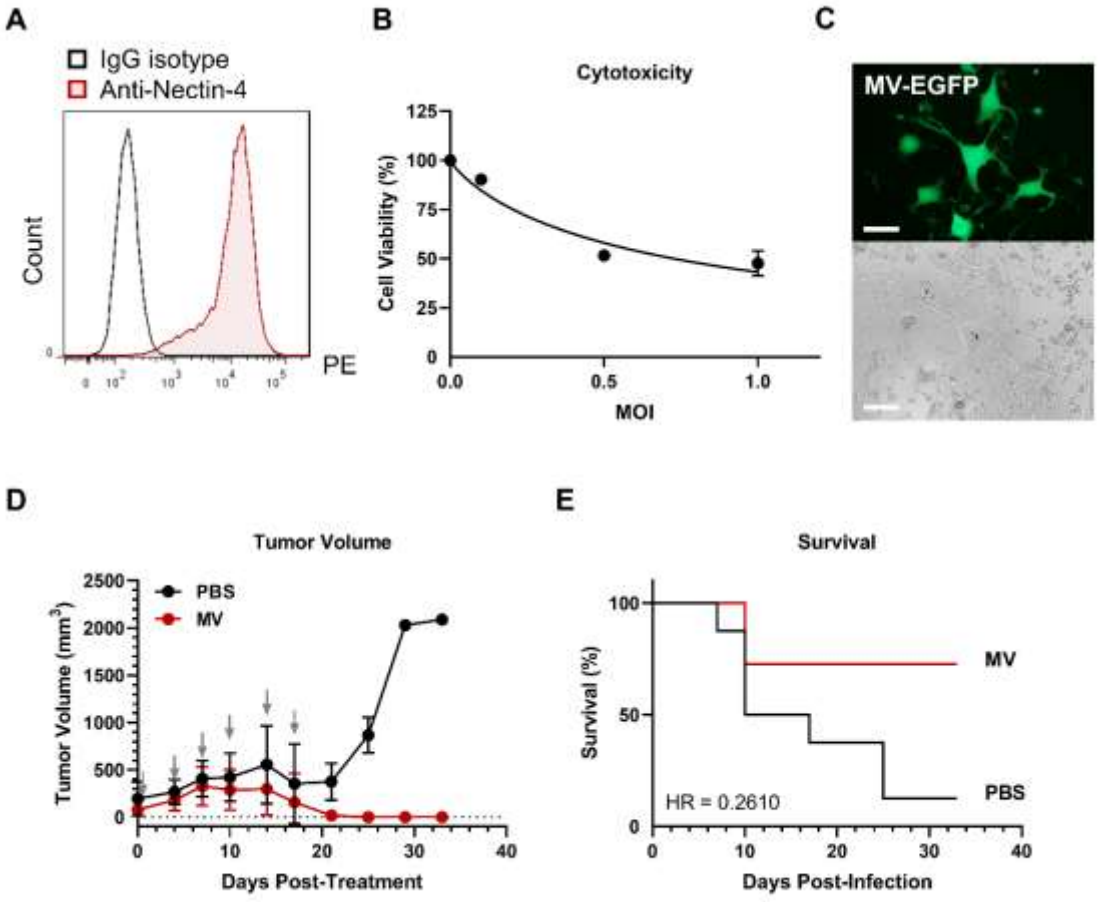

Figure 5. Oncolytic effect of MV in E0771 syngeneic mouse model.

A. Flow cytometry analysis of surface nectin-4 expression on murine breast cancer cell line E0771 overexpressing human nectin-4 (E0771.hNectin-4). **B.** Cytotoxicity of MV-EGFP (MOI 0.1, 1, and 5) in E0771.hNectin-4 at 5 dpi. Data shown are means ± SD from three independent experiments. **C.** Fluorescence microscopy of MV-EGFP infection in E0771.hNectin-4 cells (MOI 1; 5 dpi). **D.** Intratumoral MV treatment of E0771.hNectin-4 tumors in syngeneic mouse model. Seven to fourteen days after tumor cell inoculation (5×10^6 cells per mouse), mice received intratumoral treatment of PBS (control) or MV (5×10^6 $TCID_{50}$ per mouse) twice per week for 3 weeks (indicated by gray arrows). Tumor volume was measured on the twice per week. Tumor volume = $(4/3) \times \pi \times (L/2) \times (W/2) \times (D/2)$. **E.** Kaplan-Meier survival curve. Hazard ratio (HR; MV/PBS) was analyzed by log-rank method.

CHAPTER 4

CHEMOVIROTHERAPEUTIC TREATMENT OF BREAST CANCER CELLS USING CAMPTOTHECIN TO ENHANCE ONCOLYTIC MEASLES VIRUS-MEDIATED KILLING

Adapted from published manuscript with modifications: Tai CJ[1], **Liu CH[1]**, Pan YC, Wong SH, Tai CJ, Richardson CD, Lin LT. *Chemovirotherapeutic Treatment Using Camptothecin Enhances Oncolytic Measles Virus-Mediated Killing of Breast Cancer Cells.* **Sci Rep. 2019 May 1;9(1):6767.**

Author contributions: Conceived and designed the experiments: C.-J.T.[1], C.-H.L.[1], and L.-T.L. Performed the experiments: C.-H.L. and Y.-C.P. Analyzed the data: C.-J.T.[1], C.-H.L.[1], Y.-C.P., S.H.W., C.D.R., and L.-T.L. Wrote and edited the paper: C.-J.T.[1], C.-H.L.[1], S.H.W., C.D.R., and L.-T.L. All authors contributed to reagents/materials/technical support to this study.

4.1. Abstract

Oncolytic virotherapy is a novel treatment strategy for the management of cancers. Although tested in various cancers, including that of the breast, oncolytic viral vectors have had limited efficacy as monotherapy. Improving oncolytic virotherapy through combination therapy with chemotherapeutic drugs is a possible solution. Herein, we consider the use of MV as oncolytic agent and the anticancer drug agent camptothecin or CPT together for a combined chemovirotherapeutic treatment modality against breast cancer cells. Our results showed that a treatment combination using oncolytic MV plus CPT confers increased cytotoxicity to the human breast cancer MCF-7 cells, and that MV combined with a low dose of CPT induced the same treatment efficacy as high-dose CPT. Furthermore, low-dose CPT did not negatively affect MV's early viral entry steps or inhibit the viral replication. In additional experiments, we observed that the co-administration of MV and CPT induced a significant upsurge in apoptotic cell death of breast cancer cells compared to each agent alone. Altogether, our data demonstrate the merit of a novel chemovirotherapeutic approach using oncolytic MV combined with CPT against breast cancer cells, which warrants further exploration as a potential means to enhance the oncolytic activity of MV-based virotherapy.

4.2. Rationale and Aim

In the last decade oncolytic virotherapy, which employs OVs to treat cancer, has emerged as a promising treatment that can selectively target and destroy tumor cells without harming normal cells [73, 141-143]. While most cancer therapies target tumors in a non-specific manner, many OVs have a propensity to replicate in the more favorable

environment found in transformed cells [103], and various forms of OVs including wild-type, laboratory attenuated, and genetically engineered or modified viruses have been in development to treat cancers, including adenocarcinomas of the breast. The recent discovery of nectin-4, a tumor marker that is commonly overexpressed in adenocarcinomas including that of the breast [64-66, 144], as a receptor for MV [23, 24], has sparked an interest to use of this paramyxovirus as an oncolytic agent for treating breast cancer [111]. Similar to other OVs, a substantial hurdle remains in their clinical application with the observed limited efficacy when used in monotherapy [145]. This challenge could potentially be circumvented through the combination of OVs with chemotherapy, which is also referred to as 'chemovirotherapy', as a viable strategy to maximize the oncolytic potency of virotherapeutics [146].

As a natural small molecule isolated from *Camptotheca acuminata* tree bark, CPT is a quinoline alkaloid that exhibits anticancer bioactivity by acting as a DNA topoisomerase I (Topo I) inhibitor [147]. The FDA-approved CPT analogues for chemotherapy, such as irinotecan and topotecan [148], are documented to cause apoptotic cell death of tumor cells [149]. Conversely, MV infection can produce cytopathic effects including inducing the formation of syncytia (multi-nucleated giant cell) and apoptosis [8, 150, 151]. Due to their distinct mechanism of inducing cell death, a combination therapy promoting better tumor cell killing and a reduced risk of developing resistance against the individual agents [152]. As a proof-of-principle for employing such tactic, we examined the treatment effects of a recombinant wild-type MV in conjunction with CPT against breast cancer cells. Specifically, we explored optimal parameters of treatment *in vitro*,

deduced the mechanism of action involved, and illustrate the value of this strategy for future development as a therapeutic modality for clinical management of breast cancer.

4.3. Results

4.3.1. Cytotoxic effect of oncolytic MV and the chemotherapeutic drug CPT as separate agents against human breast cancer MCF-7 cells

As our first aim, we determined the individual impact of oncolytic MV and CPT in killing the human breast cancer cells MCF-7. To this end, a recombinant EGFP reporter-tagged MV at various MOI and different concentrations of CPT were administered on the seeded cells. The MCF-7 breast adenocarcinoma cell line is known to express nectin-4 on the surface of the cell, thereby making them particularly permissive to infection by MV [24]. As shown in Figure 6A and B, both CPT and oncolytic MV reduced the MCF-7 cell viability in a dose-dependent fashion with either a 3- or 5-day treatment. Over 50 % decrease in the viability of MCF-7 breast cancer cells was observed with CPT treatment at concentrations of 50 nM and above (CC_{50} = 381 nM for 3 days of treatment and 58.5 nM for 5 days of treatment) or with infection by oncolytic MV at a MOI above 0.1. Analysis using LDH release assay for evaluating cell death revealed similar results (Supplementary Figure S3). On the basis of these observations, we therefore chose to employ oncolytic MV at a MOI of 0.1 and CPT at concentrations ≤ 50 nM (10, 30, and 50 nM) for the remainder experiments in the study to examine their combined treatment effects.

4.3.2. CPT and oncolytic MV in combination treatments exert enhanced cytotoxicity in breast cancer MCF-7 cells

Following determining their individual killing profile of the MCF-7 cells, our next goal was to examine the impact of combined treatments using CPT and oncolytic MV through three types of treatment approaches to determine the most effective treatment modality (see Figure 7A for a schematic diagram). These included 'drug sensitization', in which CPT is used to pre-treat the cells before initiating MV infection. The second method is 'viral sensitization', whereby MV is first used to establish infection in the cells prior to starting CPT treatment. Lastly, the third approach is the 'co-treatment' model, wherein oncolytic MV and CPT are simultaneously added to the target cells. Chou-Talalay method [153] for evaluating treatment synergy was employed to assess the synergy level of each combination model, where the combination index or 'CI' values quantitatively defined synergistic (CI < 1), additive (CI = 1) and antagonistic (CI > 1) effects. CPT at various doses was used in combination with and their associated cytotoxicity was then measured. Data indicated that the co-treatment approach with MV at MOI 0.1 produced the greatest cytotoxic effect to MCF-7 cells across the tested concentrations of CPT (10 nM [Figure 7B], 30 nM [Figure 7C], and 50 nM [Figure 7D]). This was reflected by the reduced number of viable cells to 44.45 % (at 10 nM), 34.87 % (at 30 nM), and 30.54 % (at 50 nM) through respective concentrations of CPT co-treatment in combination with MV (Figure 7 B – D). In addition, 20 ~ 30 % more cell death was observed with the co-treatment approach compared to CPT or MV treatment as single agents. These results were corroborated by the LDH release assay (Supplementary Figure S4A) and in microscopy wherein enhanced cytotoxic effects were observed (Supplementary Figure S4B). Accordingly, CPT co-treatment (10, 30, and 50 nM) exhibited the lowest CI values which reflected synergy (0.11, 0.21, and 0.31), respectively (Figure 7E), indicating that the oncolytic activity was

synergistic against the breast cancer MCF-7 cells when MV and CPT were employed using the co-treatment model. In contrast, the CI values in the other two treatment approaches ('drug sensitization' and 'viral sensitization') revealed antagonistic effect, irrespective of the concentration evaluated for CPT (Figure 7 B – E).

4.3.3. CPT does not exhibit antiviral activity against oncolytic MV infection

To investigate possible antagonistic interactions from the co-addition of CPT and oncolytic MV, an analysis was carried to determine whether CPT treatment inhibits the early steps of MV viral entry into the breast cancer MCF-7 cells. Specifically, we examined CPT's effect on the free viral particles of oncolytic MV, their binding to host cell surface, and the post-attachment entry/fusion events (Figure 8A). For this purpose, CPT was used to treat the virus and/or cells at the specific steps of the viral entry, and the emitted EGFP fluorescence, which is expressed through viral replication upon successful establishment of the infection, was determined in subsequent cell incubation. As depicted in Figure 8 B – D, CPT treatments, for all concentrations tested, did significantly impede the early infection stages of the oncolytic MV. In contrast, the natural phytobioactive small molecule punicalagin (PUG), which was previously shown to block MV's viral entry [154] and used here as a positive control, effectively reduced the infectivity of MV. These observations indicate that CPT exhibits little or no impact on cell-free particles of oncolytic MV and its early viral entry steps into the MCF-7 cells. Other potential antiviral effects were further excluded when a time-of-addition assay was carried out for CPT treatment, by specifically adding CPT before, during, and subsequent to oncolytic MV infection (Figure 9A). Similar to the above observations, addition of CPT at various times of the viral infection (Figure 9

B – D) had little effect on the infectivity from the oncolytic MV, whereas the positive control IFN-α effectively reduced the viral infection. Likewise, CPT treatments at from the time-frame of 24 h prior to the MV challenge to immediately after the viral infection did not affect the viral titers obtained at the experimental endpoint (Figure 9E). These results therefore suggest that treatment with CPT, at the doses used in this study for combination treatment analysis, induces no significant antiviral effect nor interfere with the infection by the oncolytic MV.

4.3.4. Co-treatment combination of CPT and oncolytic MV in breast cancer MCF-7 cells induces sub-G1 cell cycle arrest and apoptosis

Following the above experiments, we next studied the mechanistic basis of the synergistic oncolytic impact produced from the oncolytic MV-CPT combination. Specifically, flow cytometry was used to analyze how the cell cycle of the breast cancer MCF-7 cells is affected by these two agents. Data from Figure 10A indicated that compared with untreated cells, adding just the oncolytic virus resulted in augmented number of sub-G1 cells (from 0 % to 25 %), while CPT alone and at all three tested concentrations (10, 30, and 50 nM) induced a G2/M cell cycle arrest that was dose-dependent. On the other hand, compared with the mono-treatment with each agent, co-treatment of oncolytic MV and CPT in combination significantly increased the cell population in sub-G1 regardless of the concentration of CPT used, and this effect was accompanied by a corresponding decrease in the G1 and G2 populations (Figure 10A). This observation of an increase in the sub-G1 population is indicative of elevated number of apoptotic cells, which was confirmed by flow cytometry analysis of double staining using Annexin V/PI, whereby the

apoptotic cell population in oncolytic MV treatment alone (~ 25 %) and CPT treatment alone (~ 13 %) rose to 40 – 60 % in the combined treatment with both agents (Figure 10B).

To further confirm that the combined treatment using oncolytic MV and CPT on the MCF-7 breast cancer cells can enhance cellular apoptosis, we subsequently analyzed the cleavage of the nuclear enzyme PARP, which is a hallmark of apoptosis [155], using Western blotting. In agreement with the Annexin V/PI double staining, the level of PARP in cleaved form was observed to be significantly increased in the cells treated with the co-treatment of oncolytic virus and CPT (Figure 11A), and the increase in the amount of cleaved PARP was dose-dependent over the range of CPT concentrations used (10, 30, and 50 nM) (Figure 11B). Together, these results showed that the treatment combination of MV and CPT produced a significantly enhanced oncolytic effect that was synergistic on the MCF-7 cells, and this outcome was at least partly due to the increase in the level of apoptosis.

4.3.5. Combination treatment using CPT and oncolytic MV also produces enhanced cytotoxicity on T-47D breast tumor cells

Lastly, we examined whether the combination using oncolytic MV and CPT can be applied to other breast cancer cells and is not restricted to only the MCF-7, the same method and combination treatment approach (described in Figure 6 and Figure 7) was used to test on the human breast adenocarcinoma T-47D cells. These tumor cells have previously been reported to be susceptible to MV infection [24]. We observed that similar to the MCF-7 cell, the T-47D cells are sensitive to treatments using CPT (10 – 50 nM) and oncolytic MV (MOI 0.01 – 10) as single agents, whereby a concentration of 50 nM CPT and MOI 0.1 of

MV effectively decreased the cell viability to near or below 50 % of the cell viability (Figure 12 A and B). Even more importantly, combining CPT (10, 30, and 50 nM) with oncolytic MV (MOI 0.1) using the co-treatment approach caused significantly greater cell death than the use of each agent alone (Figure 12 C). Analogous results were also obtained with the LDH release test for cytotoxicity (Supplementary Figure S5).

Altogether, the culminated data provide evidence that the chemotherapeutic CPT can be used with oncolytic MV in a co-treatment type of combination to enhance the oncolytic killing of the human breast cancer cells.

4.4. Discussion

To overcome the limitations of OVs as monotherapy, the strategy of combining OVs with chemotherapeutic agents has been investigated, grounded on the idea that these two agents may potentiate or act in synergism with each other [156, 157] to improve treatment outcomes. However, the compatibility and synergy of these two therapeutic approaches may depend on the context of treatment [158]. Herein, we showed for the first time that MV combined with low concentrations of CPT can enhance the lethality of human breast cancer cells. When these cells were co-treated with both agents, we observed an enhanced killing effect that was synergistic. Mechanistically, the synergistic outcome from the MV plus CPT combination led to an augmented accumulation of cell populations in sub-G1, resulting in enhancement of cell apoptosis, which is evident by the increase in the level of PARP cleavage (Figure 10 and Figure 11). In view of the fact that treatment with MV infection and CPT individually can ultimately lead to the induction of apoptosis [8, 149-151], such observation is largely anticipated.

Incidentally, it is known that MV infection can induce autophagy as a pro-viral physiological process, whereby continuous activation of autophagy can delay cell apoptosis and promote the transmission of MV between cells or the formation of syncytia before ultimately culminating in cell death [159]. Alternatively, CPT is reported to trigger both autophagy as well as apoptosis [160], and low doses of the drug (≤ 50 nM) can induce autophagy and premature senescence [161]. Since MV and CPT can both induce autophagy at the concentrations used in this study, the combination of these two agents may amplify the process of autophagy, thus facilitating the spread of the virus and concomitantly enhancing the sensitivity of the breast adenocarcinoma cells to impact from the ensuing apoptosis. In fact, preliminary experiments have shown that treatment with CPT or the oncolytic MV as individual agent alone at 24 h as well as 48 h after addition can induce the autophagy marker LC3 (‘LC3II’) (Supplementary Figure S6A). Interestingly, after 48 h of treatment, we observed an accompanying decrease in LC3II as the concentration of CPT increased in combined treatment with the oncolytic virus (Supplementary Figure S6A). This phenomenon was not due to the inhibition of autophagy, but instead due to its enhancement ("faster turnover"). Specifically, when autophagic flux was inhibited using the lysosomal inhibitor bafilomycin, there was a significant change in LC3II accumulation in the CPT-treated groups, with or without co-administration of MV (Supplementary Figure S6B), as opposed to using MV only. The potentiation effect of CPT on the inefficient autophagic flux triggered by MV may lead to its perturbation, which has been considered to promote apoptosis [162]. Additional studies are needed to clarify this observation and to tease out the nuances of virus- and drug-induced autophagy prior to

cellular commitment to apoptosis in the enhanced cytotoxic outcome of CPT combined with oncolytic MV.

Overall, the data presented indicate that oncolytic MV combined with CPT chemotherapy is a potential treatment modality that exerts synergistic killing of the breast tumor cells. Besides the fact that the chemotherapeutic drug itself does not induce antiviral effect against the oncolytic virus, the boosted efficacy from the combination also led to a reduction in each agent's effective dose required. Specifically, our results showed that CPT at low concentrations (50 nM and below) in conjunction with a low dose (MOI 0.1) of MV has the same treatment impact on breast cancer cells as high doses of each agent individually (CPT at 100 nM and MV at MOI 3). This synergistic effect can potentially reduce the toxicity associated with each agent [152], including the gastrointestinal toxicity and bone marrow suppression described for treatment using CPT as well as the associated derivatives including irinotecan [163] and topotecan [164]. To summarize, our observations in this study highlight the potential of the chemovirotherapeutic approach, especially in the context of employing MV-based oncolytics. Thus, oncolytic MV plus CPT combination therapy merits to be further explored and developed for breast cancer management.

4.5. Acknowledgements

The authors would like to thank Shun-Pang Chang, Yi-Chun Su, and Alagie Jassey for technical support. C.-H.L.[#] is a recipient of the Canadian Network on Hepatitis C (CanHepC) PhD Fellowship. This study was supported in part by funding from Taipei Medical University Hospital (105TMU-TMUH-11 to C.-J.T.[#] and L.-T.L.), the Aim for the

Top University Project–Cancer Translational Center of Taipei Medical University (TMUTOP103005-4 to L.-T.L.), and the Ministry of Science and Technology of Taiwan (MOST107-2320-B-038-034-MY3 to L.-T.L.).

4.6. Figures, Tables, and Legends

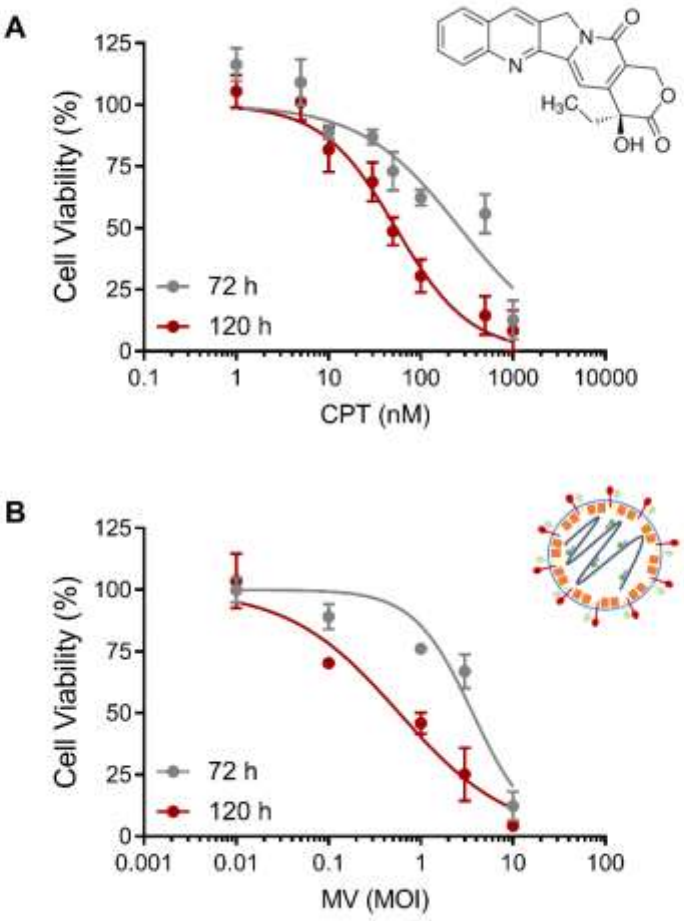

Figure 6. Camptothecin (CPT) and oncolytic MV are cytotoxic against human MCF-7 breast cancer cells.

MCF-7 cells were treated with **A.** CPT (1 – 1000 nM) or **B.** MV (MOI 0.01 – 10) for 3 or 5 days. Cell viability was analyzed by MTT assay. All data shown are means ± SD from three independent experiments. Adapted from Tai et al. Sci Rep. 2019 May 1;9(1):6767.

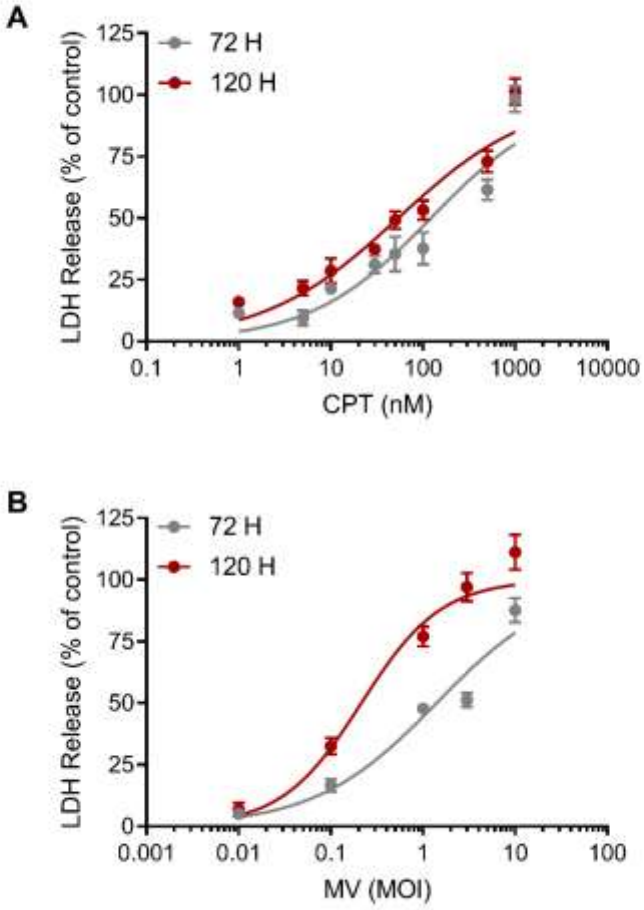

Supplementary Figure S3. Cytotoxicity of CPT and oncolytic MV on human MCF-7 breast cancer cells determined by LDH release assay.

MCF-7 cells were **A.** treated with CPT (1 – 1000 nM) or **B.** infected with MV (MOI 0.01 – 10) for 3 or 5 days and analyzed with LDH cytotoxicity detection kit. DMSO = 0.1 %. All data shown are means ± SD from three independent experiments; **P* < 0.05 compared to Mock treatment. Adapted from Tai et al. Sci Rep. 2019 May 1;9(1):6767.

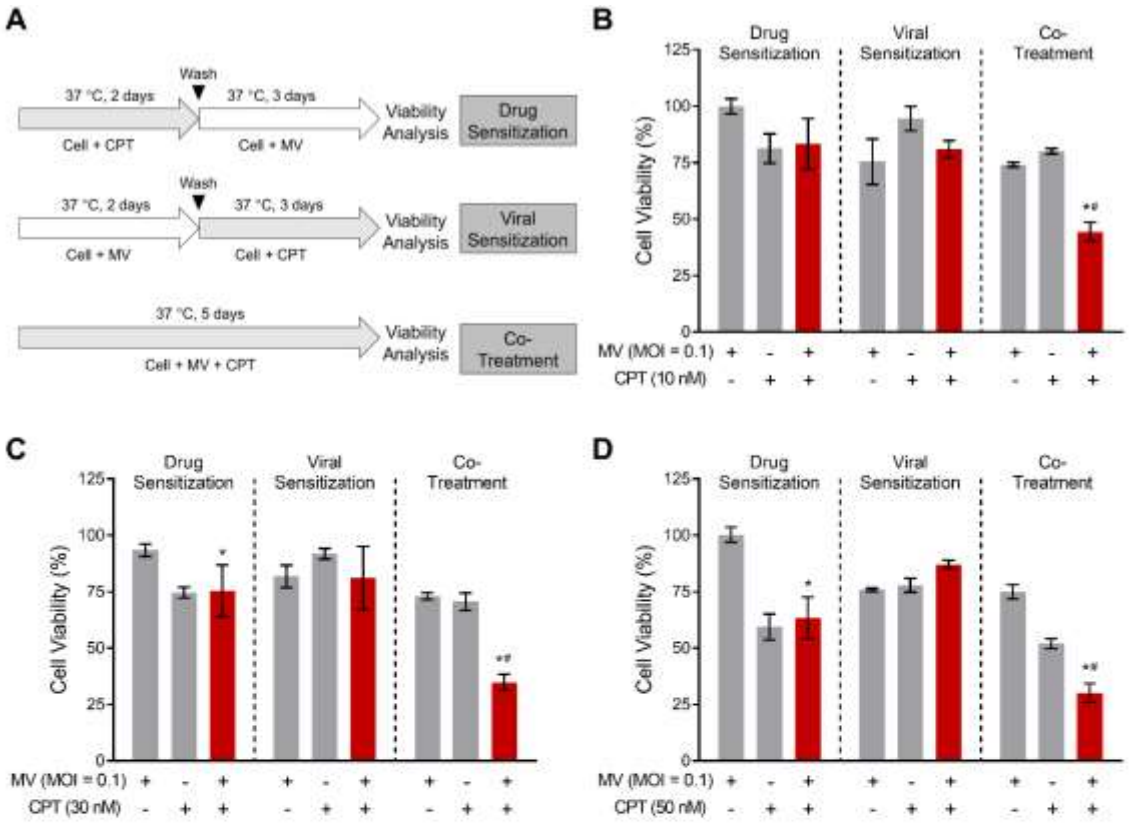

E

	MV (MOI = 0.1) + CPT (10 nM)		
	Drug sensitization	Viral sensitization	Co-treatment
CI[1]	1.34	1.66	0.11
Combination effect	Antagonism	Antagonism	Synergism
	MV (MOI = 0.1) + CPT (30 nM)		
	Drug sensitization	Viral sensitization	Co-treatment
CI[1]	1.75	2.02	0.21
Combination effect	Antagonism	Antagonism	Synergism
	MV (MOI = 0.1) + CPT (50 nM)		
	Drug sensitization	Viral sensitization	Co-treatment
CI[1]	1.2	5.12	0.31
Combination effect	Antagonism	Antagonism	Synergism
[1]Combination index (CI < 1: synergism; CI = 1: additive effect; CI > 1: antagonism)			

Figure 7. Co-treatment of MV plus CPT exhibits enhanced anticancer activity against human MCF-7 breast cancer cells.

A. Schematic representations of the different treatment models. **B** – **D.** MCF-7 cells were treated with MV (MOI 0.1) and/or **B.** 10 nM, **C.** 30 nM, **D.** 50 nM of CPT in different models (drug sensitization, viral sensitization, and co-treatment), following which cell viability was determined by MTT assay. **E.** The CI value of combination models were measured by Chou-Talalay method where CI value quantitatively defines synergism (CI < 1), additive effect (CI = 1) and antagonism (CI > 1). All data shown are means ± SD from three independent experiments; *P < 0.05 compared to MV treatment, and $^{\#}P$ < 0.05 compared to CPT treatment. Adapted from Tai et al. Sci Rep. 2019 May 1;9(1):6767.

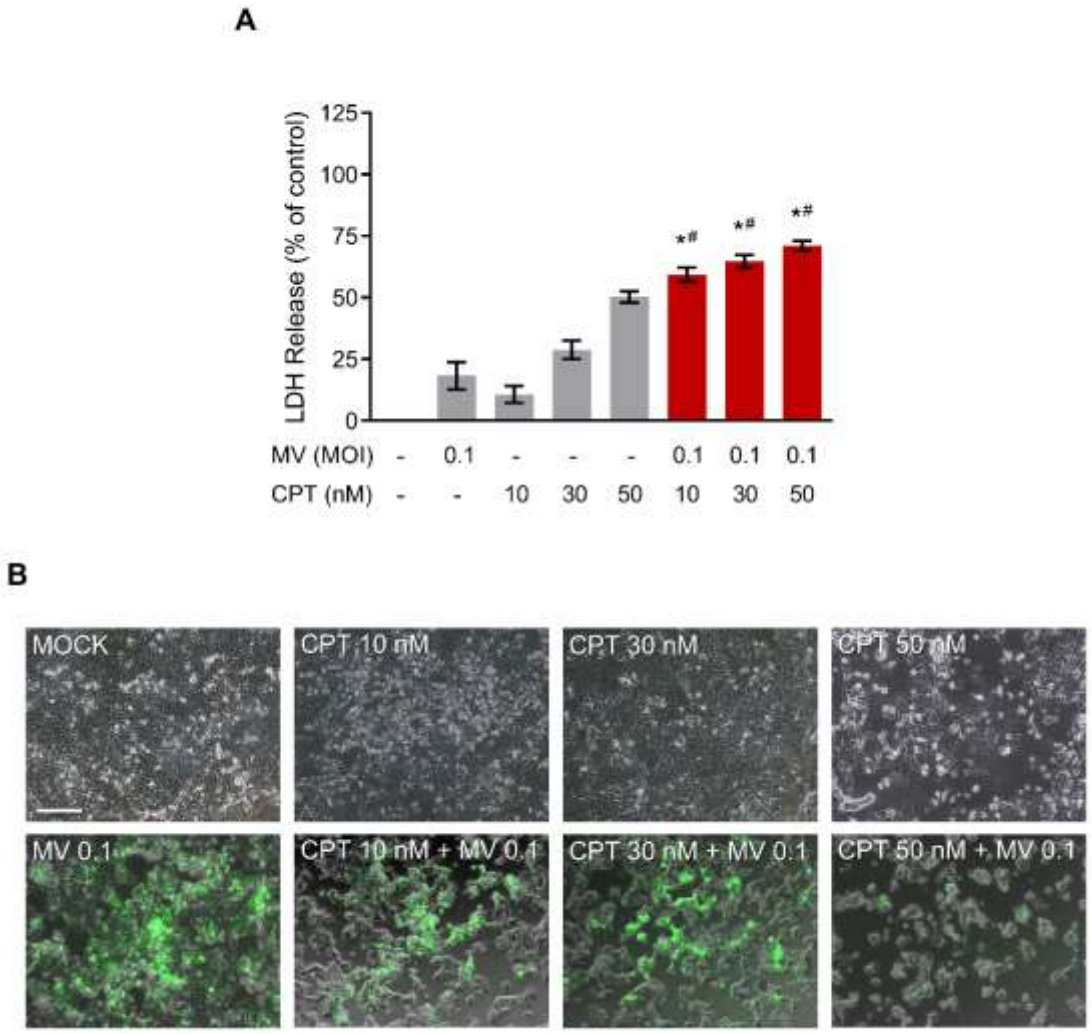

Supplementary Figure S4. Effect of MV and CPT co-treatment on human MCF-7 breast cancer cells. MCF-7 cells were treated with MV (MOI 0.1) and/or CPT (10, 30, and 50 nM) using the co-treatment model described in the text. Cell viability was then determined by **A.** LDH release assay, and **B.** cell morphology was observed by microscopy. Data shown in **A** are means ± SD from three independent experiments; $^{*}P < 0.05$ compared to MV treatment, and $^{\#}P < 0.05$ compared to CPT treatment. Representative micrographs in **B** are displayed in overlaid images of bright field (phase) with the corresponding dark field (fluorescence) pictures. Scale bar = 100 μm. Adapted from Tai et al. Sci Rep. 2019 May 1;9(1):6767.

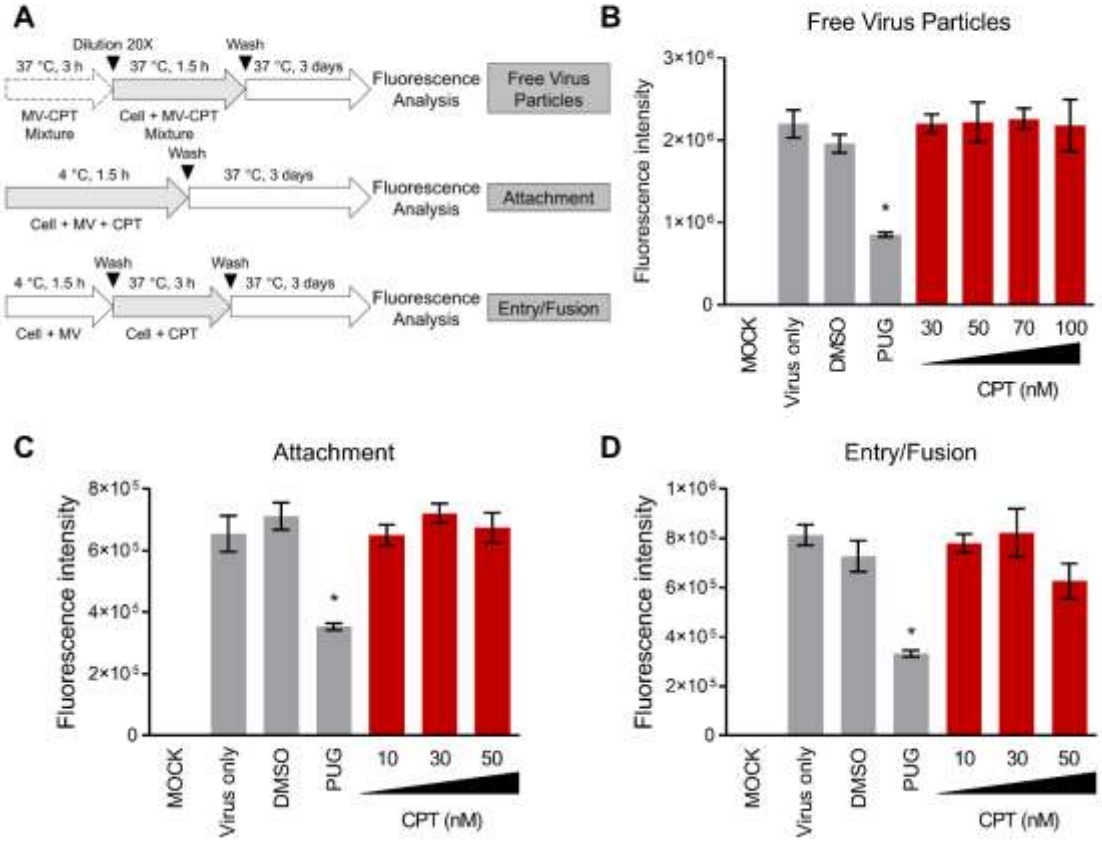

Figure 8. CPT treatment does not influence the viral entry steps of the oncolytic MV.
A. Schematic representations of synchronized infection analysis on early viral entry. **B.** CPT's effect on free MV particles. **C.** CPT's effect on MV attachment. **D.** CPT's effect on MV entry/fusion. For all experiments, final MV MOI was 0.1, 0.1 % DMSO was included as negative control, and PUG = 50 μM was included as positive control treatment in each condition. All data shown are means ± SD from three independent experiments; **P* < 0.05 compared to Virus Only treatment. Adapted from Tai et al. Sci Rep. 2019 May 1;9(1):6767.

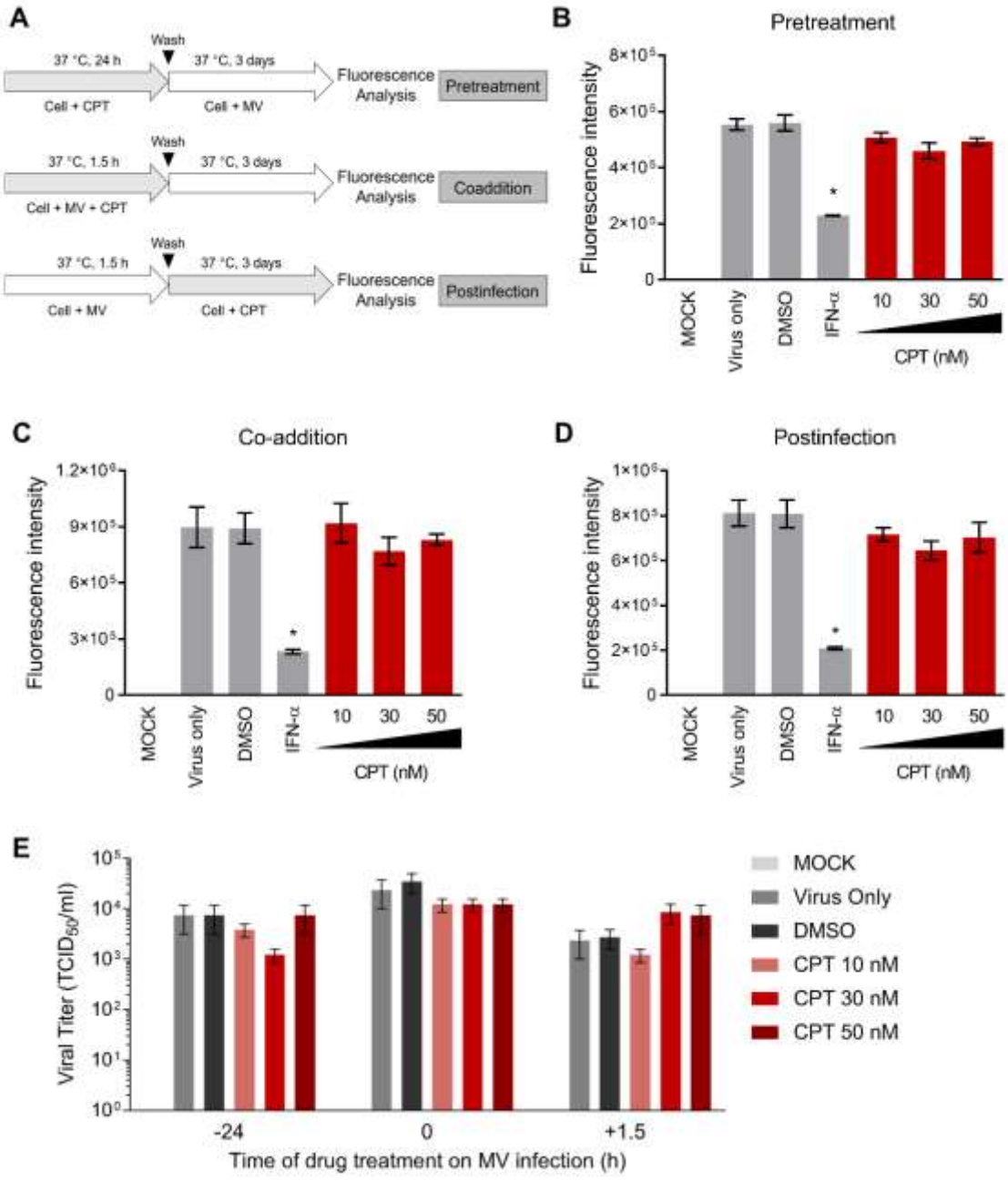

Figure 9. CPT treatment neither enhances nor exerts antiviral activity against MV infection.
A. Schematic representations of the time-of-drug-addition analysis on CPT treatment against MV infection. **B.** Pretreatment effect of CPT on MCF-7 cells before MV infection. **C.** Co-addition treatment effect of CPT on MV infection of MCF-7 cells. **D.** Post-infection treatment effect of CPT on MCF-7 cells immediately after MV infection. Results were obtained after 3 days of incubation. **E.** Viral titer readouts of CPT treatment at different time-points of MV infection as in **B** – **D**. For all experiments, MV infection was performed at MOI 0.1, 0.1 % DMSO was included as negative control, and IFN-α (1,000 IU/ml) was included as positive control treatment where indicated. All data shown are means ± SD from three independent experiments; **P* < 0.05 compared to Virus Only treatment. Adapted from Tai et al. Sci Rep. 2019 May 1;9(1):6767.

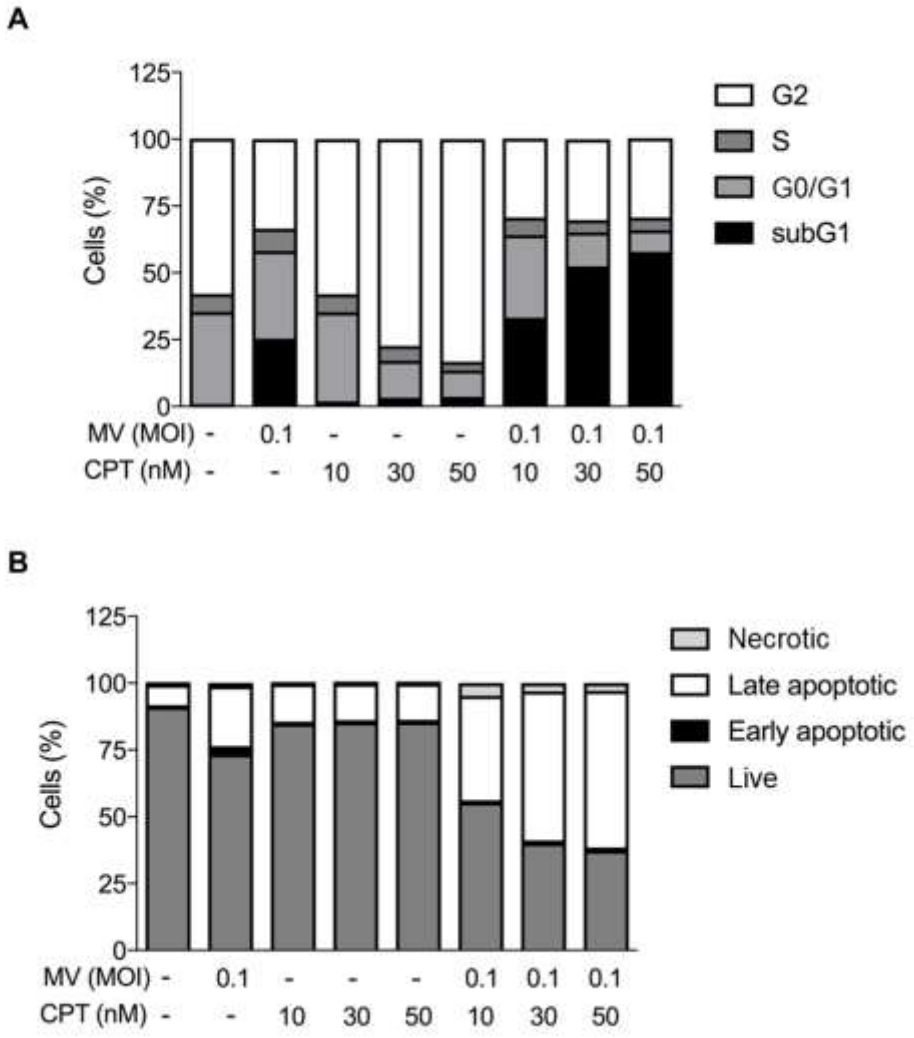

Figure 10. Oncolytic MV and CPT combinatorial treatment causes cell cycle arrest and induction of apoptosis in human MCF-7 breast cancer cells.

A. Flow cytometric cell cycle assay was performed using PI staining on MCF-7 cells following 5 days of treatment with CPT and MV in co-treatment model. **B.** Flow cytometric double stain assay was performed using PI and Annexin V (APC conjugated) staining on MCF-7 cells following 5 days of treatment with CPT and MV in co-treatment model. Percentage of cells was determined by Beckman Cytomics FC500 Flow Cytometry CXP analysis. Data shown are means from three independent experiments. Adapted from Tai et al. Sci Rep. 2019 May 1;9(1):6767.

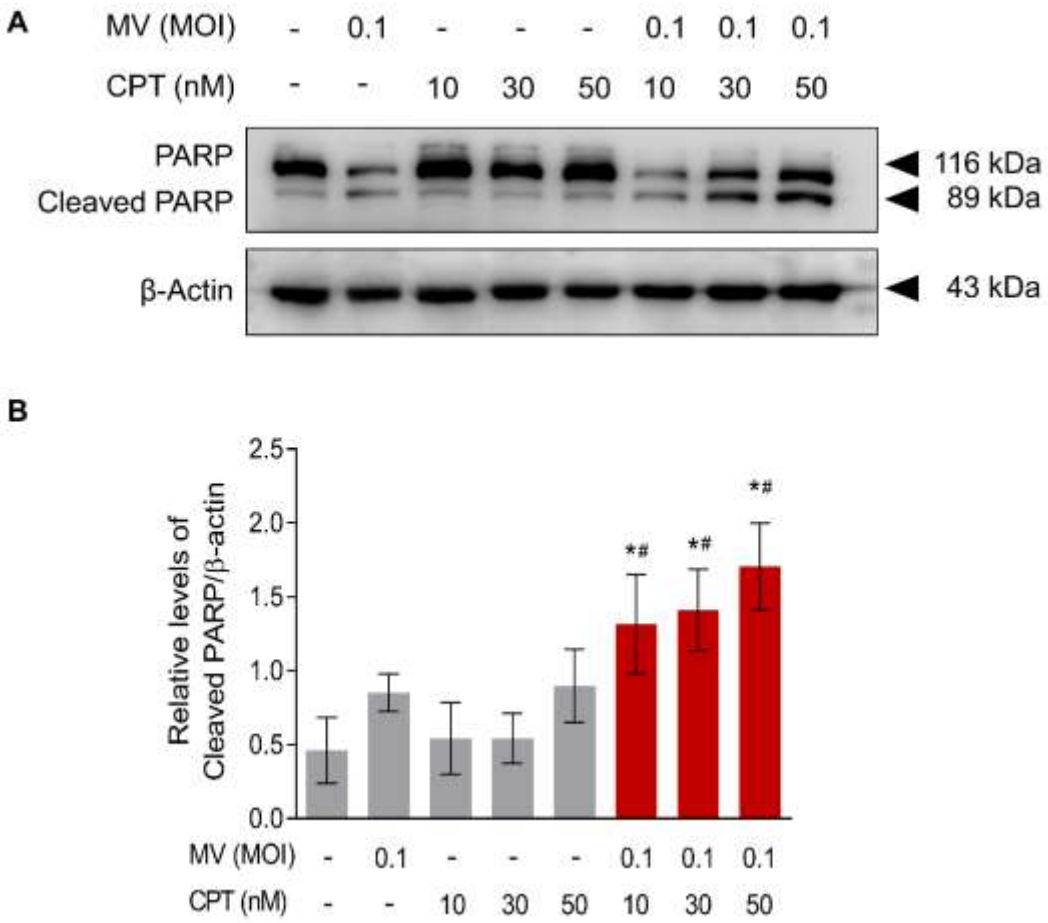

Figure 11. Combinatorial treatment of oncolytic MV with CPT induces apoptosis via PARP cleavage. **A.** Western blot analysis of PARP expression from MCF-7 cells co-treated with CPT and MV for 5 days. **B.** Quantitation of the level of cleaved PARP from **A**. The representative Western blot and average quantitative data (means ± SD) shown are from three independent experiments; $^{*}P < 0.05$ compared to MV treatment and $^{\#}P < 0.05$ compared to CPT treatment at the same concentration. Adapted from Tai et al. Sci Rep. 2019 May 1;9(1):6767.

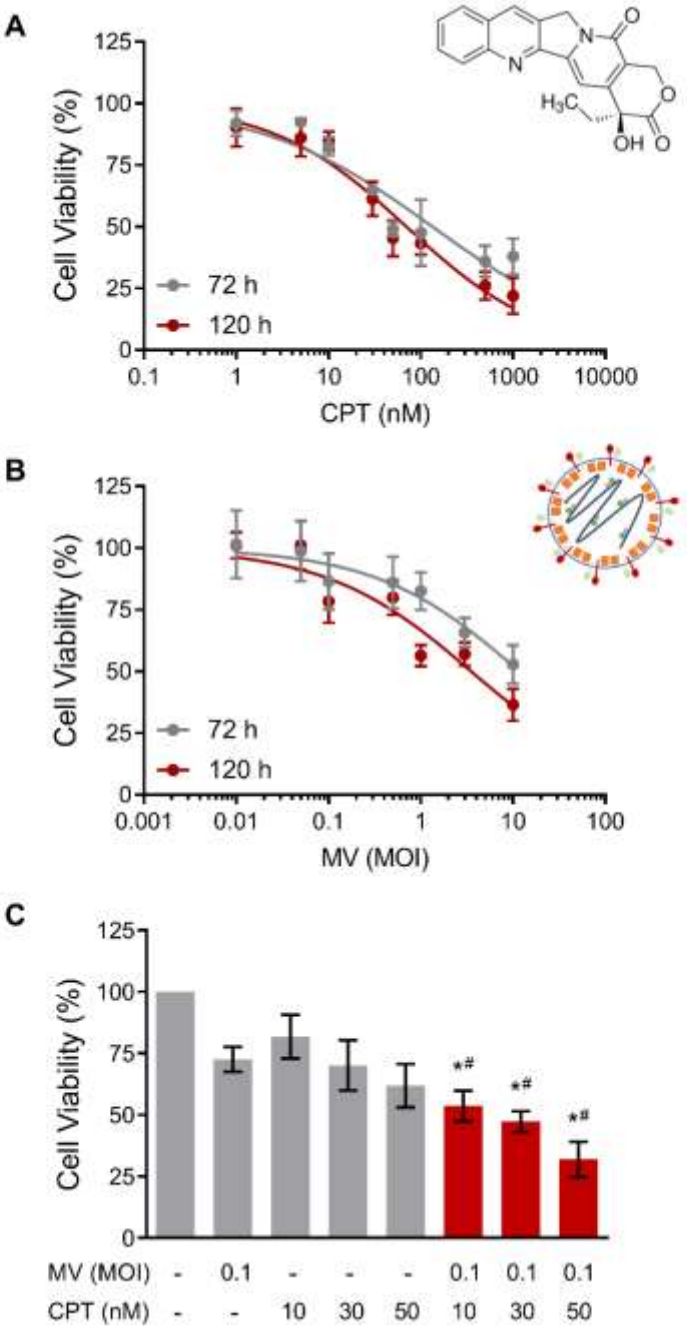

Figure 12. CPT and oncolytic MV are cytotoxic against human T-47D breast cancer cells and induce enhanced cell death in combination using the co-treatment model.

T-47D cells were **A.** treated with CPT (1 – 1000 nM) or **B.** infected with MV (MOI 0.01 – 10) for 3 or 5 days. Cell viability was analyzed by MTT assay; DMSO = 0.1 %. Data shown are means ± SD (*$P < 0.05$ compared to Mock treatment) from three independent experiments. **C.** In the co-treatment model, T-47D cells were treated with MV (MOI 0.1) and CPT (10, 30, and 50 nM). Data shown are means ± SD from three independent experiments; *$P < 0.05$ compared to MV treatment, and $^{\#}P < 0.05$ compared to CPT treatment of the same concentration. Adapted from Tai et al. Sci Rep. 2019 May 1;9(1):6767.

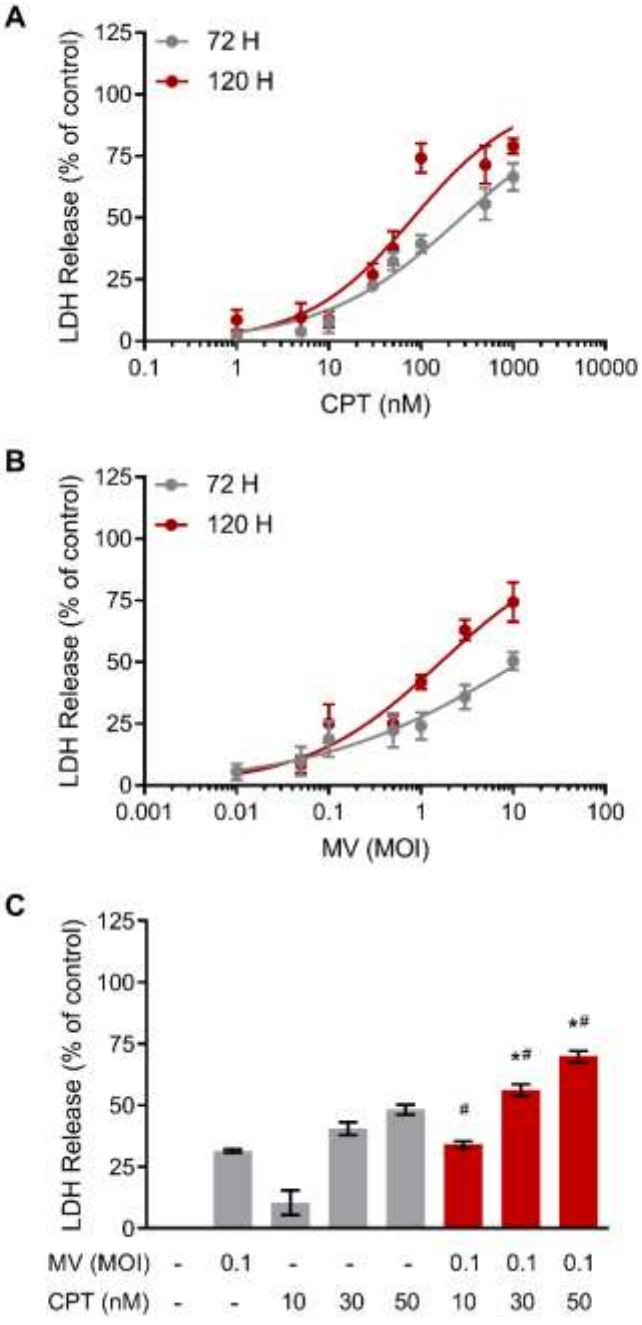

Supplementary Figure S5. Cytotoxicity of CPT and oncolytic MV on human T-47D breast cancer cells determined by LDH release assay.

T-47D cells were **A.** treated with CPT (1 – 1000 nM) or **B.** infected with MV (MOI 0.01 – 10) for 3 or 5 days before analysis by LDH release assay; DMSO = 0.1 %. Data shown are mean ± SEM from three independent experiments; **P* < 0.05 compared to Mock treatment. **C.** In the co-treatment model, T-47D cells were treated with MV (MOI 0.1) and CPT (10, 30, and 50 nM) before LDH release was measured. Data shown are means ± SD from three independent experiments; **P* < 0.05 compared to MV treatment, and $^{\#}P < 0.05$ compared to CPT treatment. Adapted from Tai et al. Sci Rep. 2019 May 1;9(1):6767.

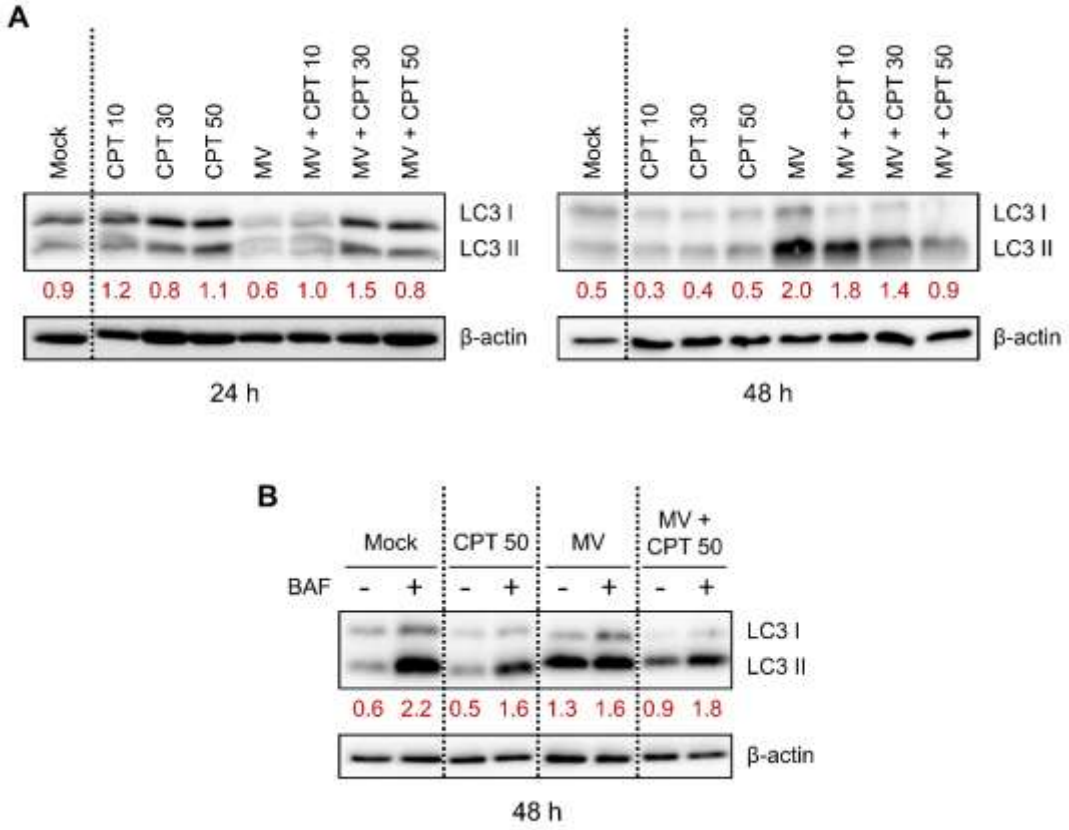

Supplementary Figure S6. Influence of MV and CPT co-treatment on autophagy.
MCF-7 cells were treated with MV (MOI 0.1) and/or CPT (10, 30, and 50 nM) using the co-treatment model. **A.** After 24 or 48 h, cells were harvested and analyzed with Western immunoblotting as described in the text. **B.** Cells were treated with bafilomycin A1 (BAF) 4 h before harvesting at 48 h. Antibodies were used to probe LC3 and β-actin. LC3 II signals were quantified and compared against the β-actin loading control using densitometry analysis. Adapted from Tai et al. Sci Rep. 2019 May 1;9(1):6767.

CHAPTER 5

POTENTIATING ONCOLYTIC MEASLES VIROTHERAPY AGAINST BREAST CANCER CELLS USING URSOLIC ACID AND ITS NANOPARTICLES

Adapted from published manuscript with modifications: **Liu CH**, Wong SH, Tai CJ, Tai CJ, Pan YC, Hsu HY, Richardson CD, and Lin LT. *Ursolic Acid and its Nanoparticles are Potentiators of Oncolytic Measles Virotherapy against Breast Cancer Cells*. **Cancers (Basel). 2021 Jan 4;13(1):136.**

Author contributions: Conceptualization, C.-H.L. and L.-T.L.; methodology, C.-H.L. and L.-T.L.; formal analysis, C.-H.L., C.-J.T. (Chen-Jei Tai), C.-J.T. (Cheng-Jeng Tai), Y.-C.P., H.-Y.H., C.D.R. and L.-T.L.; investigation, C.-H.L. and Y.-C.P.; resources, L.-T.L.; writing—original draft preparation, C.-H.L., S.H.W. and Y.-C.P.; writing—review and editing, C.-H.L., S.H.W. and L.-T.L.; supervision, L.-T.L.; funding acquisition, L.-T.L. All authors have read and agreed to the published version of the manuscript.

5.1. Abstract

OV and the phytochemical UA are two effective drug candidates for the treatment of breast cancer, the most common cancer in women worldwide. However, as single agents, the clinical efficacy of OV and UA is limited. As a common strategy to improve the efficacy of single-agent anticancer agents, we investigated a chemovirotherapeutic approach consisting of oncolytic measles (MV) targeting the breast tumor marker nectin-4 and the anticancer agent UA for the treatment of breast cancer. Our results showed that *in vitro* combination treatment with UA synergistically enhanced the killing of the MCF-7 human breast cancer cells by oncolytic MV, while UA did not interfere with the different steps of viral infection. Mechanistic studies showed that the synergistic effect of the combination treatment was mediated by the enhanced effect of UA on the MV-mediated apoptotic killing. To circumvent the poor solubility and bioavailability of UA and to improve its clinical applicability, we further developed UA-derived nanoparticles (UA-NPs) by a nanoemulsification technique. Compared with unformulated UA, UA-NPs exhibited better drug solubility and similarly synergized with oncolytic MV to induce apoptosis in breast cancer cells. This enhanced oncolytic efficacy was partly attributed to the increased autophagic flux induced by the combined treatment of UA-NPs and MV. Finally, synergistic effects of the combination of UA-NPs and MV were also observed in BT-474 and MDA-MB-468 breast cancer cells. Thus, our study highlights the potential value of oncolytic MV and UA-based chemotherapy as a therapeutic strategy for the further development of breast cancer treatment, as well as the possibility of using nanoemulsification to improve the applicability of UA.

5.2. Rationale and Aim

Nanomedicine is considered to be an important driving force of modern clinical progress, and is usually defined as the application of nanoscale (< 1000 nm) agents for the diagnosis or treatment of diseases [165, 166]. They are small in size and can be modified on the surface and/or within the particles, which provides for better solubility, bioavailability, targeting, efficacy, and safety [165] that are essential features for effective anticancer treatments. Therefore, anticancer nanomedicines, including nanoparticle-based agents and OVs, have been extensively studied and have achieved clinical success in a variety of cancers including breast cancer [165].

Formulating drugs into nanoparticles is a very popular strategy, especially for plant-based molecules, because it can effectively improve the solubility, bioavailability, and biological activity of drugs in *in vivo* setting [167]. Ursolic acid or UA (3-β-hydroxy-urs-12-en-28-oic acid), widely found in fruits and plants, is a naturally occurring pentacyclic triterpenoid. This phytochemical is recognized for its significant multimodal anti-tumor properties against various cancers [168, 169]. Its ability to inhibit breast cancer proliferation, angiogenesis, and metastasis, and induce apoptosis of breast cancer cells *in vitro* and in small animal models has been largely recognized, making it an important candidate in recent years for potential development as chemopreventive and therapeutic agent against breast cancer [170]. However, UA possess a very poor water solubility profile and hence low bioavailability [170]. Modifications by nanotechnology, such as through the preparation of nanoparticles, can effectively circumvent this problem.

Another newly emerging and promising therapeutic strategy is the use of OVs as oncolytic nanomedicine, the so-called oncolytic virotherapy [171]. This novel therapeutic

approach prevents cancer recurrence by OVs directly targeting and killing the infected tumor cells and inducing tumor-specific immunity [172]. Although they have good safety and preclinical antitumor potential, many OVs, including MV, have shown moderate efficacy when used as monotherapy [145]. Therefore, the approach of "combinatorial chemovirotherapy" is commonly used, that is, combining OVs with anticancer drug agents to improve the treatment efficacy. Combining oncolytic MV and the phytochemical UA may induce an enhanced cytotoxicity against breast cancer cells due to their different tumor-killing mechanisms. Such combination treatment has the potential to lead to better tumor killing while preventing the development of drug resistance [152]. To validate its feasibility and as a proof-of-concept, this study aims to explore the anticancer efficacy of combining a recombinant wild-type MV with UA and its nanoformulation as a new strategy for breast cancer treatment

5.3. Results

5.3.1. Oncolytic MV and the small molecule UA exert dose-dependent cytotoxicity against breast cancer cells

To first establish the individual cytotoxicity profiles of oncolytic MV and UA, different concentrations of the drug or MOI of the virus were adminstered on the human breast cancer MCF-7 cells for a 5-day treatement before testing for cell viability. The oncolytic MV is based on a wild-type strain tagged with EGFP, which can recognize nectin-4 expression that is highly expressed on the permissice MCF-7 cells [24]. On the other hand, DMSO was used as solvent to dissolve UA due to the compound's low water solubility. As shown in Figure 13A, increasing concentrations of UA from 2 – 15 μM led

to a reciprocal decrease in MCF-7 cell viability to 75 %, with 20 μM of the compound reducing the the number of viable breast cancer cells to 20 % (CC_{50} = 16.67±1.10 μM). Likewise, oncolytic MV treatment also dose-dependently diminished the MCF-7 cell vaiblity over a concentraion of MOI 0.001 – 10, with MOI 1 of the virus killing about 50 % of the breast cancer cells (Figure 13B). Based on these obserations, the concentrations of UA (≤ 10 μM) and MV (MOI 0.1 – 0.01) below their CC_{50} indices were thus chosen for the remainder of the study in exploring their combination anticancer effect.

5.3.2. Combined treatment of UA and oncolytic MV produces synergistic anticancer effect against MCF-7 breast cancer cells

To determine whether UA and oncolytic MV would exert stronger potency when used in combination, both agents were concurrently added to MCF-7 cells. Data obtained from the cell viability analysis in the ensuing incubation was then assessed by the Chou-Talalay method [153], where the combination index 'CI' value would signify the combination effect to be synergistic (CI < 1), additive (CI = 1), or antagonistic (CI > 1). While the combination of 10 μM UA with MOI 0.01 of oncolytic MV attained a similar killing effect as UA monotreatment (~ 25 %) with no obvious synergism, increasing the viral concentration to MOI 0.1 with 10 μM UA produced a significantly higher MCF-7 cell death (> 50 %) compared to each agent alone (Figure 13C). The CI value of the MV MOI 0.1 with 10 μM UA combination was 0.3 (Figure 13D), indicating that UA and oncolytic MV can act synergistically, leading to enhanced tumoricidal effect against MCF-7.

5.3.3. UA treatment does not antagonize oncolytic MV infection

While UA and MV co-treatment demonstrated synergy, precaution was taken to further examine whether UA would interfere with the oncolytic MV infection by evaluating its effect on the viral infectivity through a series of experiments, each focused on a specific stage of MV infection in MCF-7. For the early viral entry stages, three assays were performed to assess the impact of UA on (i) free oncolytic MV particles (Figure 14A), (ii) viral attachment to the target cells (Figure 14B), and (iii) post-attachment fusion with the target cells (Figure 14C). A known small-molecule MV entry inhibitor PUG [154] was included as a positive control in all experiments. Data obtained from viral reporter fluorescence showed that UA, at concentrations up to the maximum dose used in the combination treatment, did not affect the early entry steps of the oncolytic MV, similar to the DMSO solvent control. PUG, on the other hand, effectively impeded all three steps as previously reported [154]. Three time-of-drug-addition assays (pre-treatment, co-addition, and post-infection) were also performed to assess whether UA treatment administered at different time-points produces antiviral effect on the oncolytic MV infection. UA treatment generally had negligible effects on the MV infectivity for all doses tested, whereas the positive control IFN-α significantly reduced the viral infection (Figure 14D). These results therefore suggested that combinatorial treatment of UA and the oncolytic MV does not negatively modulate the viral infection.

5.3.4. UA and oncolytic MV combinatorial treatment enhances apoptotic cell death of MCF-7 breast cancer cells

Cell cycle and apoptosis analyses were next performed to study the mechanism underlying the anticancer activity of UA and oncolytic MV combinatorial treatment on

MCF-7 cells. Compared to cells treated with UA or MV alone, the combinatorial treatments caused synergistic elevation in the population of sub-G1 phase cells to approximately 25 % and 60 % for MOI 0.01 and MOI 0.1 of oncolytic MV, respectively (Figure 15A). Increased sub-G1 population suggesting apoptosis [173] was subsequently validated by flow cytometric Annexin V/PI double staining. Percentage of late apoptotic cells detected in MCF-7 cells treated with UA and MV in combination significantly increased to 33 – 69 % compared to 20 % or less when treated with each agent alone (Figure 15B). These results were further confirmed via western blot analysis of the apoptotic marker, cleavage of PARP [174]. Consistently, our finding revealed increased apoptosis as level of cleaved PARP was greatly enhanced by UA and oncolytic MV combinatorial treatments (Figure 15 C and D). Therefore, our results overall demonstrated that UA and oncolytic MV combinatorial treatment produces synergistic tumoricidal effect against MCF-7 breast cancer cells, which is mediated by increased induction of apoptotic cell death.

5.3.5. Nanoformulation changes the physicochemical properties and improves drug dissolution of UA

As UA is a triterpenoid compound with poor water solubility and low bioavailability *in vivo*, which limit its applicability, we next employed nanoemulsification using the nonionic polymer PVP to generate water soluble PVP-based UA nanoparticles (UA-NPs) as a strategy to improve these issues [167]. Physicochemical characterization of UA and UA-NP were performed and documented in Figure 16. Our optimized UA:PVP formulation (1:1 weight ratio) produced a well-suspended colloidal solution, while other formulations with 1:3 or 1:6 weight ratio were unable to maintain the dispersion state and

easily aggregate or precipitate (data not shown). The mean size of the formulated UA-NPs was 209.3 ± 1.7 nm, and the yield was 69.3 ± 9.9 % after removing the non-formulated aggregates. Electron microscopy using FESEM demonstrated a morphological change of the needle-shaped UA crystals (Figure 16A) to the nanoparticulate form of UA-NPs (Figure 16B). This observation was supported by the XRD analysis, in which the obvious crystalline peaks in the spectra of non-formulated UA and the UA-PVP physical mixture (UA-PM) disappeared in the spectra of UA-NPs that showed an amorphous state similar to PVP (Figure 16C). This physicochemical change is a favorable factor for improving UA's dissolution and thus bioavailability [175]. Our dissolution test further confirmed that UA-NPs' solubility was substantially increased over the time intervals tested as compared to non-formulated UA, which remained mostly insoluble in the water-based buffer (Figure 16D). Altogether, these results demonstrated that we have successfully generated nanoformulated UA with improved solubility.

5.3.6. UA-NPs retained synergistic tumoricidal effect in combination with oncolytic MV and enhanced apoptotic cell death in MCF-7 breast cancer cells

To confirm whether UA-NPs retained its anticancer potency, the nanoparticles were used to treat MCF-7 cells over a range of drug concentrations. For comparison, non-formulated UA mixed in water ('UA-Water'), in which it is not soluble, was also tested in MCF-7 cells. As shown in Figure 17A, the non-soluble UA-water mixture had no impact on the cell viability of the breast cancer cells. In contrast, the UA-NPs solubilized in water could dose-dependently reduce MCF-7 cell viability and the CC_{50} value was found to be 36.52 ± 1.02 μM (Figure 17B). The polymeric carrier PVP alone showed no effect in

reducing the MCF-7 breast cancer cell viability. To examine whether UA-NPs retained the synergistic tumoricidal effect in combination with oncolytic MV, 30 μM of the UA-NPs and oncolytic MV (MOI 0.01 and 0.1) were used to co-treat MCF-7 cells. As shown in Figure 17C, MCF-7 cell viability was significantly reduced with the combinatorial treatments with MV compared to each agent alone, and most potently with the MV MOI 0.1 plus UA-NPs 30 μM combination. Similar results to the above observations were obtained using LDH release assay (Supplementary Figure S7). Their corresponding CI values, 0.9 and 0.7 (Figure 17D), indicated that both groups of combinatorial treatment produced synergistic effect (CI < 1) on MCF-7 cells. Thus, we concluded that UA-NPs retained tumoricidal effect against the MCF-7 cells and could exert synergistic activity with the oncolytic MV.

Finally, cell cycle analysis showed that the combinatorial treatments of UA-NPs and oncolytic MV, at MOI 0.01 and 0.1, similarly enriched sub-G1 phase populations to 46 % and 69 %, respectively (Figure 18A). With this result predicting increased apoptosis, Annexin V/PI staining likewise demonstrated enhanced levels of apoptosis from below 20 % in the untreated and mono-treated cells, to 45 – 60 % in UA-NPs and MV co-treated cells (Figure 18B). Markedly higher levels of cleaved PARP from the western blot analysis were also observed in the combinatorial treatments compared to the respective mono-treatment doses, although the MV MOI 0.01 plus UA-NPs 30 μM combination did not show a statistical significance compared with MV MOI 0.01 (Figure 18 C and D). These observations therefore suggested that UA-NPs with improved solubility retained the tumoricidal activity and could act synergistically with the oncolytic MV through enhancing apoptosis of MCF-7 cells.

5.3.7. Oncolytic MV and UA-NPs combined treatment indcued autophagic flux

UA has been reported to induce autophagy in MCF-7 cells at the range of concentrations that we used [176], and interestingly, autophagy also plays a pro-viral role in the life cycle of MV by promoting its replication and particle production [159]. To investigate how the MV and UA-NPs combination affect the dynamic process of autophagy in MCF-7 cells, we performed a western blot to analyze the autophagic flux induced by both agents (Figure 19). In contrast to the mock control which did not induce LC3 lipidation (LC3II, an autophagy marker) at 48 h, UA-NPs treatment and MV infection each individually induced autophagy as indicated by the increase in LC3II lipidation. However, the combination of UA-NPs and MV led to a decrease in LC3 lipidation compared to UA-NPs alone and comparable to MV alone, suggesting enhanced autophagic flux, an event that could be reversed by the lysosomal inhibitor BAF. This observation in cells that were treated with the combination was also supported by the decreased level of p62, an ubiquitin- and LC3-binding protein that accumulates when autophagy is impaired, such as by BAF treatment [177]. Since enhanced autophagic flux promotes MV's replicative spread and thus the subsequent cytopathic effect [159], this may contribute to the observed augmented cancer cell death induced by UA-NPs and MV combination.

5.3.8. Synergistic killing effect of oncolytic MV and UA-NPs combined treatment on BT-474 and MDA-MB-468 breast cancer cells

Lastly, we examined whether the combined treatment using oncolytic MV and UA-NPs could also exert enhanced killing effect on other breast cancer cell lines. To this end,

we tested each agent alone or their combination in the human breast cancer BT-474 and MDA-MB-468 cells. While MCF-7 represents luminal type A breast cancer (ER+, PR+/-, HER2-), BT-474 represents luminal type B (ER+, PR+/-, HER2+) [178], and MDA-MB-468 is a TNBC cell line [179]. Both BT-474 and MDA-MB-468 are known to express nectin-4 [23, 24, 65], which is used by MV to enter the host cell [23, 24]. As shown in Figure 20, both UA-NPs (Figure 20A) and oncolytic MV (Figure 20B) induced a dose-dependent cytotoxic effect on BT-474 and MDA-MB-468 cells. Using the UA-NPs threshold concentration as mono-agent producing > 50 % viable cells for BT-474 (30 μM) and MDA-MB-468 (20 μM), its combination with MOI 0.1 of oncolytic MV caused significant increased cell death in both cell lines compared to each agent alone (Figure 20C). Similar to MCF-7 cells, this enhanced killing effect in both cell lines appeared to be synergistic (CI = 0.9 for BT-474 and 0.6 for MDA-MB-468). Increased apoptosis was also observed in both cell lines when treated with the MV and UA-NPs combination (Figure 20D). Cell viability analyses using LDH release also corroborated these results (Supplementary Figure S8 and Supplementary Figure S9).

Overall, the above data supports the notion that UA-NPs and oncolytic MV can be used as a combination to enhance breast cancer cell death.

5.4. Discussion

Despite the advent of oncolytic virotherapy, most OVs have limited clinical efficacy as single agents, and therefore, combinations with anticancer agents are being increasingly explored. We have found that the synergistic activity resulting from combining oncolytic MV with the anticancer agent UA provides an alternative strategy to

using a chemovirotherapeutic approach that provides an augmentation in anticancer activity while reducing the dose of the agent, thereby decreasing toxicity to normal cells [152].

Both Oncolytic MV and UA individually have significant anti-breast cancer potential. The newly discovered oncolytic MV receptor nectin-4, which is a tumor marker, is selectively overexpressed and identified as a therapeutic target for many cancers including primary and metastatic triple-negative breast adenocarcinomas and also bladder, pancreatic, and lung cancers [52-56, 126], making the nectin-4-specific oncolytic MV a key new tool for targeting breast and other adenocarcinomas that are nectin-4-positive [64-68, 140]. On the other hand, UA is widely known as a potent anticancer agent capable of inhibiting breast adenocarcinomas in cell culture and animal models [170]. At the concentrations used in this study, UA and MV infection have been documented to induce G0/G1 cell cycle arrest and apoptosis [150, 180, 181]. Our results revealed similar pro-apoptotic effects of MV and UA on MCF-7 breast cancer cells, and these pro-apoptotic effects were significantly enhanced when MV and UA were co-administered in combination (Figure 15), leading to the speculation that their combined use may enhance their respective tumoricidal effects. Indeed, our data showed that the combination of oncolytic MV and UA produced a synergistic impact in killing breast cancer cells (Figure 15), supporting the idea that UA enhances the MV-mediated breast cancer cell oncolysis.

Although UA has been documented to exhibit antiviral activities, notably against HSV-1 [182], human immunodeficiency virus (HIV) [183], coxsackievirus B1 (CVB1), and enterovirus 71 (EV71) [184], no interference from UA treatment on the oncolytic MV infection was observed in our study (Figure 14), suggesting that UA's antiviral effects

could be virus-specific. Thus, the absence of antagonistic effects of UA on the oncolytic MV life cycle further lends support to their use in combination therapy. Conversely, our analysis confirmed that both the UA-based nanoparticles and MV independently triggered autophagy in the MCF-7 breast cancer cells, with a further enhanced autophagic flux through their combined use (Figure 19), which provides a pro-viral environment for MV infection and its associated CPE [159]. These results may partly explain why the combination therapy promoted greater tumor cell death than each drug or viral agent alone, although further study is needed to fully elucidate the underlying mechanisms.

UA's relatively low solubility profile has severely limited its medicinal application as a potential anticancer drug. Importantly, the water solubility of crude UA at 25 °C is about 2.2 x 10^{-4} μM [185], which is significantly well below its anticancer concentration (CC_{50} = 16.67±1.10 μM) against the MCF-7 breast cancer cells when completely solubilized using DMSO as solvent. Considering UA's poor water solubility and hence low bioavailability, we have successfully overcome this hurdle in its drug dissolution profile by generating nanoformulated UA-NPs with improved solubility. Specifically, FESEM-based biophysical examination indicated that crude UA as micrometer needle-shaped crystals were rendered into amorphous-state nanoscale particles (Figure 16 B and C). This effect is likely due to the dispersion of the UA crystals by the emulsion-solvent diffusion with the water-soluble PVP excipient as supported by our XRD analysis (Figure 16D). Since a lower energy is required in the dissolution process of the amorphous UA in the UA-NPs (Figure 16E), altogether these observations thus support the use of hydrophilic PVP as a formulation strategy to improve UA's dissolution profile. More importantly, the nanoformulation permitted the UA-NPs to retain their anticancer activity that produced

synergistic effect with the oncolytic MV combination in a similar manner to crude UA dissolved in DMSO. Finally, given the known toxic effect of the DMSO solvent [186], the UA-based nanoparticles have significant advantages for the future development of anticancer treatment modalities involving UA, including the combinatorial use of oncolytic MV vectors.

5.5. Acknowledgements

The authors would like to thank Dr. Christian Buchholz for reagent and Shun-Pang Chang and Wen-Chan Hsu for their technical support. C.-H.L. has received PhD fellowship from the Canadian Network on Hepatitis C (CanHepC). CanHepC is funded by a joint initiative of the Canadian Institutes of Health Research (CIHR) (NHC-142832) and the Public Health Agency of Canada (PHAC). L.-T.L. was supported by funding from Taipei Medical University Hospital (105TMU-TMUH-11) and the Ministry of Science and Technology of Taiwan (MOST107-2320-B-038-034-MY3).

5.6. Figures, Tables, and Legends

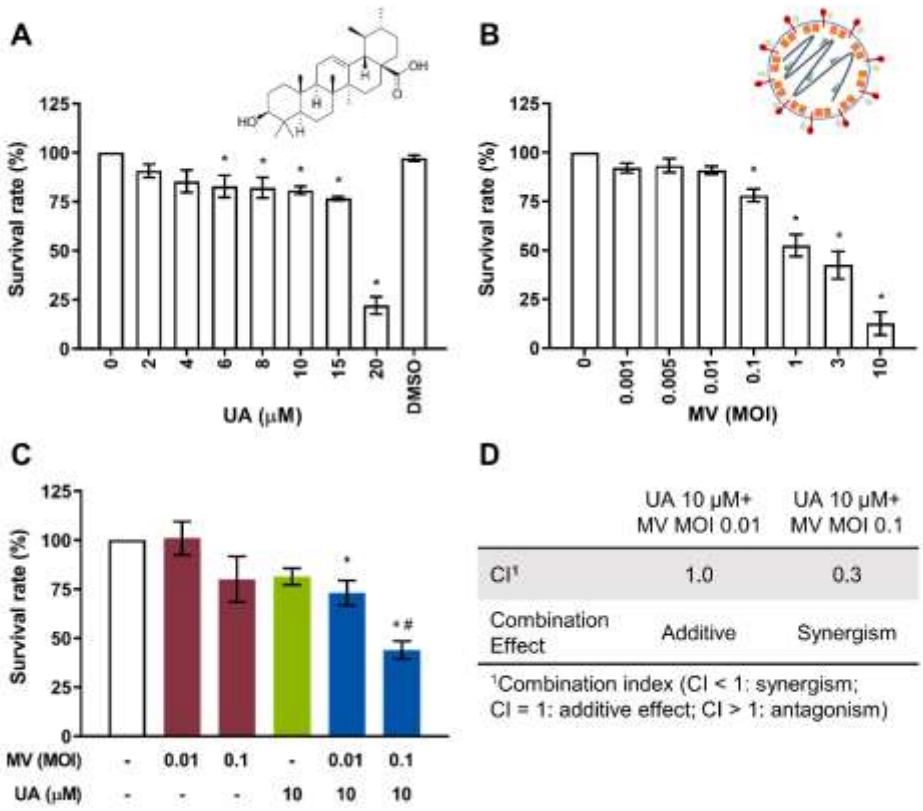

	UA 10 μM+ MV MOI 0.01	UA 10 μM+ MV MOI 0.1
CI[1]	1.0	0.3
Combination Effect	Additive	Synergism

[1]Combination index (CI < 1: synergism; CI = 1: additive effect; CI > 1: antagonism)

Figure 13. Ursolic acid (UA) and oncolytic MV are cytotoxic to human breast cancer MCF-7 cells and synergistically induce anticancer activity.

A. MTT cell viability analysis of MCF-7 cells treated with UA (2 – 20 μM) for 5 days. **B.** MTT cell viability analysis of MCF-7 cells treated with MV (multiplicity of infection, MOI 0.001 – 10) for 5 days. **C.** MTT cell viability analysis of MCF-7 cells treated with UA (10 μM) and MV (MOI 0.01 or 0.1) concurrently for 5 days. **D.** Analysis of treatment synergism using the Chou-Talalay method wherein combination index (CI) value quantitatively defines synergism (CI < 1), additive effect (CI = 1), or antagonism (CI > 1). All data shown are means ± SEM from three independent experiments; **P* < 0.05 in **A** and **B** compared to '0'; **P* < 0.05 compared with MV treatment, $^{\#}P$ < 0.05 compared with UA treatment in **C**; DMSO = 0.2 % (the maximum concentration of DMSO used). Adapted from Liu et al. Cancers (Basel). 2021 Jan 4;13(1):136.

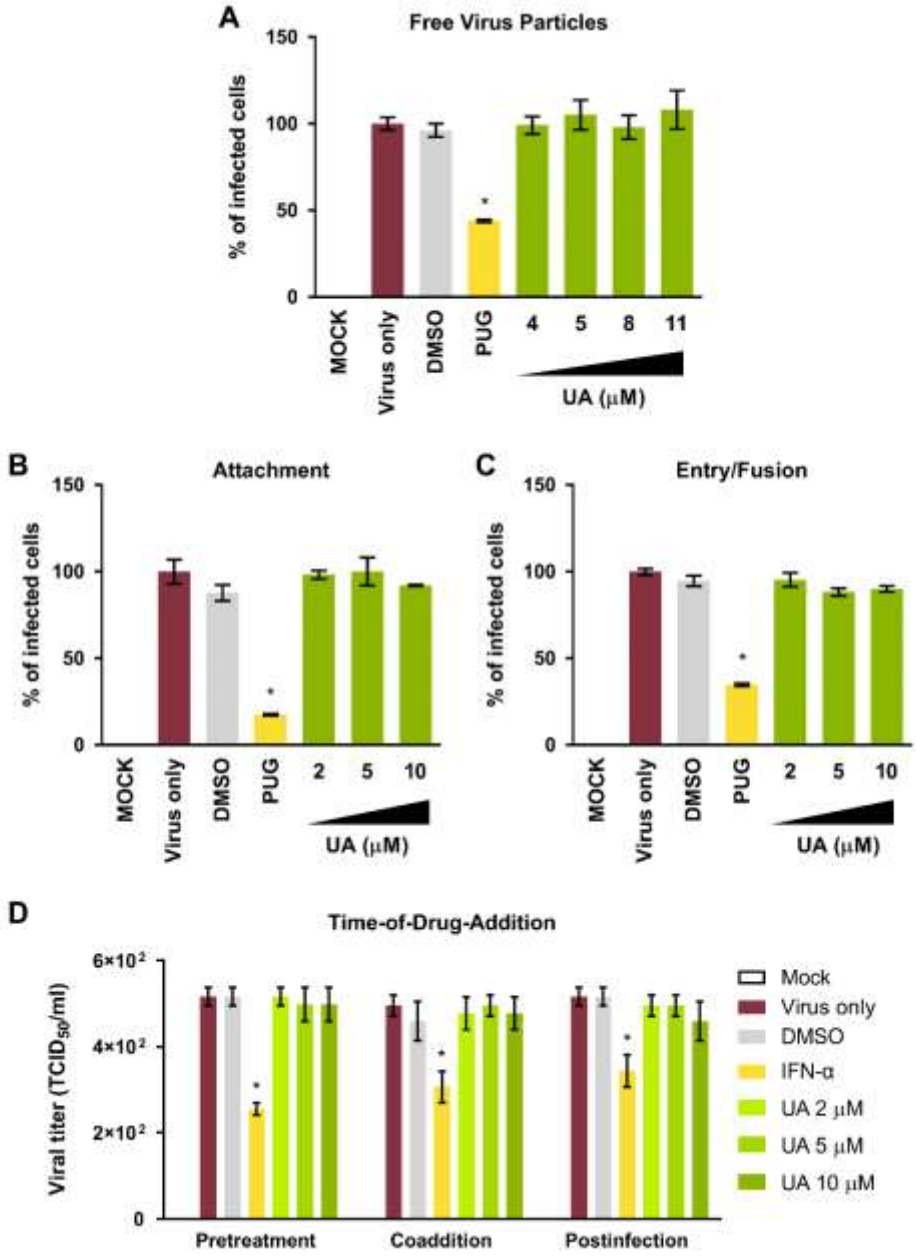

Figure 14. UA treatment does not interfere with the infection of oncolytic MV.

A. Effect of UA (4, 5, 8 and 11 μM) on free MV particles. **B.** Effect of UA (2, 5 and 10 μM) on MV attachment. **C.** Effect of UA (2, 5 and 10 μM) on MV entry/fusion. **D.** Time-of-drug-addition analysis of UA treatment on MV infection. For **A** – **C**, viral reporter fluorescence intensity reflecting the infectivity was measured using a variable mode scanner at 72 h post-infection. For **D**, supernatants from the experiment were collected at 72 h post-infection for viral titration using $TCID_{50}$. For all assays, final MV concentration = MOI 0.1; DMSO = 0.1 % (the maximum concentration of DMSO used); 50 μM punicalagin (PUG) for **A** – **C** or 1000 IU/ml interferon-α (IFN-α) for **D** was included as a positive control. All data shown are means ± SEM from three independent experiments; $*P < 0.05$. Adapted from Liu et al. Cancers (Basel). 2021 Jan 4;13(1):136.

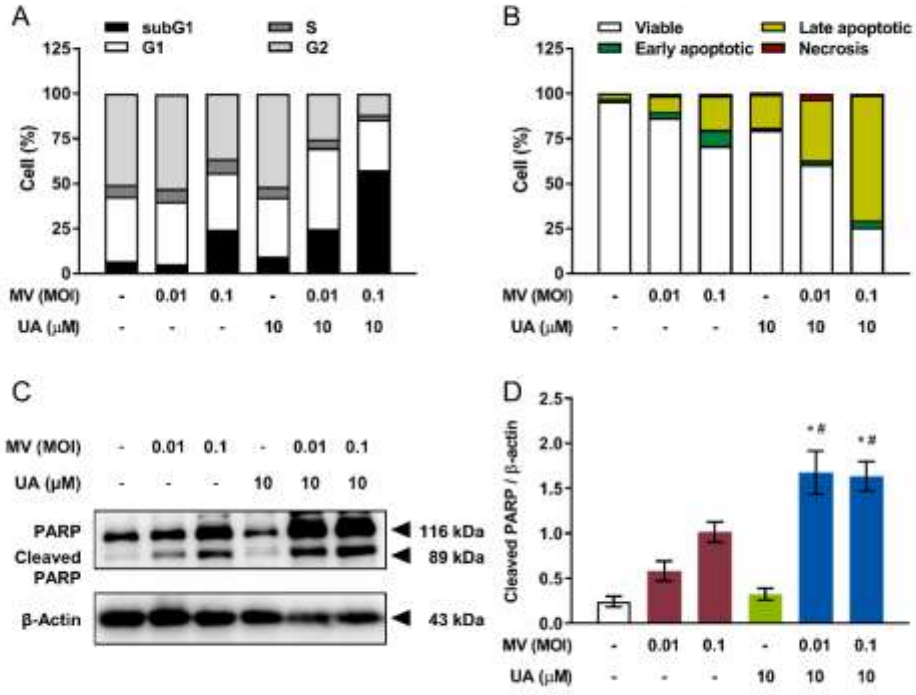

Figure 15. Co-treatment using UA and oncolytic MV enhances apoptotic cell death in human breast cancer MCF-7 cells.

MCF-7 cells were first treated with combination of UA (10 μM) and MV (MOI 0.01 or 0.1) for 5 days, then analyzed by flow cytometry for **A.** cell cycle distribution and **B.** apoptosis induction, using propidium iodide (PI) staining and double staining (PI and Annexin V conjugated with APC) respectively. Percentages shown are determined by Beckman Cytomics TM FC500 Flow Cytometry CXP analysis software. **C.** Lysates of MCF-7 cells co-treated with UA (10 μM) and MV (MOI 0.01 or 0.1) for 5 days were analyzed by western blot for poly (ADP-ribose) polymerase (PARP) cleavage. **D.** Quantitative analysis of the relative level of cleaved PARP from **C**. All quantitative data are expressed as means ± SEM from three independent experiments; $^{*}P < 0.05$ compared with MV treatment, $^{\#}P < 0.05$ compared with UA treatment. Adapted from Liu et al. Cancers (Basel). 2021 Jan 4;13(1):136.

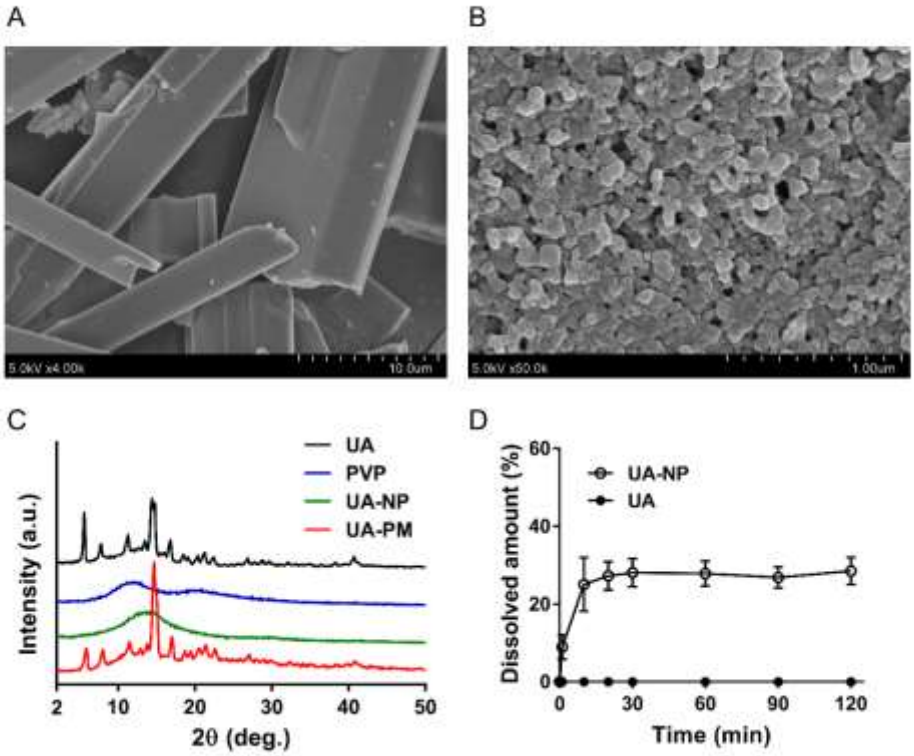

Figure 16. Physicochemical properties of UA nanoparticles (UA-NP).
A. Field emission scanning electron microscopy (FESEM) photograph of non-formulated UA (magnification: 4000X; scale bar = 10.0 μm). **B.** FESEM photograph of nanoformulated UA (magnification: 50,000X; scale bar = 1.0 μm). **C.** X-ray diffraction patterns of UA, polyvinylpyrrolidone (PVP), nanoformulated UA nanoparticles (UA-NP), and UA-PVP physical mixture (UA-PM). XRD patterns were taken from 2° to 50°with a scanning rate of 4°/min. The spectra were offset for clarity. **D.** Drug dissolution test (open circle, UA-NP; filled circle, UA). Samples containing 4.68 mg equivalent of UA were placed in 100 ml of pH 7.4 phosphate buffer and maintained at 37 ± 0.5 °C. During the dissolution process, samples were withdrawn at 0, 1, 10, 20, 30, 60, 90 and 120 min for HPLC analysis. Data points are expressed as means ± SD (n = 6). Adapted from Liu et al. Cancers (Basel). 2021 Jan 4;13(1):136.

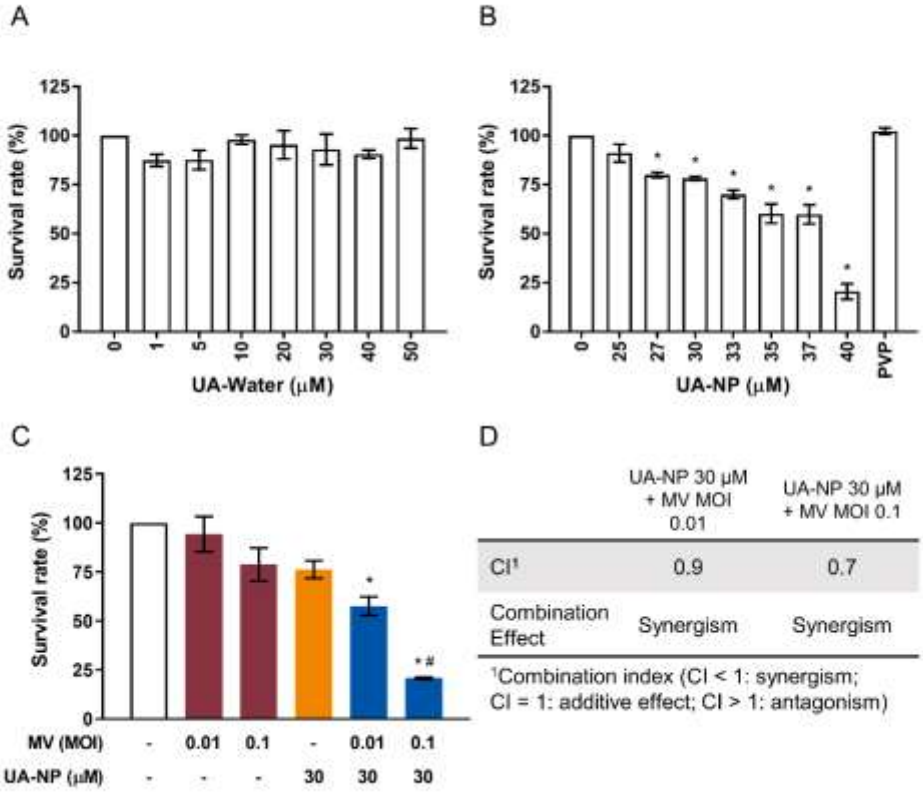

Figure 17. UA-NP retain cytotoxic activity against human breast cancer MCF-7 cells and exert synergistic anticancer activity in combination with oncolytic MV.

MCF-7 cells were treated with **A.** non-formulated UA mixed in water (UA-Water; 1 – 50 μM) or **B.** UA-NP solubilized in water (25 – 40 μM) for 5 days, and cell viability was analyzed by MTT assay; PVP = 50 μg/ml. **C.** MCF-7 cells were concurrently treated with UA-NP (30 μM) and MV (MOI 0.01 or 0.1) for 5 days, following which cell viability was determined by MTT assay. **D.** Analysis of treatment synergism using the Chou-Talalay method. All data shown are means ± SEM from three independent experiments; $^{*}P < 0.05$ in **A** and **B**; $^{*}P < 0.05$ compared with MV treatment, $^{\#}P < 0.05$ compared with UA treatment in **C**. Adapted from Liu et al. Cancers (Basel). 2021 Jan 4;13(1):136.

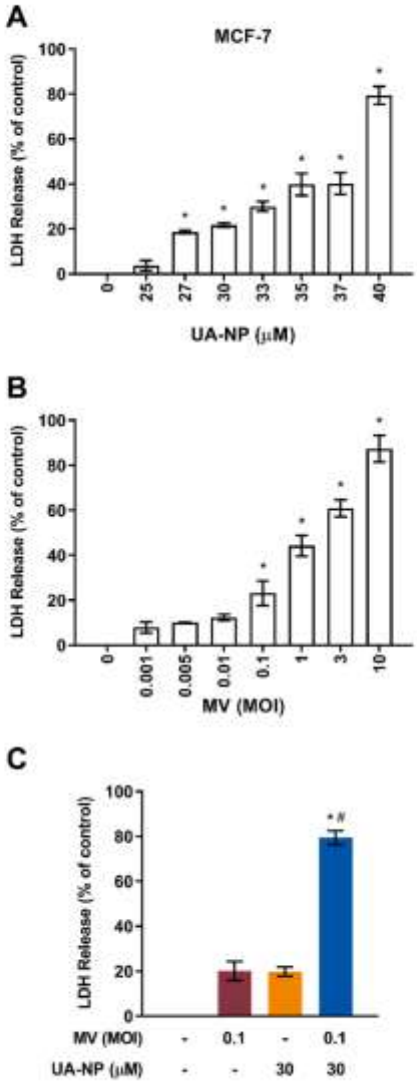

Supplementary Figure S7. LDH release assay to assess cell viability of UA-NP and oncolytic MV co-treatment in MCF-7 human breast cancer cells.

MCF-7 cells were treated with **A.** UA-NP (25 – 40 μM), **B.** MV (MOI 0.001 – 10), or **C.** concurrently treated with MV (MOI 0.1) and/or UA-NP (30 μM) for 5 days before analyzing cell viability using LDH cytotoxicity detection kit. All data shown are means ± SEM from three independent experiments; **P* < 0.05 in panels **A** and **B**; * *P* < 0.05 compared with MV treatment, $^{\#}P < 0.05$ compared with UA treatment in panel **C**. Adapted from Liu et al. Cancers (Basel). 2021 Jan 4;13(1):136

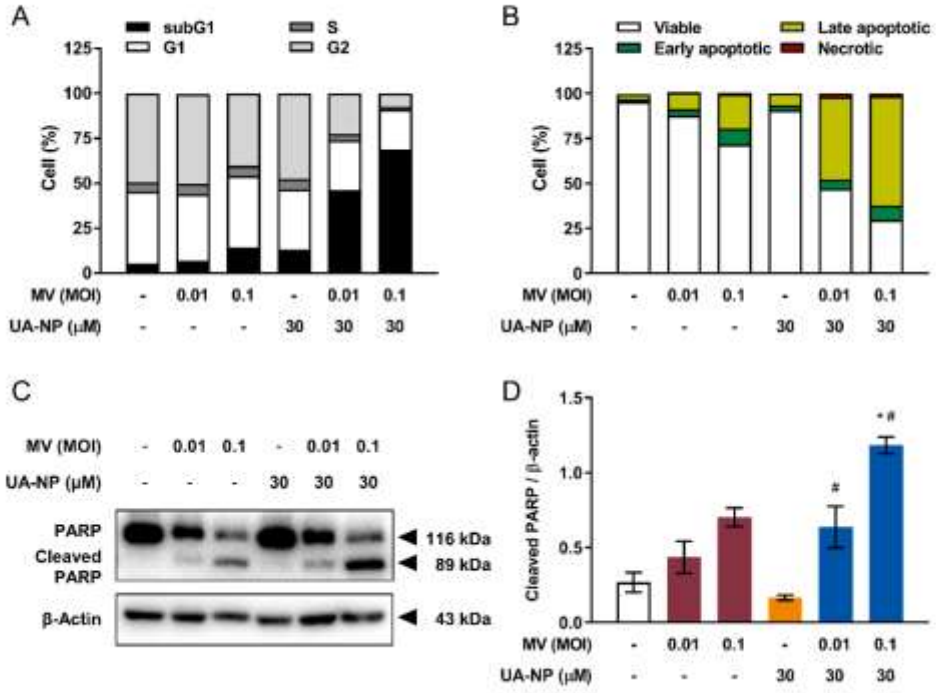

Figure 18. UA-NP and oncolytic MV co-treatment induces enhanced apoptotic cell death in human breast cancer MCF-7 cells.

MCF-7 cells were first concurrently treated with UA-NP (30 μM) and MV (MOI 0.01 or 0.1) for 5 days, then analyzed by flow cytometry for **A.** cell cycle distribution and **B.** apoptosis induction. **C.** Lysates of MCF-7 cells co-treated with UA-NP (30 μM) and MV (MOI 0.01, or 0.1) for 5 days were also analyzed for PARP cleavage by western blot. **D.** Quantitation of the relative level of cleaved PARP from **C**. All quantitative data are expressed as means ± SEM from three independent experiments; $^{*}P < 0.05$ compared with MV treatment, $^{\#}P < 0.05$ compared with UA treatment. Adapted from Liu et al. Cancers (Basel). 2021 Jan 4;13(1):136.

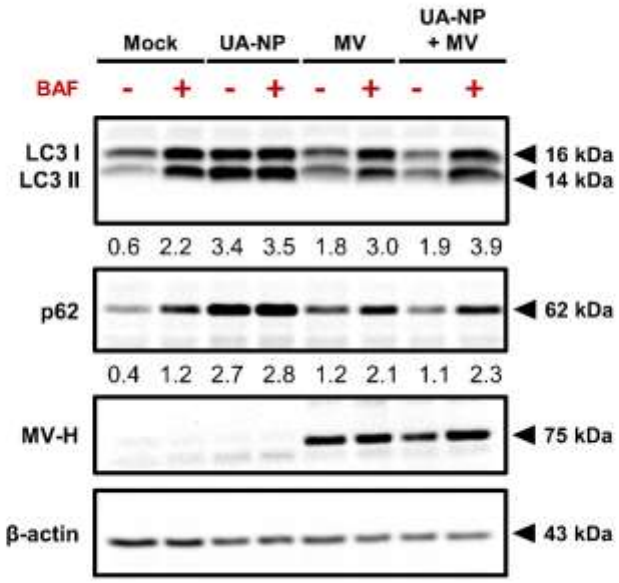

Figure 19. UA-NP and oncolytic MV co-treatment enhances autophagic flux in MCF-7 cells.
MCF-7 cells were treated with UA-NP (30 μM), MV (MOI 0.1), or concurrently with both agents for 48 h before being harvested and analyzed for LC3, p62, MV H protein, and β-actin expression using western blot. Bafilomycin (BAF, 100 nM) was added to the indicated groups 4 h before harvesting the cells. LC3II and p62 signals were quantified and normalized to the β-actin loading control. Adapted from Liu et al. Cancers (Basel). 2021 Jan 4;13(1):136.

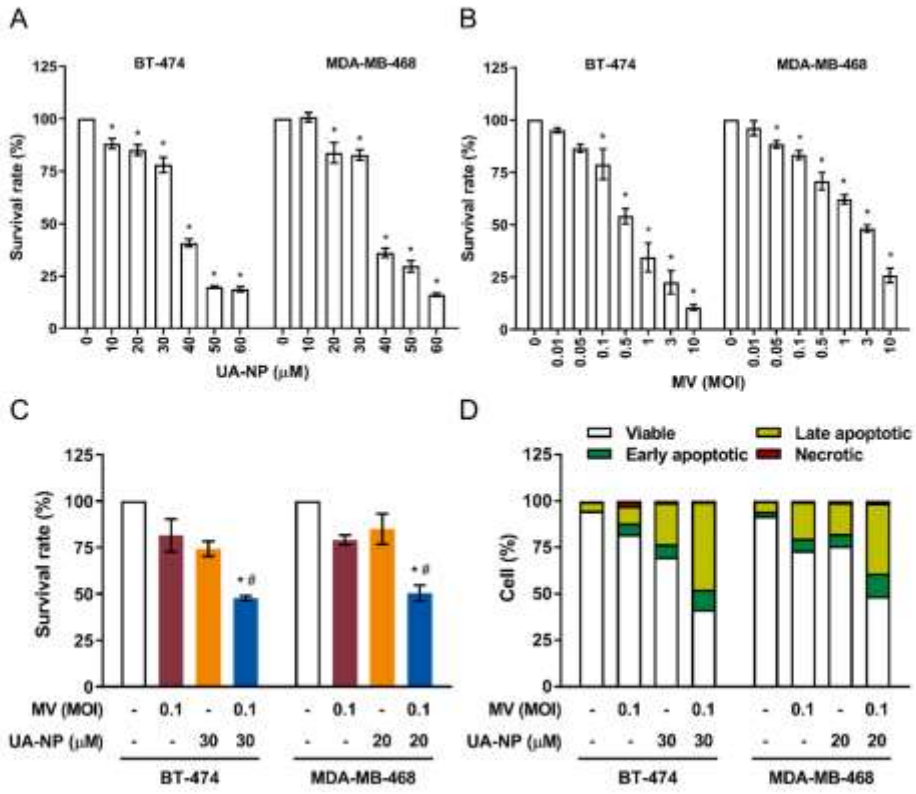

Figure 20. Combination treatment using UA-NP and oncolytic MV exerts enhanced anticancer effect against human breast cancer BT-474 and MDA-MB-468 cells.

BT-474 and MDA-MB-468 cells were treated with **A.** UA-NP (10 – 60 μM) or **B.** MV (MOI 0.01 – 10) for 5 days before analysis of cell viability using MTT assay. DMSO = 0.1 %. **C.** BT-474 and MDA-MB-468 cells were co-treated MV (MOI 0.1) and/or UA-NP (30 μM for BT-474 and 20 μM for MDA-MB-468), following which cell viability was determined by MTT assay. **D.** BT-474 and MDA-MB-468 cells were first concurrently treated with UA-NP (30 or 20 μM) and MV (MOI 0.1) for 5 days, and then analyzed by flow cytometry for apoptosis induction. Data shown are means ± SEM from three independent experiments; $*P <$ 0.05 in **A** and **B**; $*P < 0.05$ compared with MV treatment, $^{\#}P < 0.05$ compared with UA treatment in **C**. Adapted from Liu et al. Cancers (Basel). 2021 Jan 4;13(1):136.

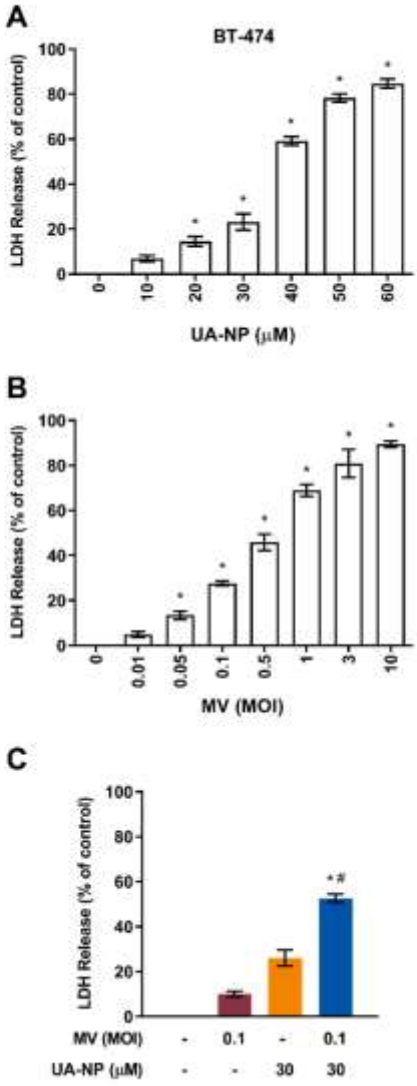

Supplementary Figure S8. LDH release assay to assess cell viability of UA-NP and oncolytic MV co-treatment in BT-474 human breast cancer cells.

BT-474 cells were treated with **A.** UA-NP (10 – 60 μM), **B.** MV (MOI 0.01 – 10), or **C.** concurrently treated with MV (MOI 0.1) and/or UA-NP (30 μM) for 5 days before analyzing cell viability using LDH cytotoxicity detection kit. All data shown are means ± SEM from three independent experiments; **P* < *0.05* in panels **A** and **B**; **P* < 0.05 compared with MV treatment, $^{\#}P < 0.05$ compared with UA treatment in panel **C**. Adapted from Liu et al. Cancers (Basel). 2021 Jan 4;13(1):136.

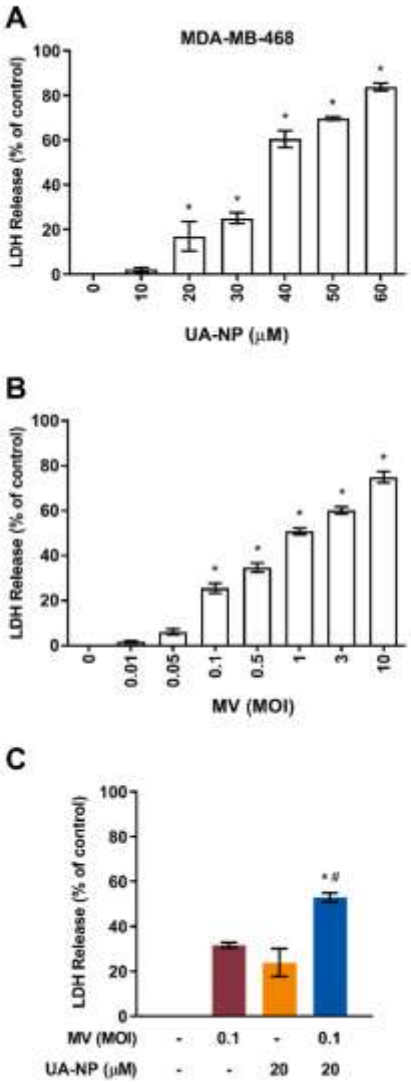

Supplementary Figure S9. LDH release assay to assess cell viability of UA-NP and oncolytic MV co-treatment in MDA-MB-468 human breast cancer cells.

MDA-MB-468 cells were treated with **A.** UA-NP (10 – 60 μM), **B.** MV (MOI 0.01 – 10), or **C.** concurrently treated with MV (MOI 0.1) and/or UA-NP (20 μM) for 5 days before analyzing cell viability using LDH cytotoxicity detection. All data shown are means ± SEM from three independent experiments; **P* < 0.05 in panels **A** and **B**; **P* < 0.05 compared with MV treatment, $^{\#}P$ < 0.05 compared with UA treatment in panel **C**. Adapted from Liu et al. Cancers (Basel). 2021 Jan 4;13(1):136.

CHAPTER 6

THE USE OF ONCOLYTIC MEASLES-BASED VECTORS FOR TARGETED TREATMENT OF HEPATITIS C VIRUS-INDUCED LIVER CANCER

6.1. Abstract

Although direct antiviral drugs now offer a treatment for hepatitis C, treatment options for HCV-associated HCC remain limited. Current treatments for HCC include surgical resection, radiofrequency ablation, embolization, liver transplantation, and chemotherapy, but these therapies are ineffective for advanced HCC, and conditions such as risk of recurrence, contraindications, lack of donor livers, and varied responses contribute to poor disease prognosis. These problems highlight the importance of developing new therapies for HCC, particularly for patients with chronic hepatitis C. Recently, nectin-4, a tumor marker found on many epithelial malignancies, including HCC, was identified as one of the receptors for MV. This finding highlights the potential use of MV-based oncolytic vectors for the treatment of HCC including scenarios of HCV-associated HCC. Analysis of the Oncomine online dataset revealed that nectin-4 was upregulated in HCC samples, including those infected with HCV, compared to normal liver tissue. HCC cell lines expressing nectin-4 can be targeted by a recombinant wild-type MV vector and exhibit a dose-dependent response to the MV-induced oncolysis. More importantly, the increased infectivity and propagation of MV in hepatocellular carcinoma cell lines with replicating HCV subgenomes suggests that suppression of cell innate immunity due to HCV activity may influence the infectivity of oncolytic vectors. Finally, MV-based oncolytic treatment effectively infected and inhibited *in vivo* xenograft tumor growth, an effect that was further enhanced in an immunocompetent syngeneic mouse model. Taken together, these results suggest that MV oncolytic virotherapy has potential for the treatment of HCC, including in the context of HCV-associated HCC and merits to be further explored.

6.2. Rationale and Aim

Recombinant MV has been explored in recent years as an oncolytic agent, including against non-small-cell lung carcinoma [58], glioblastoma [59], ovarian cancer [60], osteosarcoma [61], acute myeloid leukemia [62], among others. It has been proposed that nectin-4 expression in HCC is associated with larger tumor size, presence of metastasis and vascular invasion, and later cancer stages, suggesting that it could serve as a novel prognostic biomarker and therapeutic target in liver cancer [69]. Interestingly, the MV receptor nectin-4 has also been documented to be highly expressed in late-stage HCC [69]. These evidences point to using MV oncolytics to target and treat HCC through nectin-4.

In addition, HCV infection is known to depress the host cell innate immune system [187], which can be advantageous to alleviate antiviral response against oncolytic MV when targeting the HCV-induced tumor cells. These lines of evidence advocate the use of MV oncolytics for potential treatment of HCC, including those related to hepatitis C. We therefore propose to take advantage of the nectin-4 targeting ability of MV and explore the use of recombinant MV as an oncolytic agent to target HCC, particularly in the context of hepatitis C-induced HCC. These studies should help establish a foundation for using oncolytic MV vector for virotherapy of HCC, particularly in the context of HCV-induced liver cancer, and expand the scope of treatment strategies for the management of HCC.

6.3. Results

6.3.1. Nectin-4 expression is upregulated in clinical HCC specimens

To determine whether nectin-4 is generally upregulated in clinical HCC specimens, we first analyzed the copy number of nectin-4 in publicly available microarray datasets

deposited in Oncomine (http://www.oncomine.org). Four DNA copy number datasets (Chiang Liver 2 [188], Guichard Liver [189], Guichard Liver 2 [189], and TCGA Liver) containing data from HCC and corresponding non-tumor tissues were analyzed. As shown in Figure 21A, DNA copy numbers of nectin-4 were significantly higher in the tumor (T) tissues compared to the non-tumor (NT) tissues in all four datasets. We next examined whether nectin-4 expression correlates with Tumor, Node, Metastasis (TNM) stage as previously suggested [69]. While we did not observe a higher nectin-4 expression in later TNM stages (data not shown), an increasing trend was found from low to high Edmonson-Steiner grades (Figure 21B), the most commonly accepted histological grading of HCC to predict disease prognosis [190]. In addition, nectin-4 upregulation was present in both hepatitis viruses positive (HBV or HCV) and negative (NBNC) HCC samples (Figure 21C). These results suggest that nectin-4 is upregulated in HCC compared to non-tumor tissues and potentially increased with higher grades, and may be a relevant target for the application of MV oncolytics in HCC including those of viral etiology.

6.3.2. Human HCC cell lines express nectin-4 and are susceptible to MV oncolysis

To evaluate the oncolytic activity of MV *in vitro*, human hepatoma cell lines Huh-7, HepG2, Hep3B, and PLC/PRF/5 were assessed for their nectin-4 expression by flow cytometry analysis (Figure 22A). All four cell lines expressed certain levels of nectin-4 on cell surface, suggesting that targeting these cells with MV is feasible. Vero cells with and without Nectin-4 overexpression were included as positive and negative controls. Indeed, these cell lines appeared susceptible to MV infection as indicated by the fluorescent viral syncytia formation (Figure 22B), and cell death was induced 7 days post infection (dpi) in

a dose-dependent manner (Figure 22C), with Huh-7 and PLC/PRF/5 being the most sensitive cell lines. Of note, we also included PH5CH8, a non-neoplastic immortalized human hepatocyte cell line [191], as a control to assess MV's specificity. As shown in Figure 22, PH5CH8 did not express nectin-4 and was resistant to MV infection and cytotoxicity. These results suggest that MV is a HCC-specific oncolytic agent that selectively causes cancer cell death.

6.3.3. Treatment impact of oncolytic MV in the context of HCV infection and immune evasion

Following our proof-of-concept analysis of the nectin-4-selective oncolytic MV in HCC in the above experiments, we next look at its potency in the context of HCV-associated HCC setting. For this purpose, we evaluated MV infection in two Huh-7-based replicons containing HCV subgenomes — AB12-A2 (genotype 1b) [113] and sbJFH1-B2 (genotype 2a) [114]. These cells derived from G418-resistant clones that were electroporated with HCV replicon RNAs encoding a neomycin-resistance gene and the nonstructural proteins (NS) NS3 to NS5B (Figure 23A). Interestingly, MV infection of these replicon cells resulted in more widespread syncytia formation (Figure 23B) and enhanced MV replication as demonstrated by increased EGFP reporter intensity (Figure 23C) compared to the parental Huh-7 cells, eventually leading to more oncolysis in the replicon cells (Figure 23D). When the replicon cells were treated with IFN-α (200 IU/ml) for 2 weeks to eliminate HCV RNA, the above effects were reversed. Similar observations were made with daclatasvir-cured cells. We speculated that the suppressed cellular innate immunity might have contributed to these observations, as the HCV NS3/4A protease is

known to cleave the mitochondrial antiviral-signaling protein (MAVS) and the TLR signaling molecule TIR domain-containing adaptor protein-inducing IFN-β (TRIF) following initial infection to disrupt downstream IFN-β production [192]. Indeed, IFN-β production was induced in Huh-7 cells when the cells were stimulated with poly I:C, a synthetic double-stranded (dsRNA) that simulates viral infection, but not in the HCV replicon cells (Figure 23E). Although MV infection could inhibit this antiviral activation in the Huh-7 cells (Figure 23E) as previously suggested [193], the predisposed immune suppression in the replicon cell likely contributes to an easier establishment of MV infection and thereafter reaching a more efficient spread, as there are less obstacles imposed by the HCV-subverted cell innate immune system. We further examined the impact of HCV NS3/4A on MV replication using an adenovirus vector to transiently express the protease. HCV NS3/4A alone was able to enhance MV replication (Figure 23F), indicating that this scenario of antiviral innate immunity-suppressed hepatocyte microenvironment, which occurs in chronic hepatitis C and its associated liver cancer, could prove to be advantageous for application of viral oncolytics, including our proposed MV vector.

6.3.4. Oncolytic MV infection in HCC tumor spheres

To assess the feasibility of treating HCC tumors with oncolytic MV, we then performed MV infection of HCC tumor spheres. Single Huh-7 cells were seeded on low attachment plates to allow sphere formation in suspension, and then the spheres were infected with MV-EGFP. As shown in Figure 24A, viral infection was observed starting from 3 dpi, and the fluorescent syncytia increased in size over 7 days of observation.

Confocal microscope imaging of infected spheres along the Z stack further demonstrates an extension of EGFP signal (Figure 24B). These results indicate that MV could effectively spread within HCC tumor spheres.

6.4. Discussion

Current management of HCC relies on the Barcelona Clinic Liver Cancer (BCLC) staging system, which evaluates the patients' liver function, performance status, and tumor burden to determine the most optimal treatment for them. While patients with early stages are eligible for curative treatments including ablation, resection, and liver transplantation, treatment options including locoregional therapies and systemic chemotherapies for patients with intermediate or advanced stages remain non-curative, resulting in significantly shorter survival [194]. This underscores the drastic need for further treatment options for these relatively incurable individuals. To date, clinical trials evaluating oncolytic virotherapies for HCC are rather limited [195]. The vaccinia virus-derived JX-594 represents the lead agent in this field. The vector has been assessed in several randomized clinical trials, demonstrating well tolerance, tumor perfusion, and induction of immune responses when administered intratumorally alone [196] or following intravenous infusion [197]. However, JX-594 failed to improve the overall survival as a second-line therapy after sorafenib treatment failure [197] or as a sensitizing agent to improve sorafenib treatment, thus its phase III randomized trial (NCT02562755) was halted in 2019 [198]. Nonetheless, the locoregional treatment of conventional HCC management provides a window for intratumoral administration of oncolytic viral vectors, which in the case of MV vector may be helpful in shielding the virus from pre-existing humoral immunity.

HCC often results from chronic hepatitis B or chronic hepatitis C [194], which likely contribute to the immunosuppressive microenvironment in HCC [199]. However, we found that the suppressed cell innate immunity in HCC cells containing HCV subgenomes may be helpful for MV spread and oncolysis *in vitro* (Figure 23), indicating the feasibility of using MV virotherapy in HCV infection scenario. On the other hand, while previous study has shown that HBX expression from HBV infection could confer HCC cells resistant to reovirus oncolysis by activating signal transducer and activator of transcription 1 (STAT1) [200], MV was able to infect the HBV genome-containing Hep3B cells and reached 50 % cytotoxicity around MOI 5 (Figure 22). Along with the observation that MV receptor nectin-4 is upregulated in HCC tissues (Figure 21) and that HCC cells and tumor spheres are permissive to MV's oncolytic infection *in vitro* (Figure 22 and Figure 24), these results suggest that MV is worth further development as an oncolytic vector for HCC including those of viral etiologies. Animal studies to further validate MV's *in vivo* application for HCC treatment are being explored next.

6.5. Figures, Tables, and Legends

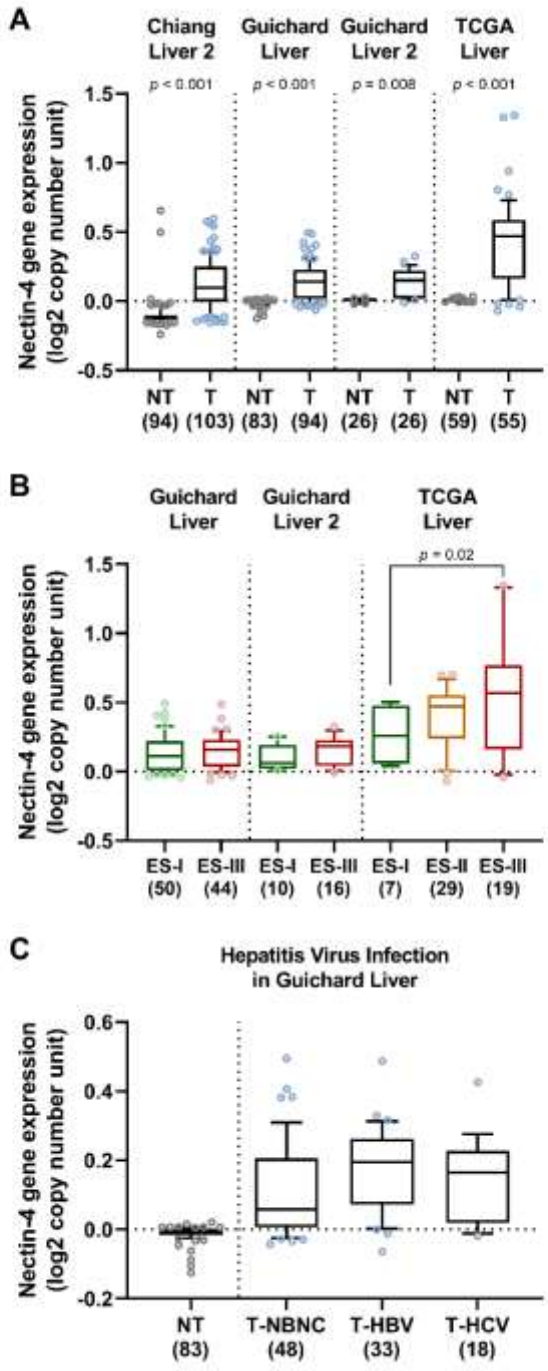

Figure 21. Assessment of nectin-4 expression in clinical hepatocellular carcinoma (HCC) specimens using DNA microarray datasets.

A. DNA copy numbers of nectin-4 in HCC tumor (T) tissues and their non-tumor (NT) counterparts from Chiang Liver 2, Guichard Liver, Guichard Liver 2, and TGCA datasets deposited in Oncomine. **B.** DNA copy numbers of nectin-4 in HCC samples with different Edmondson-Steiner tumor grades (ES-I, ES-II, and ES-III). **C.** Viral hepatitis status of HCC samples in Guichard Liver. Data shown are box and whiskers with 10 – 90 percentile, and the sample number in each group is indicated in parentheses. P values were calculated by one-way ANOVA followed by Sidak's multiple comparisons tests.

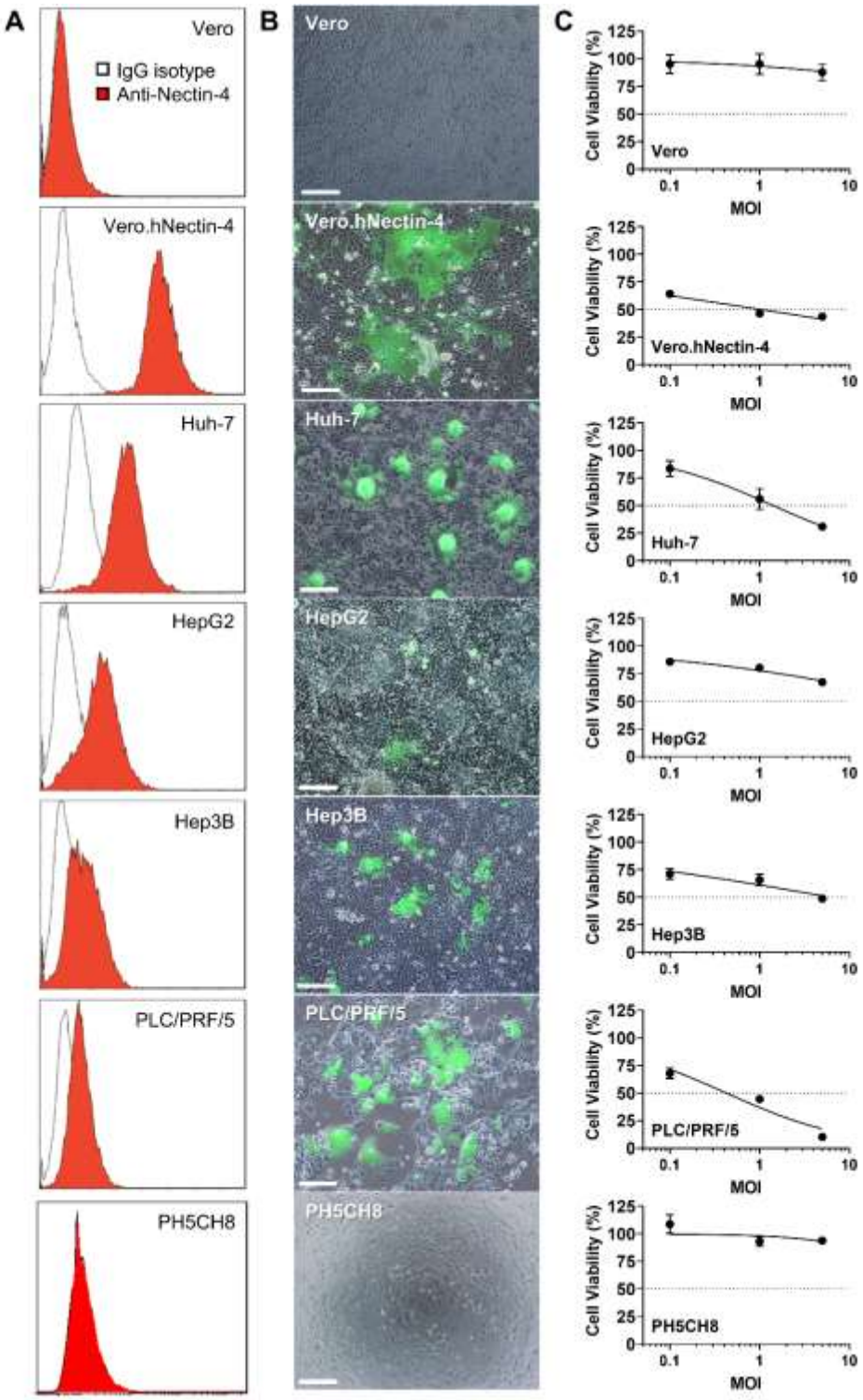

Figure 22. Nectin-4 expression and oncolytic MV infection of human HCC cell lines.
A. Flow cytometry analysis of surface Nectin-4 expression. **B.** Representative micrographs of MV-EGFP infection at 3 dpi (MOI 5). Scale bar = 200 μm. **C.** Cytotoxicity of MV-EGFP (MOI 0.1 – 5) at 7 dpi in each cell line. Data shown are means ± SD from three independent experiments. Vero and PH5CH8 serve as negative controls, and Vero.hNectin-4 is a positive control.

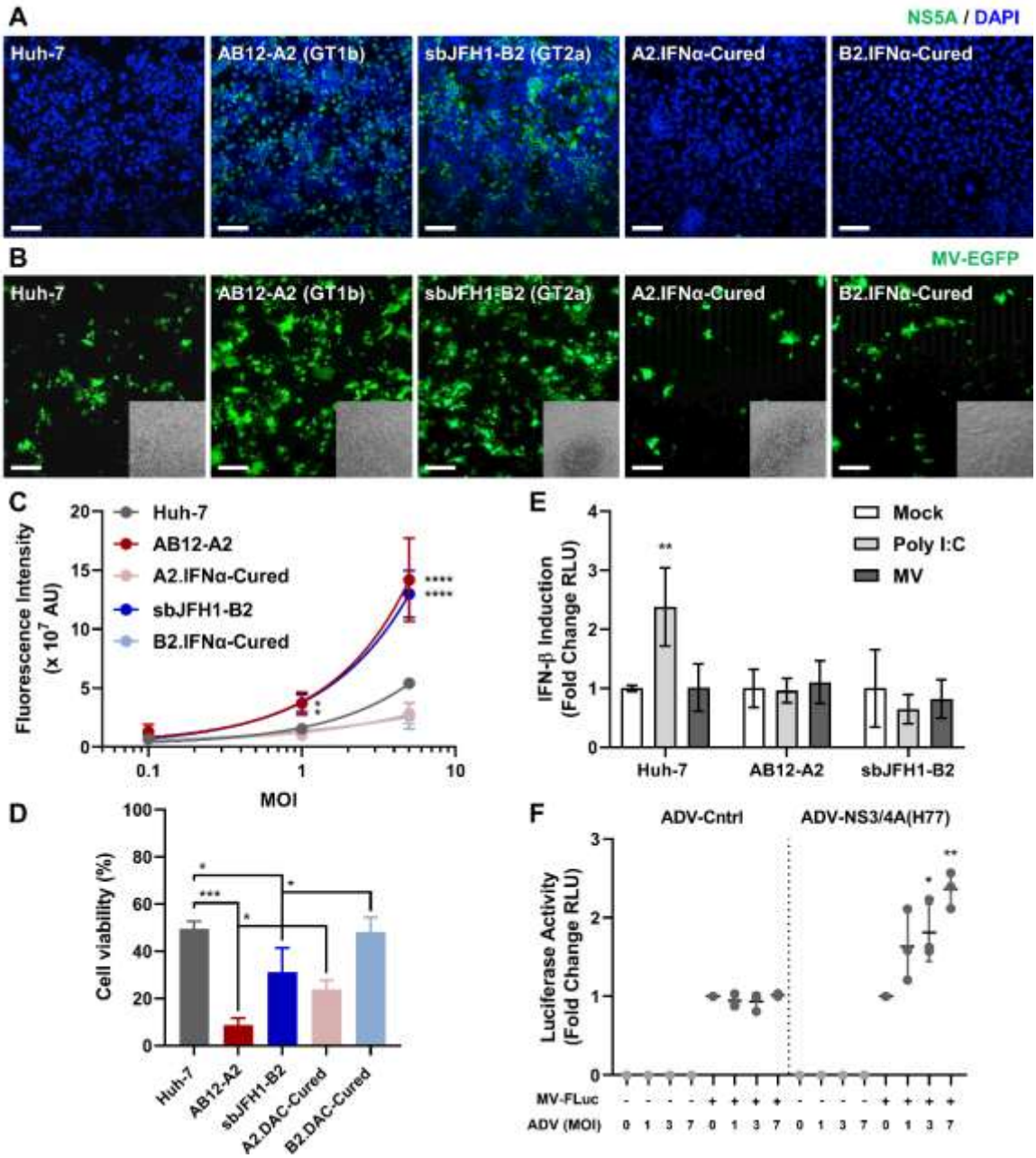

Figure 23. MV infection of Huh-7-based HCV replicons.

A. Immunofluorescence staining of HCV NS5A (Alexa fluor 488) and nuclei (DAPI) in Huh-7, its derivatives HCV replicon cells harboring genotype 1b (AB12-A2) and genotype 2a (sbJFH1-B2) subgenomes, and cured replicon cells. **B.** MV-EGFP infection (MOI 5; 3 dpi) in Huh-7 and HCV replicon cells. All scale bar = 400 μm. **C.** EGFP fluorescence intensity of **B** quantified. **D.** Cytotoxicity of MV measured at 5 dpi. **E.** IFN-β induction in Huh-7 and replicon cells stimulated with poly I:C or MV (MOI 5) for 20 h. **F.** Effect of HCV NS3/4A on MV-FLuc replication. NS3/4A was transiently expressed in Huh-7 cells using the adenoviral vector ADV-NS3/4A(H77) before the cells were infected with MV-Fluc (MOI 0.1; 3 dpi). Luciferase activities were measured and normalized to MV-infected cells without ADV transduction. The control vector ADV-Cntrl served as a negative control. Data shown are means ± SD from three independent experiments. Data were analyzed by ANOVA (*$P < 0.05$; **$P < 0.01$; ****$P < 0.0001$). AU: arbitrary unit; RLU: relative light unit.

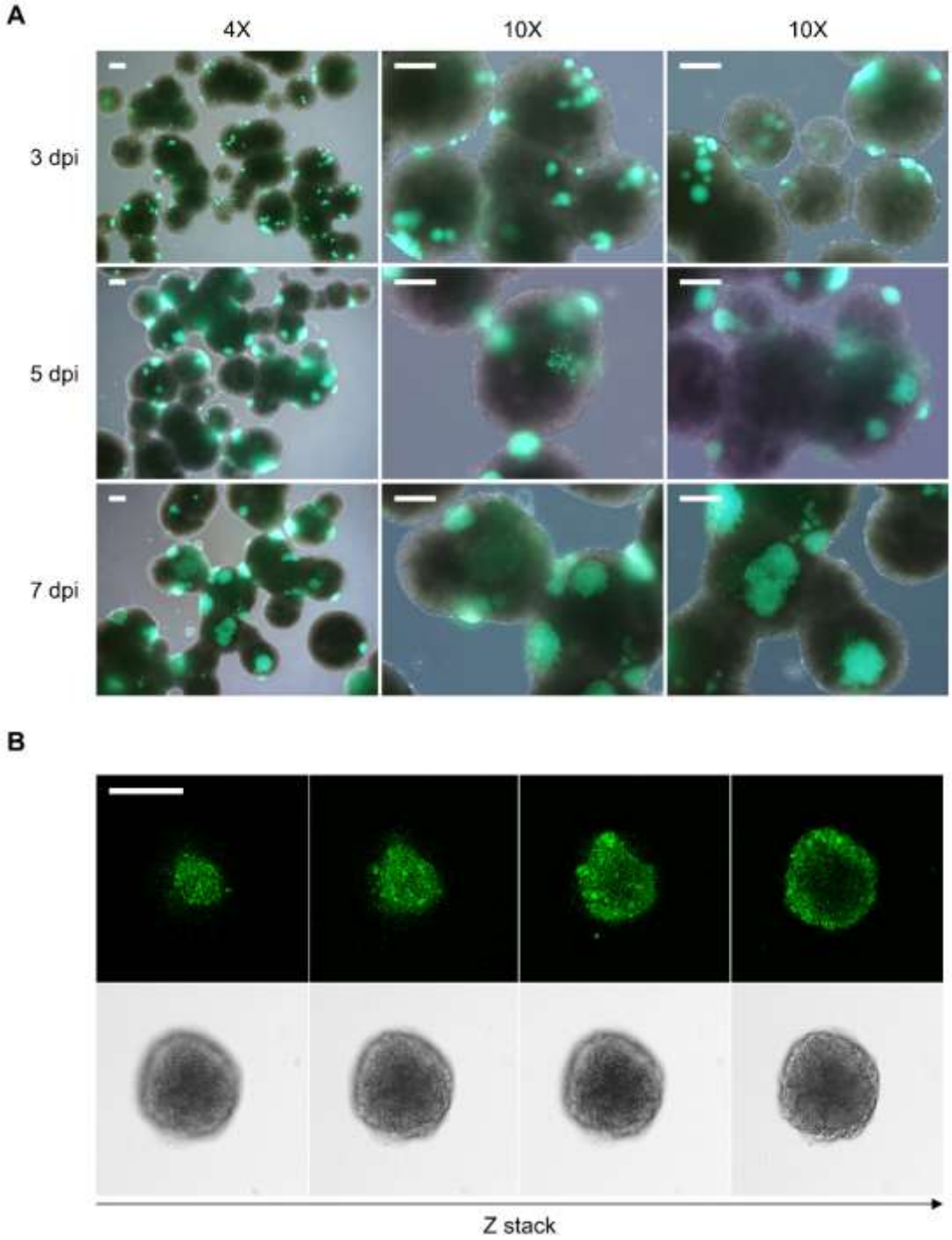

Figure 24. MV infection of Huh-7 tumor spheres.
A. Huh-7 cells were seeded 10-cm dishes (1 x 10^5 cells per dish) coated with 1 % agarose and cultured in 15 ml 10 % FBS DMEM for 7 days before MV infection. Approximately 120 spheres were transferred to a 5 ml tube and infected with MV-EGFP (10^5 $TCID_{50}$) for 2 h, then the virus was removed and spheres were resuspended in 10 % FBS DMEM and cultured in ultra-low attachment 6-well plate. **B.** Confocal microscopy of an infected sphere along the Z stack. Scale bar = 200 μm.

CHAPTER 7 DISCUSSION AND FUTURE DIRECTIONS

7.1. MV as an Oncolytic Agent

Arising in the dawn of 19th century from a unique history of human patient hematological cancer regressions induced by naturally acquired viral infections, including influenza, herpes, viral hepatitis, and notably MV [201], OVs have serendipitously proven their anticancer potential. However fruitful development of safe non-lethal viral agents for therapeutic administrations then was withheld until the availability of recombinant genetic engineering and reverse genetics technology by early 1990s [201], which rekindled and rapidly advanced oncolytic virotherapy research, leading eventually to the first commercial oncolytic viruses – Oncorine H101 (recombinant ADV) approved for treating head and neck cancer in China in 2005, and recombinant HSV-1-based T-VEC approved for metastatic melanoma in the USA, Europe, and Australia in 2015 [202]. Oncorine is licensed as combination treatment with chemotherapy, and T-VEC is the first monotherapy oncolytic virus licensed [202]. Nonetheless as monotherapy, including for T-VEC, the anticancer therapeutic efficacy of oncolytic viruses is most often limited due to premature clearance by patient's immune system, therefore combinatorial administrations commonly with chemotherapy, radiotherapy, and immunotherapy (immunosuppressants, checkpoint inhibitors) are extensively explored as strategies to boost anticancer potency of oncolytic viruses without resorting to increased and/or repeated dosing [157, 202]. Especially, in the case of oncolytic MV, anti-measles immunity is highly prevalent due to widespread routine vaccination, hence the challenge of pre-existing immunity on therapeutic efficacy of MV-

based oncolytics is anticipated particularly for systemic administration, and amelioration by genetic modification and combination therapy could be valuable [46].

Oncolytic MV of various forms (unmodified, recombinant) and strains (wild-type, vaccine) have been used against hematological malignancies as well as different solid tumors [46]. Predominantly, oncolytic MV vectors are derivatives of vaccine strains MV, with a large majority based on the Edmonston-B attenuated vaccine strain (MV-Edm), including the oncolytic recombinant MV engineered to express thyroidal sodium iodide symporter (MV-NIS) [46]. Indeed, eengineered oncolytic MV has gained attention for development as a potential treatment against many cancers, and several MV oncolytics-based clinical trials are ongoing against various cancers, including malignant mesothelioma (NCT01503177), ovarian, fallopian, or peritoneal cancer (NCT02068794, NCT02364713, NCT00408590), metastatic head and neck cancer, breast cancer (NCT01846091), malignant peripheral nerve sheath tumor and neurofibromatosis (NCT02700230), and multiple myeloma (NCT00450814, NCT02192775) [46, 128].

Vaccine lineage MV vectors are conventionally favoured based on two main considerations: firstly, their safety over wild-type pathogenic MV, and secondly the early notion that MV-Edm vaccine strain uses CD46 which is frequently overexpressed in breast and many other cancers. However, the discovery of nectin-4 tumor marker of breast, lung, and ovarian cancers [64-66] as a receptor for MV [23, 24] raised strong attention on the suitability of MV bearing wild-type glycoproteins as oncolytic vectors for targeting nectin-4-positive tumors. Nectin-4 is more selectively overexpressed in tumors and in particular adenocarcinomas including breast, lung, pancreatic, bladder, and ovarian cancers [64-68], and hence a better therapeutic target as compared to CD46 which is ubiquitously expressed

in all nucleated cells although upregulated in different cancer cells [46]. As such, compared to vaccine strain, the wild-type MV glycoprotein is considered to be more specific to nectin-4 as it does not target to CD46 [111]. The use of MV oncolytic vectors with wild-type glycoproteins is thus justified for oncolytic development targeting nectin-4, and further genetic engineering such as by removing the C and V proteins expression [203] or recombination with a vaccine strain backbone could be incorporated to improve its safety. In the current study, the results presented as a proof of concept, the use of a recombinant wild-type MV as oncolytic agent, and demonstrated its ability to efficiently target the nectin-4-expressing breast and HCC tumors cells *in vitro* and *in vivo*. The results from this study along with the above reasons therefore suggest that MV bearing wild-type glycoproteins may serve as a suitable oncolytic vector for treating nectin-4-expressing cancers. Ablation of additional receptor SLAM recognition ("SLAM-blind virus") is possible [204, 205], and has been shown to be a viable strategy to increase nectin-4-specificity of wild-type MV glycoproteins against cancer cells [206-209]. Such approach should also be considered in optimizing MV vectors for future therapeutic development.

7.2. Targeting Nectin-4 as an Oncolytic Strategy

Several studies have looked into how nectin-4 is related to carcinogenesis, particularly in breast cancer models. It was suggested that the extracellular portion of nectin-4 promotes nectin-1-dependent cell-to-cell attachment that contributes to the anchorage-independent growth of cancer cells, and its *cis*-interaction with integrin β4 to activate the Src family kinases may be crucial for the survival of these clustering cells [210]. Nectin-4 is also considered a marker of breast cancer stem cells, as its presence enhances

cell invasion and epithelial-mesenchymal transition and activates the Wnt/β-catenin pathway through the PI3K/Akt axis [211]. In addition, the ectodomain of nectin-4, which could be detected in the sera of breast cancer [212], lung cancer [66], and ovarian cancer [64, 213] patients, has been proposed to *trans*-interact with endothelial integrin β4 to promote angiogenesis through Src-regulated PI3K/Akt pathway [214]. Consistent with the proposed mechanisms, nectin-4 expression positively correlates with tumor size, histopathological grading, and angiogenic markers in clinical specimens, and increased nectin-4 level is associated with metastasis and recurrence [215].

Given nectin-4's limited expression profile in normal tissues including the lung, trachea, skin, and hair follicles, [63, 216], but elevated expression levels in many adenocarcinomas such as breast, bladder, lung, ovarian, and pancreatic cancers [64-68], nectin-4 has risen as an important tumor marker and target for therapy. In breast cancer, it is a hallmark indicative of advanced stage or highly metastatic cancer phenotype [65, 212]. Specifically, nectin-4 has been reported to promote cell survival and proliferation of the breast tumor cells [210]. In addition, the soluble form of nectin-4, which is present and can be detected in the sera from patients with breast or lung cancer [66, 212], could have diagnostic applications for the screening of these cancers. Supporting the role of nectin-4 in cancer progression, it has been shown that blocking nectin-4 using antibodies could inhibit the growth of cell line-derived [210] and patient-derived [138] breast cancer mouse xenografts. In fact, nectin-4 antibodies that are conjugated to anti-neoplastic agents have been developed as a potential treatment to target nectin-4-expressing cancers including primary and metastatic triple-negative breast cancers, as well as cancers of the bladder, lung, and pancreas [133, 138]. Recently, enfortumab vedotin (Padcev; Astellas Pharma US,

Inc.), a nectin-4-directed antibody conjugated with the microtubule-disrupting agent monomethyl auristatin E (MMAE), has been granted accelerated approval by the FDA for the treatment of metastatic urothelial cancer [217]. The antibody-drug conjugate (ADC) has been demonstrated to inhibit breast, bladder, pancreatic, and lung cancer xenografts in mouse models [133] and yielded an objective response rate (ORR) of 43 % in its phase I clinical trial [218]. Enfortumab vedotin has also completed a multicenter phase 2 study (EV-201; NCT03219333) [219] and a global phase 3 study (EV-301; NCT03474107) [220], highlighting the potential of developing targeted therapies for nectin-4-positive cancers. Similarly, the ability of MV to target nectin-4 makes it an advantageous OV platform for development of nectin-4-targeting oncolytic agent.

7.3. Oncolytic Combination Treatment Using Chemovirotherapeutic Approach

Due to their unique viral replicative mechanism, oncolytic viruses kill both chemotherapeutic-sensitive and -resistant tumor cells. Hence, they do not have cross-resistance issues with currently existing therapies and could possibly be potentiated and benefited by supportive treatments. The use of chemotherapeutics can tailor oncolytics as a means to enhance its efficacy through combinatorial treatments [221]. For these reasons, oncolytic virotherapy is often studied in combination with chemotherapy in primary and adjuvant therapy settings [126, 127] to enhance therapeutic outcome. Indeed many combinations reportedly demonstrated synergistic potency plausibly enabled by the distinct anti-cancer mechanisms of oncolytic virotherapy and chemotherapy [222-224], although the combined effect is ultimately dependent on the specific virus and drug used and the cancer type treated [157]. Until now, with the exception cyclophosphamide (CPA)

[222, 225] and doxorubicin [224], there have been few studies combining chemotherapeutic agents with MV therapy. Our findings that combination treatment of CPT or UA-nanoparticles can boost MV efficacy expands the scope of chemovirotherapeutic strategies that can enhance MV oncolytics. Some research studies had examined engineered prodrug convertase-encoding MV as an alternative strategy, such that chemotherapeutic prodrugs can be converted [128]. For example, MV can be armed to encode purine nucleoside phosphorylase (MV-PNP) [226-229], which is responsible for catalyzing the conversion of 2-fluoroadenine and 6-methylpurine from fludarabine and 6-methylpurine-2'-deoxyriboside (MePdR), respectively. Another example is the engineered MV to encode super cytosine deaminase (MV-SCD) [230-234] that mediates the conversion of 5-fluorocytosine (5-FC) into 5-fluorouracil (5-FU). For CPT, the clinically available prodrug is the analog irinotecan, whose active metabolite 7-ethyl-10-hydroxycamptothecin (SN-38, also a topoisomerase I inhibitor) is generated following conversion in the liver and circulates to kill the tumor cells [235]. Over time, most of the SN-38 eventually transforms into its inactive form, which is the metabolite SN-38 glucuronide (SN-38G) that is secreted for elimination in the intestinal lumen where it could be regenerated by the bacterial beta-glucuronidase back into SN-38 [236]. It has been shown that combining intravenous injection of irinotecan and intratumoral injection of oncolytic ADV that expresses beta-glucuronidase yields significantly stronger antitumor activity as compared to treatment with single-agent *in vivo* [237]. Such observation suggests that the combination of CPT or its derivatives with a beta-glucuronidase-expressing oncolytic MV vector could be further explored as a potential strategy to enhance its tumor killing efficacy. Specificity of these chemovirotherapeutic combinations could

also be examined to ensure the safety of this approach and identify potential off-target effects.

7.4. Oncolytic Immunogenicity in the Tumor Microenvironment

Interestingly, while we were exploring the oncolytic potency of MV against breast adenocarcinomas *in vivo* in both immune-deficient and immune-competent mouse models (CHAPTER 3), we observed an enhanced and accelerated treatment outcome in the syngeneic mouse model, implying that the activation of the immune system by the oncolytic MV during infection and lysis of the breast adenocarcinoma cells is critical to ablate the tumors *in vivo*. This effect could possibly be linked to ICD and pro-inflammatory signals released into the tumor microenvironment (TME) during the virus-mediated tumor cell oncolysis, with the recruitment and simulation of immune cells to the tumor site and processing of neo-antigens [75-78]. Indeed, recent studies illustrated that the anti-tumor immune response provoked by ICD, which is accompanied by the exposure and release of the damage-associated molecular patterns (DAMPs) that exert potent adjuvant properties on dying cancer cells for detection by the antigen-presenting cells (APCs), can lead to prolonged therapeutic effects [238, 239]. DAMPs, similar to the pattern-associated molecular patterns (PAMPs) from microbial counterparts, serve as adjuvants and impart a state of crisis in the organism, and includes surface-exposed calreticulin (CRT), secreted adenosine triphosphate (ATP), annexin A1 (ANXA1), released high mobility group protein B1 (HMGB1), heat shock proteins (HSPs), and type I IFNs, among other signals [238]. Collectively, the immunogenicity conferred by tumor cell death in an ICD state involves both the antigenicity induced by neo-antigenic epitopes and adjuvanticity produced by the

specific DAMPs. It is noteworthy that, while apoptosis used to be considered as non-immunogenic, it has been suggested apoptotic cells may also trigger antigen-specific immune response [240]. Indeed, recent studies have observed how OVs can induce ICD in the TME, and ICD hallmarks triggered by MV has previously been observed in mesothelioma [78], melanoma [241], HCC [242], glioblastoma [243] cells, suggesting that MV-induced cancer cell death may be immunogenic [244]. Whether the enhanced oncolytic potency observed in our *in vivo* studies is also associated with ICD remains to be explored.

Nonetheless, the ability of OVs to selectively stimulate a dysfunctional antitumor immune system (transiting the TME from "immune-cold" to "immune-hot") by causing incessant exposure of DAMPs which promotes pathological inflammatory responses, highlights their utility as ICD inducers. As such, OVs have also been explored as a novel system to sensitize tumor cells for promising immunotherapies, and coining the concept of "viro-immunotherapy". For instance, researchers have attempted to introduce cell death inducing factors in OV vectors for an efficient immune-oncolytic therapeutic outcome. Van Hoecke *et al.* demonstrated that intratumoral delivery of mRNA encoding for mixed lineage kinase domain-like (MLKL), a necroptosis (a form of ICD) inducing factor, induced tumor lysis and mediated anti-tumor immunity in tumor mouse models [245]. In follow up studies, they employed vaccinia virus (VACV) for targeted intratumoral delivery of MLKL which led to activation of necroptosis-like tumor cell death *in vitro* [246]. MLKL expressing-VACV vectors induced a noticeable anti-tumor activity, which was coupled with potent intrinsic anti-tumor immunity against neo-antigenic epitopes [246]. Alternatively, expression of CD40 ligand (CD40L) to CD40 receptor on APCs leads to

cancer cell apoptosis and Th-1 immune response, followed by cytotoxic T cells activation and nullified immunosuppression. Using chimeric adenovirus, a groups showed that Ad5/3-hTERT-E1A-hCD40L, which codes for expression of CD40L in the viral backbone, significantly inhibited tumor growth via oncolytic and apoptotic properties *in vivo* [247]. Specifically, the oncolysis mediated by Ad5/3-hTERT-E1A-hCD40L was accompanied by DAMP signals including HMGB1 and ATP release, and augmented CRT exposure, which were indicative of immunogenicity. *In vivo* therapeutic intervention of immunocompromised mice with Ad5/3-hTERT-E1A-hCD40L construct failed to respond with adaptive immune response, while in contrast, immunocompetent mice showed antitumor effects [247]. This antitumor response was characterized by the recruitment and activation of APCs, which led to infiltration of $CD45^+$ cells, macrophages, and T cells with concomitant upregulation of Th-1 cytokines, including IFN-γ, RANTES (aka 'regulated upon activation, normal T cell expressed and secreted'), and tumor necrosis factor-alpha (TNF-α) [247]. Finally, temozolomide (TMZ) is an alkylating agent currently preferred as first-line chemotherapeutic drug for glioblastoma treatment and second-line therapy for astrocytoma, due to its DNA damaging effect followed by apoptotic cell death [248]. Preclinically, Liikanen *et al.* showed that triple combination of oncolytic adenovirus Ad5/3-D24-GMCSF, TMZ, and the alkylating agent CPA on prostate cancer cells, resulted in increased tumor cell autophagy, and triggered ICD indicated by elevated ATP, CRT, and HMGB1 [249]. In an initial clinical trial, they observed anti- and pro-inflammatory cytokines, neutralizing antibodies, and release of HMGB1 which appeared to correlate with tumor-specific T cell responses and resulted in disease control in 67 % of patient cases [249]. These results suggesting the efficacy of oncolytic adenovirus with low-dose TMZ

and CPA in inducing ICD and its oncolytic potency for clinical application. Altogether, these examples illustrate the involvement of ICD with the oncolytic activity of OVs in the presence of immune system and points towards the possibility to enhance efficacy through enhancing the OVs' ability in inducing ICD.

7.5. Conclusion

In conclusion, this thesis has explored the use of recombinant wild-type MV for targeting nectin-4 positive breast and liver cancers, and demonstrated the possibility to enhance MV's oncolytic potency using chemotherapeutics and nanoparticles. This study provides a foundation for future development of MV-based oncolytic virotherapy in the management of breast and liver cancers through targeting nectin-4-positive tumors, and the tailoring of such treatment modality to enhance efficacy.

REFERENCES

1. Holzmann H, Hengel H, Tenbusch M, Doerr HW: **Eradication of measles: remaining challenges**. *Med Microbiol Immunol* 2016, **205**(3):201-208.
2. Tanne JH: **Measles cases and deaths are increasing worldwide, warn health agencies**. *BMJ* 2020, **371**:m4450.
3. Brechot C, Bryant J, Endtz H, Garry RF, Griffin DE, Lewin SR, Mercer N, Osterhaus A, Picot V, Vahlne A *et al*: **2018 international meeting of the Global Virus Network**. *Antiviral Res* 2019, **163**:140-148.
4. Paules CI, Marston HD, Fauci AS: **Measles in 2019 - Going Backward**. *N Engl J Med* 2019, **380**(23):2185-2187.
5. **WHO New Measles Surveillance Data for 2019** [https://www.who.int/immunization/newsroom/measles-data-2019/en/]
6. Guerra FM, Bolotin S, Lim G, Heffernan J, Deeks SL, Li Y, Crowcroft NS: **The basic reproduction number (R**. *Lancet Infect Dis* 2017, **17**(12):e420-e428.
7. Moss WJ: **Measles**. *Lancet* 2017, **390**(10111):2490-2502.
8. Griffin DE: **Measles Virus**. In: *Fields Virology 6th edition.* edn. Edited by Knipe DMH, P.M. Philadelphia: Wolters Kluwer Health/Lippincott Williams & Wilkins; 2013.
9. Roberts L: **Why measles deaths are surging - and coronavirus could make it worse**. *Nature* 2020, **580**(7804):446-447.
10. Strebel PM, Orenstein WA: **Measles**. *N Engl J Med* 2019, **381**(4):349-357.
11. SOMMER A: **Vitamin A prophylaxis**. *Archives of Disease in Childhood* 1997, **77**(3):191-194.
12. Coughlin MM, Beck AS, Bankamp B, Rota PA: **Perspective on Global Measles Epidemiology and Control and the Role of Novel Vaccination Strategies**. *Viruses* 2017, **9**(1).
13. Bankamp B, Takeda M, Zhang Y, Xu W, Rota PA: **Genetic characterization of measles vaccine strains**. *J Infect Dis* 2011, **204 Suppl 1**:S533-548.
14. **Package Insert - M-M-R® II (Measles, Mumps, and Rubella Virus Vaccine Live)** [https://www.fda.gov/vaccines-blood-biologics/vaccines/measles-mumps-and-rubella-virus-vaccine-live]
15. **The immunological basis for immunization series: module 7: measles. Update 2020.** Geneva: World Health Organization; 2020.
16. Pless RP, Bentsi-Enchill AD, Duclos P: **Monitoring vaccine safety during measles mass immunization campaigns: clinical and programmatic issues**. *J Infect Dis* 2003, **187 Suppl 1**:S291-298.
17. Vaccines IoMCtRAEo, Stratton KR, Clayton EW: **Adverse effects of vaccines: evidence and causality**: National Academies Press Washington, DC; 2012.
18. Shaffer JA, Bellini WJ, Rota PA: **The C protein of measles virus inhibits the type I interferon response**. *Virology* 2003, **315**(2):389-397.
19. Schuhmann KM, Pfaller CK, Conzelmann KK: **The measles virus V protein binds to p65 (RelA) to suppress NF-kappaB activity**. *J Virol* 2011, **85**(7):3162-3171.
20. Gotoh B, Komatsu T, Takeuchi K, Yokoo J: **Paramyxovirus accessory proteins as interferon antagonists**. *Microbiol Immunol* 2001, **45**(12):787-800.
21. Griffin DE, Lin WH, Pan CH: **Measles virus, immune control, and persistence**. *FEMS Microbiol Rev* 2012, **36**(3):649-662.

22. Tatsuo H, Ono N, Tanaka K, Yanagi Y: **SLAM (CDw150) is a cellular receptor for measles virus**. *Nature* 2000, **406**(6798):893-897.

23. Mühlebach MD, Mateo M, Sinn PL, Prüfer S, Uhlig KM, Leonard VH, Navaratnarajah CK, Frenzke M, Wong XX, Sawatsky B *et al*: **Adherens junction protein nectin-4 is the epithelial receptor for measles virus**. *Nature* 2011, **480**(7378):530-533.

24. Noyce RS, Bondre DG, Ha MN, Lin LT, Sisson G, Tsao MS, Richardson CD: **Tumor cell marker PVRL4 (nectin 4) is an epithelial cell receptor for measles virus**. *PLoS Pathog* 2011, **7**(8):e1002240.

25. Naniche D, Varior-Krishnan G, Cervoni F, Wild TF, Rossi B, Rabourdin-Combe C, Gerlier D: **Human membrane cofactor protein (CD46) acts as a cellular receptor for measles virus**. *J Virol* 1993, **67**(10):6025-6032.

26. Dorig RE, Marcil A, Chopra A, Richardson CD: **The human CD46 molecule is a receptor for measles virus (Edmonston strain)**. *Cell* 1993, **75**(2):295-305.

27. Iorio RM, Melanson VR, Mahon PJ: **Glycoprotein interactions in paramyxovirus fusion**. *Future Virol* 2009, **4**(4):335-351.

28. Gonçalves-Carneiro D, McKeating JA, Bailey D: **The Measles Virus Receptor SLAMF1 Can Mediate Particle Endocytosis**. *J Virol* 2017, **91**(7).

29. Delpeut S, Sisson G, Black KM, Richardson CD: **Measles Virus Enters Breast and Colon Cancer Cell Lines through a PVRL4-Mediated Macropinocytosis Pathway**. *J Virol* 2017, **91**(10).

30. Crimeen-Irwin B, Ellis S, Christiansen D, Ludford-Menting MJ, Milland J, Lanteri M, Loveland BE, Gerlier D, Russell SM: **Ligand binding determines whether CD46 is internalized by clathrin-coated pits or macropinocytosis**. *J Biol Chem* 2003, **278**(47):46927-46937.

31. Frecha C, Lévy C, Costa C, Nègre D, Amirache F, Buckland R, Russell SJ, Cosset FL, Verhoeyen E: **Measles virus glycoprotein-pseudotyped lentiviral vector-mediated gene transfer into quiescent lymphocytes requires binding to both SLAM and CD46 entry receptors**. *J Virol* 2011, **85**(12):5975-5985.

32. Plemper RK, Brindley MA, Iorio RM: **Structural and mechanistic studies of measles virus illuminate paramyxovirus entry**. *PLoS Pathog* 2011, **7**(6):e1002058.

33. Hashiguchi T, Ose T, Kubota M, Maita N, Kamishikiryo J, Maenaka K, Yanagi Y: **Structure of the measles virus hemagglutinin bound to its cellular receptor SLAM**. *Nature structural & molecular biology* 2011, **18**(2):135-141.

34. Jurgens EM, Mathieu C, Palermo LM, Hardie D, Horvat B, Moscona A, Porotto M: **Measles fusion machinery is dysregulated in neuropathogenic variants**. *mBio* 2015, **6**(1).

35. Mathieu C, Huey D, Jurgens E, Welsch JC, DeVito I, Talekar A, Horvat B, Niewiesk S, Moscona A, Porotto M: **Prevention of measles virus infection by intranasal delivery of fusion inhibitor peptides**. *J Virol* 2015, **89**(2):1143-1155.

36. Watanabe S, Shirogane Y, Sato Y, Hashiguchi T, Yanagi Y: **New Insights into Measles Virus Brain Infections**. *Trends Microbiol* 2019, **27**(2):164-175.

37. Ferren M, Horvat B, Mathieu C: **Measles Encephalitis: Towards New Therapeutics**. *Viruses* 2019, **11**(11).

38. Rima BK, Duprex WP: **The measles virus replication cycle**. *Curr Top Microbiol Immunol* 2009, **329**:77-102.

39. Iwasaki M, Takeda M, Shirogane Y, Nakatsu Y, Nakamura T, Yanagi Y: **The matrix protein of measles virus regulates viral RNA synthesis and assembly by interacting with the nucleocapsid protein**. *J Virol* 2009, **83**(20):10374-10383.

40. Tedcastle A, Cawood R, Di Y, Fisher KD, Seymour LW: **Virotherapy--cancer targeted pharmacology**. *Drug Discov Today* 2012, **17**(5-6):215-220.

41. Seymour LW, Fisher KD: **Oncolytic viruses: finally delivering**. *British journal of cancer* 2016, **114**(4):357-361.

42. Yu W, Fang H: **Clinical trials with oncolytic adenovirus in China**. *Current cancer drug targets* 2007, **7**(2):141-148.

43. Orloff M: **Spotlight on talimogene laherparepvec for the treatment of melanoma lesions in the skin and lymph nodes**. *Oncolytic virotherapy* 2016, **5**:91-98.

44. Cattaneo R, Miest T, Shashkova EV, Barry MA: **Reprogrammed viruses as cancer therapeutics: targeted, armed and shielded**. *Nature reviews Microbiology* 2008, **6**(7):529-540.

45. Kemp V, Lamfers MLM, van der Pluijm G, van den Hoogen BG, Hoeben RC: **Developing oncolytic viruses for clinical use: A consortium approach**. *Cytokine Growth Factor Rev* 2020, **56**:133-140.

46. Msaouel P, Opyrchal M, Dispenzieri A, Peng KW, Federspiel MJ, Russell SJ, Galanis E: **Clinical Trials with Oncolytic Measles Virus: Current Status and Future Prospects**. *Current cancer drug targets* 2018, **18**(2):177-187.

47. Bommareddy PK, Shettigar M, Kaufman HL: **Integrating oncolytic viruses in combination cancer immunotherapy**. *Nat Rev Immunol* 2018, **18**(8):498-513.

48. Kaufman HL, Kohlhapp FJ, Zloza A: **Oncolytic viruses: a new class of immunotherapy drugs**. *Nat Rev Drug Discov* 2015, **14**(9):642-662.

49. Farrera-Sal M, Fillat C, Alemany R: **Effect of Transgene Location, Transcriptional Control Elements and Transgene Features in Armed Oncolytic Adenoviruses**. *Cancers (Basel)* 2020, **12**(4).

50. Peters C, Rabkin SD: **Designing Herpes Viruses as Oncolytics**. *Mol Ther Oncolytics* 2015, **2**.

51. Geletneky K, Hajda J, Angelova AL, Leuchs B, Capper D, Bartsch AJ, Neumann JO, Schoning T, Husing J, Beelte B *et al*: **Oncolytic H-1 Parvovirus Shows Safety and Signs of Immunogenic Activity in a First Phase I/IIa Glioblastoma Trial**. *Mol Ther* 2017, **25**(12):2620-2634.

52. Samson A, Scott KJ, Taggart D, West EJ, Wilson E, Nuovo GJ, Thomson S, Corns R, Mathew RK, Fuller MJ *et al*: **Intravenous delivery of oncolytic reovirus to brain tumor patients immunologically primes for subsequent checkpoint blockade**. *Sci Transl Med* 2018, **10**(422).

53. Saga K, Kaneda Y: **Oncolytic Sendai virus-based virotherapy for cancer: recent advances**. *Oncolytic virotherapy* 2015, **4**:141-147.

54. Ammayappan A, Russell SJ, Federspiel MJ: **Recombinant mumps virus as a cancer therapeutic agent**. *Mol Ther Oncolytics* 2016, **3**:16019.

55. Fox CR, Parks GD: **Parainfluenza Virus Infection Sensitizes Cancer Cells to DNA-Damaging Agents: Implications for Oncolytic Virus Therapy**. *J Virol* 2018, **92**(7).

56. Varudkar N, Oyer JL, Copik A, Parks GD: **Oncolytic parainfluenza virus combines with NK cells to mediate killing of infected and non-infected lung cancer cells within 3D spheroids: role of type I and type III interferon signaling**. *J Immunother Cancer* 2021, **9**(6).

57. Schirrmacher V, van Gool S, Stuecker W: **Breaking Therapy Resistance: An Update on Oncolytic Newcastle Disease Virus for Improvements of Cancer Therapy**. *Biomedicines* 2019, **7**(3).

58. Patel MR, Jacobson BA, Belgum H, Raza A, Sadiq A, Drees J, Wang H, Jay-Dixon J, Etchison R, Federspiel MJ *et al*: **Measles vaccine strains for virotherapy of non-small-cell lung carcinoma**. *J Thorac Oncol* 2014, **9**(8):1101-1110.

59. Al-Shammari AM, Ismaeel FE, Salih SM, Yaseen NY: **Live attenuated measles virus vaccine therapy for locally established malignant glioblastoma tumor cells**. *Oncolytic virotherapy* 2014, **3**:57-68.

60. Zhou S, Li Y, Huang F, Zhang B, Yi T, Li Z, Luo H, He X, Zhong Q, Bian C *et al*: **Live-attenuated measles virus vaccine confers cell contact loss and apoptosis of ovarian cancer cells via ROS-induced silencing of E-cadherin by methylation**. *Cancer Lett* 2012, **318**(1):14-25.

61. Domingo-Musibay E, Allen C, Kurokawa C, Hardcastle JJ, Aderca I, Msaouel P, Bansal A, Jiang H, DeGrado TR, Galanis E: **Measles Edmonston vaccine strain derivatives have potent oncolytic activity against osteosarcoma**. *Cancer Gene Ther* 2014, **21**(11):483-490.

62. Zhang LF, Tan DQ, Jeyasekharan AD, Hsieh WS, Ho AS, Ichiyama K, Ye M, Pang B, Ohba K, Liu X *et al*: **Combination of vaccine-strain measles and mumps virus synergistically kills a wide range of human hematological cancer cells: Special focus on acute myeloid leukemia**. *Cancer Lett* 2014, **354**(2):272-280.

63. Reymond N, Fabre S, Lecocq E, Adelaide J, Dubreuil P, Lopez M: **Nectin4/PRR4, a new afadin-associated member of the nectin family that trans-interacts with nectin1/PRR1 through V domain interaction**. *J Biol Chem* 2001, **276**(46):43205-43215.

64. Derycke MS, Pambuccian SE, Gilks CB, Kalloger SE, Ghidouche A, Lopez M, Bliss RL, Geller MA, Argenta PA, Harrington KM *et al*: **Nectin 4 overexpression in ovarian cancer tissues and serum: potential role as a serum biomarker**. *American journal of clinical pathology* 2010, **134**(5):835-845.

65. Fabre-Lafay S, Monville F, Garrido-Urbani S, Berruyer-Pouyet C, Ginestier C, Reymond N, Finetti P, Sauvan R, Adelaide J, Geneix J *et al*: **Nectin-4 is a new histological and serological tumor associated marker for breast cancer**. *BMC cancer* 2007, **7**:73.

66. Takano A, Ishikawa N, Nishino R, Masuda K, Yasui W, Inai K, Nishimura H, Ito H, Nakayama H, Miyagi Y *et al*: **Identification of nectin-4 oncoprotein as a diagnostic and therapeutic target for lung cancer**. *Cancer research* 2009, **69**(16):6694-6703.

67. Nishiwada S, Sho M, Yasuda S, Shimada K, Yamato I, Akahori T, Kinoshita S, Nagai M, Konishi N, Nakajima Y: **Nectin-4 expression contributes to tumor proliferation, angiogenesis and patient prognosis in human pancreatic cancer**. *J Exp Clin Cancer Res* 2015, **34**:30.

68. Cancer Genome Atlas Research N: **Comprehensive molecular characterization of urothelial bladder carcinoma**. *Nature* 2014, **507**(7492):315-322.

69. Ma J, Sheng Z, Lv Y, Liu W, Yao Q, Pan T, Xu Z, Zhang C, Xu G: **Expression and clinical significance of Nectin-4 in hepatocellular carcinoma**. *OncoTargets and therapy* 2016, **9**:183-190.

70. Billeter MA, Naim HY, Udem SA: **Reverse genetics of measles virus and resulting multivalent recombinant vaccines: applications of recombinant measles viruses**. *Curr Top Microbiol Immunol* 2009, **329**:129-162.

71. Goldberg KB, Blumenthal GM, McKee AE, Pazdur R: **The FDA Oncology Center of Excellence and precision medicine**. *Exp Biol Med (Maywood)* 2017:1535370217740861.

72. Seymour CW, Gomez H, Chang CH, Clermont G, Kellum JA, Kennedy J, Yende S, Angus DC: **Precision medicine for all? Challenges and opportunities for a precision medicine approach to critical illness**. *Crit Care* 2017, **21**(1):257.

73. Russell SJ, Peng KW, Bell JC: **Oncolytic virotherapy**. *Nature biotechnology* 2012, **30**(7):658-670.

74. Miest TS, Cattaneo R: **New viruses for cancer therapy: meeting clinical needs**. *Nature reviews Microbiology* 2014, **12**(1):23-34.

75. Sobol PT, Boudreau JE, Stephenson K, Wan Y, Lichty BD, Mossman KL: **Adaptive antiviral immunity is a determinant of the therapeutic success of oncolytic virotherapy**. *Mol Ther* 2011, **19**(2):335-344.

76. Benencia F, Courreges MC, Conejo-Garcia JR, Mohamed-Hadley A, Zhang L, Buckanovich RJ, Carroll R, Fraser N, Coukos G: **HSV oncolytic therapy upregulates interferon-inducible chemokines and recruits immune effector cells in ovarian cancer**. *Mol Ther* 2005, **12**(5):789-802.

77. Prestwich RJ, Errington F, Ilett EJ, Morgan RS, Scott KJ, Kottke T, Thompson J, Morrison EE, Harrington KJ, Pandha HS *et al*: **Tumor infection by oncolytic reovirus primes adaptive antitumor immunity**. *Clinical cancer research : an official journal of the American Association for Cancer Research* 2008, **14**(22):7358-7366.

78. Gauvrit A, Brandler S, Sapede-Peroz C, Boisgerault N, Tangy F, Gregoire M: **Measles virus induces oncolysis of mesothelioma cells and allows dendritic cells to cross-prime tumor-specific CD8 response**. *Cancer research* 2008, **68**(12):4882-4892.

79. Pardoll DM: **The blockade of immune checkpoints in cancer immunotherapy**. *Nature reviews Cancer* 2012, **12**(4):252-264.

80. Workenhe ST, Verschoor ML, Mossman KL: **The role of oncolytic virus immunotherapies to subvert cancer immune evasion**. *Future oncology* 2015, **11**(4):675-689.

81. Twumasi-Boateng K, Pettigrew JL, Kwok YYE, Bell JC, Nelson BH: **Oncolytic viruses as engineering platforms for combination immunotherapy**. *Nature reviews Cancer* 2018, **18**(7):419-432.

82. Lin SF, Gao SP, Price DL, Li S, Chou TC, Singh P, Huang YY, Fong Y, Wong RJ: **Synergy of a herpes oncolytic virus and paclitaxel for anaplastic thyroid cancer**. *Clinical cancer research : an official journal of the American Association for Cancer Research* 2008, **14**(5):1519-1528.

83. Marchini A, Scott EM, Rommelaere J: **Overcoming Barriers in Oncolytic Virotherapy with HDAC Inhibitors and Immune Checkpoint Blockade**. *Viruses* 2016, **8**(1).

84. Dornan MH, Krishnan R, Macklin AM, Selman M, El Sayes N, Son HH, Davis C, Chen A, Keillor K, Le PJ *et al*: **First-in-class small molecule potentiators of cancer virotherapy**. *Scientific reports* 2016, **6**:26786.

85. Gujar S, Bell J, Diallo JS: **SnapShot: Cancer Immunotherapy with Oncolytic Viruses**. *Cell* 2019, **176**(5):1240-1240 e1241.

86. Stojdl DF, Lichty BD, tenOever BR, Paterson JM, Power AT, Knowles S, Marius R, Reynard J, Poliquin L, Atkins H *et al*: **VSV strains with defects in their ability to shutdown innate immunity are potent systemic anti-cancer agents**. *Cancer Cell* 2003, **4**(4):263-275.

87. Russell SJ, Federspiel MJ, Peng KW, Tong C, Dingli D, Morice WG, Lowe V, O'Connor MK, Kyle RA, Leung N *et al*: **Remission of disseminated cancer after systemic oncolytic virotherapy**. *Mayo Clin Proc* 2014, **89**(7):926-933.

88. Knuchel MC, Marty RR, Morin TN, Ilter O, Zuniga A, Naim HY: **Relevance of a pre-existing measles immunity prior immunization with a recombinant measles virus vector**. *Human vaccines & immunotherapeutics* 2013, **9**(3):599-606.

89. Ricca JM, Oseledchyk A, Walther T, Liu C, Mangarin L, Merghoub T, Wolchok JD, Zamarin D: **Pre-existing Immunity to Oncolytic Virus Potentiates Its Immunotherapeutic Efficacy**. *Molecular Therapy* 2018, **26**(4):1008-1019.

90. Dhar D, Spencer JF, Toth K, Wold WSM: **Effect of Preexisting Immunity on Oncolytic Adenovirus Vector INGN 007 Antitumor Efficacy in Immunocompetent and Immunosuppressed Syrian Hamsters**. *Journal of Virology* 2009, **83**(5):2130-2139.

91. Fukuhara H, Ino Y, Todo T: **Oncolytic virus therapy: A new era of cancer treatment at dawn**. *Cancer science* 2016, **107**(10):1373-1379.

92. Franke V, Berger DMS, Klop WMC, van der Hiel B, van de Wiel BA, Ter Meulen S, Wouters M, van Houdt WJ, van Akkooi ACJ: **High response rates for T-VEC in early metastatic melanoma (stage IIIB/C-IVM1a)**. *Int J Cancer* 2019, **145**(4):974-978.

93. **World Health Organization (WHO). http://www.who.int/**

94. Reale A, Vitiello A, Conciatori V, Parolin C, Calistri A, Palu G: **Perspectives on immunotherapy via oncolytic viruses**. *Infect Agent Cancer* 2019, **14**:5.

95. Msaouel P, Opyrchal M, Domingo Musibay E, Galanis E: **Oncolytic measles virus strains as novel anticancer agents**. *Expert opinion on biological therapy* 2013, **13**(4):483-502.

96. Nosaki K, Hamada K, Takashima Y, Sagara M, Matsumura Y, Miyamoto S, Hijikata Y, Okazaki T, Nakanishi Y, Tani K: **A novel, polymer-coated oncolytic measles virus overcomes immune suppression and induces robust antitumor activity**. *Mol Ther Oncolytics* 2016, **3**:16022.

97. Mader EK, Maeyama Y, Lin Y, Butler GW, Russell HM, Galanis E, Russell SJ, Dietz AB, Peng KW: **Mesenchymal Stem Cell Carriers Protect Oncolytic Measles Viruses from Antibody Neutralization in an Orthotopic Ovarian Cancer Therapy Model**. *Clinical Cancer Research* 2009, **15**(23):7246-7255.

98. Castleton A, Dey A, Beaton B, Patel B, Aucher A, Davis DM, Fielding AK: **Human mesenchymal stromal cells deliver systemic oncolytic measles virus to treat acute lymphoblastic leukemia in the presence of humoral immunity**. *Blood* 2014, **123**(9):1327-1335.

99. **Oncolytic Virus Clinical Trials, 2017.** [www.ta-scan.com]

100. Sung H, Ferlay J, Siegel RL, Laversanne M, Soerjomataram I, Jemal A, Bray F: **Global Cancer Statistics 2020: GLOBOCAN Estimates of Incidence and Mortality Worldwide for 36 Cancers in 185 Countries**. *CA Cancer J Clin* 2021, **71**(3):209-249.

101. American Cancer Society: **Breast cancer facts & figures 2019-2020**. In. Atlanta: American Cancer Society, Inc.; 2019.

102. Siegel RL, Miller KD, Jemal A: **Cancer statistics, 2020**. *CA Cancer J Clin* 2020, **70**(1):7-30.

103. Cody JJ, Hurst DR: **Promising oncolytic agents for metastatic breast cancer treatment**. *Oncolytic virotherapy* 2015, **4**:63-73.

104. Cardoso F, Senkus E, Costa A, Papadopoulos E, Aapro M, Andre F, Harbeck N, Aguilar Lopez B, Barrios CH, Bergh J *et al*: **4th ESO-ESMO International Consensus Guidelines for Advanced Breast Cancer (ABC 4)dagger**. *Ann Oncol* 2018, **29**(8):1634-1657.

105. **Paclitaxel (conventional): Drug information** [https://www.uptodate.com/contents/paclitaxel-conventional-drug-information]

106. **Doxorubicin (conventional): Drug information** [https://www.uptodate.com/contents/doxorubicin-conventional-drug-information]

107. Farazi PA, DePinho RA: **Hepatocellular carcinoma pathogenesis: from genes to environment**. *Nature reviews Cancer* 2006, **6**(9):674-687.

108. **Canadian Cancer Statistics Advisory Committee. Canadian Cancer Statistics 2013. Toronto, ON: Canadian Cancer Society**. 2013.

109. El-Serag HB: **Hepatocellular carcinoma**. *N Engl J Med* 2011, **365**(12):1118-1127.

110. Lin S, Hoffmann K, Schemmer P: **Treatment of hepatocellular carcinoma: a systematic review**. *Liver cancer* 2012, **1**(3-4):144-158.

111. Lin LT, Richardson CD: **The Host Cell Receptors for Measles Virus and Their Interaction with the Viral Hemagglutinin (H) Protein**. *Viruses* 2016, **8**(9).

112. Liszewski MK, Post TW, Atkinson JP: **Membrane cofactor protein (MCP or CD46): newest member of the regulators of complement activation gene cluster**. *Annual review of immunology* 1991, **9**:431-455.

113. Wilson JA, Jayasena S, Khvorova A, Sabatinos S, Rodrigue-Gervais IG, Arya S, Sarangi F, Harris-Brandts M, Beaulieu S, Richardson CD: **RNA interference blocks gene expression and RNA**

synthesis from hepatitis C replicons propagated in human liver cells. *Proc Natl Acad Sci U S A* 2003, **100**(5):2783-2788.

114. Lin LT, Chung CY, Hsu WC, Chang SP, Hung TC, Shields J, Russell RS, Lin CC, Li CF, Yen MH *et al*: **Saikosaponin b2 is a naturally occurring terpenoid that efficiently inhibits hepatitis C virus entry**. *J Hepatol* 2015, **62**(3):541-548.

115. Chou T-C: **Theoretical Basis, Experimental Design, and Computerized Simulation of Synergism and Antagonism in Drug Combination Studies**. *Pharmacological Reviews* 2006, **58**(3):621-681.

116. Tai CJ, Li CL, Tai CJ, Wang CK, Lin LT: **Early Viral Entry Assays for the Identification and Evaluation of Antiviral Compounds**. *J Vis Exp* 2015(105):e53124.

117. Lin LT, Chen TY, Chung CY, Noyce RS, Grindley TB, McCormick C, Lin TC, Wang GH, Lin CC, Richardson CD: **Hydrolyzable tannins (chebulagic acid and punicalagin) target viral glycoprotein-glycosaminoglycan interactions to inhibit herpes simplex virus 1 entry and cell-to-cell spread**. *J Virol* 2011, **85**(9):4386-4398.

118. Rasbach A, Abel T, Munch RC, Boller K, Schneider-Schaulies J, Buchholz CJ: **The receptor attachment function of measles virus hemagglutinin can be replaced with an autonomous protein that binds Her2/neu while maintaining its fusion-helper function**. *J Virol* 2013, **87**(11):6246-6256.

119. Liu CH, Lin CC, Hsu WC, Chung CY, Lin CC, Jassey A, Chang SP, Tai CJ, Tai CJ, Shields J *et al*: **Highly bioavailable silibinin nanoparticles inhibit HCV infection**. *Gut* 2017, **66**(10):1853-1861.

120. Convention USP: **The United States Pharmacopeia : USP 29 : the National Formulary : NF 24 : by authority of the United States Pharmacopeial Convention, Inc., meeting at Washington, D.C., March 9-13, 2005**: Rockville, Md. : United States Pharmacopeial Convention, cop. 2005.; 2005.

121. Liu P, De Wulf O, Laru J, Heikkila T, van Veen B, Kiesvaara J, Hirvonen J, Peltonen L, Laaksonen T: **Dissolution studies of poorly soluble drug nanosuspensions in non-sink conditions**. *AAPS PharmSciTech* 2013, **14**(2):748-756.

122. Sun DD, Wen H, Taylor LS: **Non-Sink Dissolution Conditions for Predicting Product Quality and In Vivo Performance of Supersaturating Drug Delivery Systems**. *J Pharm Sci* 2016, **105**(9):2477-2488.

123. Lin R, Genin P, Mamane Y, Hiscott J: **Selective DNA binding and association with the CREB binding protein coactivator contribute to differential activation of alpha/beta interferon genes by interferon regulatory factors 3 and 7**. *Mol Cell Biol* 2000, **20**(17):6342-6353.

124. Dekkers JF, Alieva M, Wellens LM, Ariese HCR, Jamieson PR, Vonk AM, Amatngalim GD, Hu H, Oost KC, Snippert HJG *et al*: **High-resolution 3D imaging of fixed and cleared organoids**. *Nat Protoc* 2019, **14**(6):1756-1771.

125. Torre LA, Bray F, Siegel RL, Ferlay J, Lortet-Tieulent J, Jemal A: **Global cancer statistics, 2012**. *CA Cancer J Clin* 2015, **65**(2):87-108.

126. Pol JG, Levesque S, Workenhe ST, Gujar S, Le Boeuf F, Clements DR, Fahrner JE, Fend L, Bell JC, Mossman KL *et al*: **Trial watch: oncolytic viro-immunotherapy of hematologic and solid tumors**. *Oncoimmunology* 2018, **7**(12):e1503032.

127. Raja J, Ludwig JM, Gettinger SN, Schalper KA, Kim HS: **Oncolytic virus immunotherapy: future prospects for oncology**. *J Immunother Cancer* 2018, **6**(1):140.

128. Aref S, Bailey K, Fielding A: **Measles to the rescue: a review of oncolytic measles virus**. *Viruses* 2016, **8**(10).

129. Takai Y, Miyoshi J, Ikeda W, Ogita H: **Nectins and nectin-like molecules: roles in contact inhibition of cell movement and proliferation**. *Nat Rev Mol Cell Biol* 2008, **9**(8):603-615.

130. Deng H, Shi H, Chen L, Zhou Y, Jiang J: **Over-expression of Nectin-4 promotes progression of esophageal cancer and correlates with poor prognosis of the patients**. *Cancer Cell Int* 2019, **19**:106.

131. Zhang Y, Chen P, Yin W, Ji Y, Shen Q, Ni Q: **Nectin-4 promotes gastric cancer progression via the PI3K/AKT signaling pathway**. *Hum Pathol* 2018, **72**:107-116.

132. Zhang J, Liu K, Peng P, Li S, Ye Z, Su Y, Liu S, Qin M, Huang J: **Upregulation of nectin-4 is associated with ITGB1 and vasculogenic mimicry and may serve as a predictor of poor prognosis in colorectal cancer**. *Oncol Lett* 2019, **18**(2):1163-1170.

133. Challita-Eid PM, Satpayev D, Yang P, An Z, Morrison K, Shostak Y, Raitano A, Nadell R, Liu W, Lortie DR *et al*: **Enfortumab Vedotin Antibody-Drug Conjugate Targeting Nectin-4 Is a Highly Potent Therapeutic Agent in Multiple Preclinical Cancer Models**. *Cancer research* 2016, **76**(10):3003-3013.

134. Lemos de Matos A, Franco LS, McFadden G: **Oncolytic Viruses and the Immune System: The Dynamic Duo**. *Mol Ther Methods Clin Dev* 2020, **17**:349-358.

135. Pulaski BA, Ostrand-Rosenberg S: **Mouse 4T1 breast tumor model**. *Current protocols in immunology / edited by John E Coligan [et al]* 2001, **Chapter 20**:Unit 20 22.

136. Rashid OM, Nagahashi M, Ramachandran S, Dumur C, Schaum J, Yamada A, Terracina KP, Milstien S, Spiegel S, Takabe K: **An improved syngeneic orthotopic murine model of human breast cancer progression**. *Breast Cancer Res Treat* 2014, **147**(3):501-512.

137. Le Naour A, Rossary A, Vasson MP: **EO771, is it a well-characterized cell line for mouse mammary cancer model? Limit and uncertainty**. *Cancer Med* 2020, **9**(21):8074-8085.

138. M-Rabet M, Cabaud O, Josselin E, Finetti P, Castellano R, Farina A, Agavnian-Couquiaud E, Saviane G, Collette Y, Viens P *et al*: **Nectin-4: a new prognostic biomarker for efficient therapeutic targeting of primary and metastatic triple-negative breast cancer**. *Ann Oncol* 2017, **28**(4):769-776.

139. Lattanzio R, Ghasemi R, Brancati F, Sorda RL, Tinari N, Perracchio L, Iacobelli S, Mottolese M, Natali PG, Piantelli M: **Membranous Nectin-4 expression is a risk factor for distant relapse of T1-T2, N0 luminal-A early breast cancer**. *Oncogenesis* 2014, **3**:e118.

140. Rajc J, Gugic D, Frohlich I, Marjanovic K, Dumencic B: **Prognostic role of Nectin-4 expression in luminal B (HER2 negative) breast cancer**. *Pathol Res Pract* 2017, **213**(9):1102-1108.

141. Russell SJ, Peng KW: **Viruses as anticancer drugs**. *Trends in pharmacological sciences* 2007, **28**(7):326-333.

142. Ribacka C, Hemminki A: **Virotherapy as an approach against cancer stem cells**. *Current gene therapy* 2008, **8**(2):88-96.

143. Ingemarsdotter CK, Baird SK, Connell CM, Oberg D, Hallden G, McNeish IA: **Low-dose paclitaxel synergizes with oncolytic adenoviruses via mitotic slippage and apoptosis in ovarian cancer**. *Oncogene* 2010, **29**(45):6051-6063.

144. Myers R, Greiner S, Harvey M, Soeffker D, Frenzke M, Abraham K, Shaw A, Rozenblatt S, Federspiel MJ, Russell SJ *et al*: **Oncolytic activities of approved mumps and measles vaccines for therapy of ovarian cancer**. *Cancer Gene Ther* 2005, **12**(7):593-599.

145. Fountzilas C, Patel S, Mahalingam D: **Review: Oncolytic virotherapy, updates and future directions**. *Oncotarget* 2017, **8**(60):102617-102639.

146. Simpson GR, Relph K, Harrington K, Melcher A, Pandha H: **Cancer immunotherapy via combining oncolytic virotherapy with chemotherapy: recent advances**. *Oncolytic virotherapy* 2016, **5**:1-13.

147. Pommier Y: **Topoisomerase I inhibitors: camptothecins and beyond**. *Nature reviews Cancer* 2006, **6**(10):789-802.

148. Gupta M, Fan S, Zhan Q, Kohn KW, O'Connor PM, Pommier Y: **Inactivation of p53 increases the cytotoxicity of camptothecin in human colon HCT116 and breast MCF-7 cancer cells**. *Clinical cancer research : an official journal of the American Association for Cancer Research* 1997, **3**(9):1653-1660.

149. Legarza K, Yang LX: **New molecular mechanisms of action of camptothecin-type drugs**. *Anticancer Res* 2006, **26**(5A):3301-3305.

150. Esolen LM, Park SW, Hardwick JM, Griffin DE: **Apoptosis as a cause of death in measles virus-infected cells**. *J Virol* 1995, **69**(6):3955-3958.

151. Bhaskar A, Bala J, Varshney A, Yadava P: **Expression of measles virus nucleoprotein induces apoptosis and modulates diverse functional proteins in cultured mammalian cells**. *PLoS One* 2011, **6**(4):e18765.

152. Binz E, Lauer UM: **Chemovirotherapy: combining chemotherapeutic treatment with oncolytic virotherapy**. *Oncolytic virotherapy* 2015, **4**:39-48.

153. Chou TC: **Drug combination studies and their synergy quantification using the Chou-Talalay method**. *Cancer research* 2010, **70**(2):440-446.

154. Lin LT, Chen TY, Lin SC, Chung CY, Lin TC, Wang GH, Anderson R, Lin CC, Richardson CD: **Broad-spectrum antiviral activity of chebulagic acid and punicalagin against viruses that use glycosaminoglycans for entry**. *BMC microbiology* 2013, **13**:187.

155. Chaitanya GV, Steven AJ, Babu PP: **PARP-1 cleavage fragments: signatures of cell-death proteases in neurodegeneration**. *Cell Commun Signal* 2010, **8**:31.

156. Ottolino-Perry K, Diallo JS, Lichty BD, Bell JC, McCart JA: **Intelligent design: combination therapy with oncolytic viruses**. *Mol Ther* 2010, **18**(2):251-263.

157. Wennier ST, Liu J, McFadden G: **Bugs and drugs: oncolytic virotherapy in combination with chemotherapy**. *Curr Pharm Biotechnol* 2012, **13**(9):1817-1833.

158. Nguyen A, Ho L, Wan Y: **Chemotherapy and Oncolytic Virotherapy: Advanced Tactics in the War against Cancer**. *Front Oncol* 2014, **4**:145.

159. Rozieres A, Viret C, Faure M: **Autophagy in Measles Virus Infection**. *Viruses* 2017, **9**(12).

160. Lamparska-Przybysz M, Gajkowska B, Motyl T: **Cathepsins and BID are involved in the molecular switch between apoptosis and autophagy in breast cancer MCF-7 cells exposed to camptothecin**. *J Physiol Pharmacol* 2005, **56 Suppl 3**:159-179.

161. Zhang JW, Zhang SS, Song JR, Sun K, Zong C, Zhao QD, Liu WT, Li R, Wu MC, Wei LX: **Autophagy inhibition switches low-dose camptothecin-induced premature senescence to apoptosis in human colorectal cancer cells**. *Biochem Pharmacol* 2014, **90**(3):265-275.

162. Chung Y, Lee J, Jung S, Lee Y, Cho JW, Oh YJ: **Dysregulated autophagy contributes to caspase-dependent neuronal apoptosis**. *Cell Death Dis* 2018, **9**(12):1189.

163. **Irinotecan (conventional): Drug information** [https://www.uptodate.com/contents/irinotecan-conventional-drug-information]

164. **Topotecan: Drug information** [https://www.uptodate.com/contents/topotecan-drug-information]

165. Tran S, DeGiovanni PJ, Piel B, Rai P: **Cancer nanomedicine: a review of recent success in drug delivery**. *Clin Transl Med* 2017, **6**(1):44.

166. Sebastian R: **Nanomedicine - the Future of Cancer Treatment: A Review**. *J Cancer Prev Curr Res* 2017, **8**(1).

167. Gunasekaran T, Haile T, Nigusse T, Dhanaraju MD: **Nanotechnology: an effective tool for enhancing bioavailability and bioactivity of phytomedicine**. *Asian Pac J Trop Biomed* 2014, **4**(Suppl 1):S1-7.

168. Wozniak L, Skapska S, Marszalek K: **Ursolic Acid--A Pentacyclic Triterpenoid with a Wide Spectrum of Pharmacological Activities**. *Molecules* 2015, **20**(11):20614-20641.

169. Seo DY, Lee SR, Heo JW, No MH, Rhee BD, Ko KS, Kwak HB, Han J: **Ursolic acid in health and disease**. *Korean J Physiol Pharmacol* 2018, **22**(3):235-248.

170. Iqbal J, Abbasi BA, Ahmad R, Mahmood T, Kanwal S, Ali B, Khalil AT, Shah SA, Alam MM, Badshah H: **Ursolic acid a promising candidate in the therapeutics of breast cancer: Current status and future implications**. *Biomed Pharmacother* 2018, **108**:752-756.

171. Badrinath N, Heo J, Yoo SY: **Viruses as nanomedicine for cancer**. *Int J Nanomedicine* 2016, **11**:4835-4847.

172. Maroun J, Munoz-Alia M, Ammayappan A, Schulze A, Peng KW, Russell S: **Designing and building oncolytic viruses**. *Future Virol* 2017, **12**(4):193-213.

173. Kajstura M, Halicka HD, Pryjma J, Darzynkiewicz Z: **Discontinuous fragmentation of nuclear DNA during apoptosis revealed by discrete "sub-G1" peaks on DNA content histograms**. *Cytometry A* 2007, **71**(3):125-131.

174. Kaufmann SH, Desnoyers S, Ottaviano Y, Davidson NE, Poirier GG: **Specific proteolytic cleavage of poly(ADP-ribose) polymerase: an early marker of chemotherapy-induced apoptosis**. *Cancer research* 1993, **53**(17):3976-3985.

175. Jambhekar SS, Breen PJ: **Drug dissolution: significance of physicochemical properties and physiological conditions**. *Drug Discovery Today* 2013, **18**(23-24):1173-1184.

176. Zhao C, Yin S, Dong Y, Guo X, Fan L, Ye M, Hu H: **Autophagy-dependent EIF2AK3 activation compromises ursolic acid-induced apoptosis through upregulation of MCL1 in MCF-7 human breast cancer cells**. *Autophagy* 2013, **9**(2):196-207.

177. Tanida I, Waguri S: **Measurement of autophagy in cells and tissues**. *Methods Mol Biol* 2010, **648**:193-214.

178. Holliday DL, Speirs V: **Choosing the right cell line for breast cancer research**. *Breast Cancer Res* 2011, **13**(4):215.

179. Lacroix M, Leclercq G: **Relevance of breast cancer cell lines as models for breast tumours: an update**. *Breast Cancer Res Tr* 2004, **83**(3):249-289.

180. Ito M, Yamamoto T, Watanabe M, Ihara T, Kamiya H, Sakurai M: **Detection of measles virus-induced apoptosis of human monocytic cell line (THP-1) by DNA fragmentation ELISA**. *FEMS Immunol Med Microbiol* 1996, **15**(2-3):115-122.

181. Wang JS, Ren TN, Xi T: **Ursolic acid induces apoptosis by suppressing the expression of FoxM1 in MCF-7 human breast cancer cells**. *Med Oncol* 2012, **29**(1):10-15.

182. Ryu SY, Lee CK, Lee CO, Kim HS, Zee OP: **Antiviral triterpenes from *Prunella vulgaris***. *Archives of Pharmacal Research* 1992, **15**(3):242-245.

183. Xu HX, Zeng FQ, Wan M, Sim KY: **Anti-HIV triterpene acids from Geum japonicum**. *J Nat Prod* 1996, **59**(7):643-645.

184. Chiang LC, Ng LT, Cheng PW, Chiang W, Lin CC: **Antiviral activities of extracts and selected pure constituents of Ocimum basilicum**. *Clin Exp Pharmacol Physiol* 2005, **32**(10):811-816.

185. Kim S, Thiessen PA, Bolton EE, Chen J, Fu G, Gindulyte A, Han L, He J, He S, Shoemaker BA *et al*: **PubChem Substance and Compound databases**. *Nucleic Acids Res* 2016, **44**(D1):D1202-1213.

186. Galvao J, Davis B, Tilley M, Normando E, Duchen MR, Cordeiro MF: **Unexpected low-dose toxicity of the universal solvent DMSO**. *FASEB J* 2014, **28**(3):1317-1330.

187. Rosen HR: **Emerging concepts in immunity to hepatitis C virus infection**. *The Journal of clinical investigation* 2013, **123**(10):4121-4130.

188. Chiang DY, Villanueva A, Hoshida Y, Peix J, Newell P, Minguez B, LeBlanc AC, Donovan DJ, Thung SN, Sole M *et al*: **Focal gains of VEGFA and molecular classification of hepatocellular carcinoma**. *Cancer research* 2008, **68**(16):6779-6788.

189. Guichard C, Amaddeo G, Imbeaud S, Ladeiro Y, Pelletier L, Maad IB, Calderaro J, Bioulac-Sage P, Letexier M, Degos F *et al*: **Integrated analysis of somatic mutations and focal copy-number changes identifies key genes and pathways in hepatocellular carcinoma**. *Nat Genet* 2012, **44**(6):694-698.

190. Martins-Filho SN, Paiva C, Azevedo RS, Alves VAF: **Histological Grading of Hepatocellular Carcinoma-A Systematic Review of Literature**. *Front Med (Lausanne)* 2017, **4**:193.

191. Ikeda M, Sugiyama K, Mizutani T, Tanaka T, Tanaka K, Sekihara H, Shimotohno K, Kato N: **Human hepatocyte clonal cell lines that support persistent replication of hepatitis C virus**. *Virus Res* 1998, **56**(2):157-167.

192. Horner SM, Gale M, Jr.: **Regulation of hepatic innate immunity by hepatitis C virus**. *Nat Med* 2013, **19**(7):879-888.

193. Gerlier D, Valentin H: **Measles virus interaction with host cells and impact on innate immunity**. *Curr Top Microbiol Immunol* 2009, **329**:163-191.

194. Villanueva A: **Hepatocellular Carcinoma**. *N Engl J Med* 2019, **380**(15):1450-1462.

195. Li Y, Shen Y, Zhao R, Samudio I, Jia W, Bai X, Liang T: **Oncolytic virotherapy in hepato-bilio-pancreatic cancer: The key to breaking the log jam?** *Cancer Med* 2020, **9**(9):2943-2959.

196. Heo J, Reid T, Ruo L, Breitbach CJ, Rose S, Bloomston M, Cho M, Lim HY, Chung HC, Kim CW *et al*: **Randomized dose-finding clinical trial of oncolytic immunotherapeutic vaccinia JX-594 in liver cancer**. *Nat Med* 2013, **19**(3):329-336.

197. Moehler M, Heo J, Lee HC, Tak WY, Chao Y, Paik SW, Yim HJ, Byun KS, Baron A, Ungerechts G *et al*: **Vaccinia-based oncolytic immunotherapy Pexastimogene Devacirepvec in patients with advanced hepatocellular carcinoma after sorafenib failure: a randomized multicenter Phase IIb trial (TRAVERSE)**. *Oncoimmunology* 2019, **8**(8):1615817.

198. **Pexa-Vec/Nexavar combination fails phase III trial in liver cancer** [https://www.genengnews.com/news/pexa-vec-nexavar-combination-fails-phase-iii-trial-in-liver-cancer/]

199. Pardee AD, Butterfield LH: **Immunotherapy of hepatocellular carcinoma: Unique challenges and clinical opportunities**. *Oncoimmunology* 2012, **1**(1):48-55.

200. Park EH, Koh SS, Srisuttee R, Cho IR, Min HJ, Jhun BH, Lee YS, Jang KL, Kim CH, Johnston RN *et al*: **Expression of HBX, an oncoprotein of hepatitis B virus, blocks reoviral oncolysis of hepatocellular carcinoma cells**. *Cancer Gene Ther* 2009, **16**(5):453-461.

201. Kelly E, Russell SJ: **History of oncolytic viruses: genesis to genetic engineering**. *Mol Ther* 2007, **15**(4):651-659.

202. Russell L, Peng KW: **The emerging role of oncolytic virus therapy against cancer**. *Chin Clin Oncol* 2018, **7**(2):16.

203. Devaux P, Hodge G, McChesney MB, Cattaneo R: **Attenuation of V- or C-defective measles viruses: infection control by the inflammatory and interferon responses of rhesus monkeys**. *J Virol* 2008, **82**(11):5359-5367.

204. Vongpunsawad S, Oezgun N, Braun W, Cattaneo R: **Selectively receptor-blind measles viruses: Identification of residues necessary for SLAM- or CD46-induced fusion and their localization on a new hemagglutinin structural model**. *Journal of Virology* 2004, **78**(1):302-313.

205. Leonard VH, Hodge G, Reyes-Del Valle J, McChesney MB, Cattaneo R: **Measles virus selectively blind to signaling lymphocytic activation molecule (SLAM; CD150) is attenuated and induces strong adaptive immune responses in rhesus monkeys**. *J Virol* 2010, **84**(7):3413-3420.

206. Sugiyama T, Yoneda M, Kuraishi T, Hattori S, Inoue Y, Sato H, Kai C: **Measles virus selectively blind to signaling lymphocyte activation molecule as a novel oncolytic virus for breast cancer treatment**. *Gene Ther* 2013, **20**(3):338-347.

207. Fujiyuki T, Yoneda M, Amagai Y, Obayashi K, Ikeda F, Shoji K, Murakami Y, Sato H, Kai C: **A measles virus selectively blind to signaling lymphocytic activation molecule shows anti-tumor activity against lung cancer cells**. *Oncotarget* 2015, **6**(28):24895-24903.

208. Amagai Y, Fujiyuki T, Yoneda M, Shoji K, Furukawa Y, Sato H, Kai C: **Oncolytic Activity of a Recombinant Measles Virus, Blind to Signaling Lymphocyte Activation Molecule, Against Colorectal Cancer Cells**. *Scientific reports* 2016, **6**:24572.

209. Fujiyuki T, Amagai Y, Shoji K, Kuraishi T, Sugai A, Awano M, Sato H, Hattori S, Yoneda M, Kai C: **Recombinant SLAMblind Measles Virus Is a Promising Candidate for Nectin-4-Positive Triple Negative Breast Cancer Therapy**. *Mol Ther Oncolytics* 2020, **19**:127-135.

210. Pavlova NN, Pallasch C, Elia AE, Braun CJ, Westbrook TF, Hemann M, Elledge SJ: **A role for PVRL4-driven cell-cell interactions in tumorigenesis**. *eLife* 2013, **2**:e00358.

211. Siddharth S, Goutam K, Das S, Nayak A, Nayak D, Sethy C, Wyatt MD, Kundu CN: **Nectin-4 is a breast cancer stem cell marker that induces WNT/beta-catenin signaling via Pi3k/Akt axis**. *Int J Biochem Cell Biol* 2017, **89**:85-94.

212. Fabre-Lafay S, Garrido-Urbani S, Reymond N, Goncalves A, Dubreuil P, Lopez M: **Nectin-4, a new serological breast cancer marker, is a substrate for tumor necrosis factor-alpha-converting enzyme (TACE)/ADAM-17**. *J Biol Chem* 2005, **280**(20):19543-19550.

213. Buchanan PC, Boylan KLM, Walcheck B, Heinze R, Geller MA, Argenta PA, Skubitz APN: **Ectodomain shedding of the cell adhesion molecule Nectin-4 in ovarian cancer is mediated by ADAM10 and ADAM17**. *J Biol Chem* 2017, **292**(15):6339-6351.

214. Siddharth S, Nayak A, Das S, Nayak D, Panda J, Wyatt MD, Kundu CN: **The soluble nectin-4 ecto-domain promotes breast cancer induced angiogenesis via endothelial Integrin-beta4**. *Int J Biochem Cell Biol* 2018, **102**:151-160.

215. Sethy C, Goutam K, Nayak D, Pradhan R, Molla S, Chatterjee S, Rout N, Wyatt MD, Narayan S, Kundu CN: **Clinical significance of a pvrl 4 encoded gene Nectin-4 in metastasis and angiogenesis for tumor relapse**. *J Cancer Res Clin Oncol* 2020, **146**(1):245-259.

216. Jelani M, Chishti MS, Ahmad W: **Mutation in PVRL4 gene encoding nectin-4 underlies ectodermal-dysplasia-syndactyly syndrome (EDSS1)**. *J Hum Genet* 2011, **56**(5):352-357.

217. **FDA grants accelerated approval to enfortumab vedotin-ejfv for metastatic urothelial cancer** [https://www.fda.gov/drugs/resources-information-approved-drugs/fda-grants-accelerated-approval-enfortumab-vedotin-ejfv-metastatic-urothelial-cancer]

218. Rosenberg J, Sridhar SS, Zhang J, Smith D, Ruether D, Flaig TW, Baranda J, Lang J, Plimack ER, Sangha R *et al*: **EV-101: A Phase I Study of Single-Agent Enfortumab Vedotin in Patients With Nectin-4-Positive Solid Tumors, Including Metastatic Urothelial Carcinoma**. *J Clin Oncol* 2020, **38**(10):1041-1049.

219. Rosenberg JE, O'Donnell PH, Balar AV, McGregor BA, Heath EI, Yu EY, Galsky MD, Hahn NM, Gartner EM, Pinelli JM *et al*: **Pivotal Trial of Enfortumab Vedotin in Urothelial Carcinoma After Platinum and Anti-Programmed Death 1/Programmed Death Ligand 1 Therapy**. *J Clin Oncol* 2019, **37**(29):2592-2600.

220. Powles T, Rosenberg JE, Sonpavde GP, Loriot Y, Duran I, Lee JL, Matsubara N, Vulsteke C, Castellano D, Wu C *et al*: **Enfortumab Vedotin in Previously Treated Advanced Urothelial Carcinoma**. *N Engl J Med* 2021, **384**(12):1125-1135.

221. Mahoney DJ, Stojdl DF: **Potentiating oncolytic viruses by targeted drug intervention**. *Curr Opin Mol Ther* 2010, **12**(4):394-402.

222. Peng KW, Myers R, Greenslade A, Mader E, Greiner S, Federspiel MJ, Dispenzieri A, Russell SJ: **Using clinically approved cyclophosphamide regimens to control the humoral immune response to oncolytic viruses**. *Gene Ther* 2013, **20**(3):255-261.

223. Tai CJ, Liu CH, Pan YC, Wong SH, Tai CJ, Richardson CD, Lin LT: **Chemovirotherapeutic Treatment Using Camptothecin Enhances Oncolytic Measles Virus-Mediated Killing of Breast Cancer Cells**. *Scientific reports* 2019, **9**(1):6767.

224. Weiland T, Lampe J, Essmann F, Venturelli S, Berger A, Bossow S, Berchtold S, Schulze-Osthoff K, Lauer UM, Bitzer M: **Enhanced killing of therapy-induced senescent tumor cells by oncolytic measles vaccine viruses**. *Int J Cancer* 2014, **134**(1):235-243.

225. Myers RM, Greiner SM, Harvey ME, Griesmann G, Kuffel MJ, Buhrow SA, Reid JM, Federspiel M, Ames MM, Dingli D *et al*: **Preclinical pharmacology and toxicology of intravenous MV-NIS, an oncolytic measles virus administered with or without cyclophosphamide**. *Clinical pharmacology and therapeutics* 2007, **82**(6):700-710.

226. Ungerechts G, Springfeld C, Frenzke ME, Lampe J, Johnston PB, Parker WB, Sorscher EJ, Cattaneo R: **Lymphoma chemovirotherapy: CD20-targeted and convertase-armed measles virus can synergize with fludarabine**. *Cancer research* 2007, **67**(22):10939-10947.

227. Ungerechts G, Springfeld C, Frenzke ME, Lampe J, Parker WB, Sorscher EJ, Cattaneo R: **An immunocompetent murine model for oncolysis with an armed and targeted measles virus**. *Mol Ther* 2007, **15**(11):1991-1997.

228. Bossow S, Grossardt C, Temme A, Leber MF, Sawall S, Rieber EP, Cattaneo R, von Kalle C, Ungerechts G: **Armed and targeted measles virus for chemovirotherapy of pancreatic cancer**. *Cancer Gene Ther* 2011, **18**(8):598-608.

229. Ungerechts G, Frenzke ME, Yaiw KC, Miest T, Johnston PB, Cattaneo R: **Mantle cell lymphoma salvage regimen: synergy between a reprogrammed oncolytic virus and two chemotherapeutics**. *Gene Ther* 2010, **17**(12):1506-1516.

230. Hartkopf AD, Bossow S, Lampe J, Zimmermann M, Taran FA, Wallwiener D, Fehm T, Bitzer M, Lauer UM: **Enhanced killing of ovarian carcinoma using oncolytic measles vaccine virus armed with a yeast cytosine deaminase and uracil phosphoribosyltransferase**. *Gynecol Oncol* 2013, **130**(2):362-368.

231. Kaufmann JK, Bossow S, Grossardt C, Sawall S, Kupsch J, Erbs P, Hassel JC, von Kalle C, Enk AH, Nettelbeck DM *et al*: **Chemovirotherapy of malignant melanoma with a targeted and armed oncolytic measles virus**. *J Invest Dermatol* 2013, **133**(4):1034-1042.

232. Lampe J, Bossow S, Weiland T, Smirnow I, Lehmann R, Neubert W, Bitzer M, Lauer UM: **An armed oncolytic measles vaccine virus eliminates human hepatoma cells independently of apoptosis**. *Gene Ther* 2013, **20**(11):1033-1041.

233. Lange S, Lampe J, Bossow S, Zimmermann M, Neubert W, Bitzer M, Lauer UM: **A novel armed oncolytic measles vaccine virus for the treatment of cholangiocarcinoma**. *Hum Gene Ther* 2013, **24**(5):554-564.

234. Yurttas C, Berchtold S, Malek NP, Bitzer M, Lauer UM: **Pulsed versus continuous application of the prodrug 5-fluorocytosine to enhance the oncolytic effectiveness of a measles vaccine virus armed with a suicide gene**. *Hum Gene Ther Clin Dev* 2014, **25**(2):85-96.

235. Mathijssen RH, van Alphen RJ, Verweij J, Loos WJ, Nooter K, Stoter G, Sparreboom A: **Clinical pharmacokinetics and metabolism of irinotecan (CPT-11)**. *Clinical cancer research : an official journal of the American Association for Cancer Research* 2001, **7**(8):2182-2194.

236. Yamamoto M, Kurita A, Asahara T, Takakura A, Katono K, Iwasaki M, Ryuge S, Wada M, Onoda S, Yanaihara T *et al*: **Metabolism of irinotecan and its active metabolite SN-38 by intestinal microflora in rats**. *Oncol Rep* 2008, **20**(4):727-730.

237. Huang PT, Chen KC, Prijovich ZM, Cheng TL, Leu YL, Roffler SR: **Enhancement of CPT-11 antitumor activity by adenovirus-mediated expression of beta-glucuronidase in tumors**. *Cancer Gene Ther* 2011, **18**(6):381-389.

238. Fucikova J, Kepp O, Kasikova L, Petroni G, Yamazaki T, Liu P, Zhao L, Spisek R, Kroemer G, Galluzzi L: **Detection of immunogenic cell death and its relevance for cancer therapy**. *Cell Death Dis* 2020, **11**(11):1013.

239. Krysko DV, Garg AD, Kaczmarek A, Krysko O, Agostinis P, Vandenabeele P: **Immunogenic cell death and DAMPs in cancer therapy**. *Nature reviews Cancer* 2012, **12**(12):860-875.

240. Galluzzi L, Buque A, Kepp O, Zitvogel L, Kroemer G: **Immunogenic cell death in cancer and infectious disease**. *Nat Rev Immunol* 2017, **17**(2):97-111.

241. Donnelly OG, Errington-Mais F, Steele L, Hadac E, Jennings V, Scott K, Peach H, Phillips RM, Bond J, Pandha H *et al*: **Measles virus causes immunogenic cell death in human melanoma**. *Gene Ther* 2013, **20**(1):7-15.

242. Chen A, Zhang Y, Meng G, Jiang D, Zhang H, Zheng M, Xia M, Jiang A, Wu J, Beltinger C *et al*: **Oncolytic measles virus enhances antitumour responses of adoptive CD8(+)NKG2D(+) cells in hepatocellular carcinoma treatment**. *Scientific reports* 2017, **7**(1):5170.

243. Rajaraman S, Canjuga D, Ghosh M, Codrea MC, Sieger R, Wedekink F, Tatagiba M, Koch M, Lauer UM, Nahnsen S *et al*: **Measles Virus-Based Treatments Trigger a Pro-inflammatory Cascade and a Distinctive Immunopeptidome in Glioblastoma**. *Mol Ther Oncolytics* 2019, **12**:147-161.

244. Pidelaserra-Marti G, Engeland CE: **Mechanisms of measles virus oncolytic immunotherapy**. *Cytokine Growth Factor Rev* 2020, **56**:28-38.

245. Van Hoecke L, Van Lint S, Roose K, Van Parys A, Vandenabeele P, Grooten J, Tavernier J, De Koker S, Saelens X: **Treatment with mRNA coding for the necroptosis mediator MLKL induces antitumor immunity directed against neo-epitopes**. *Nat Commun* 2018, **9**(1):3417.

246. Van Hoecke L, Riederer S, Saelens X, Sutter G, Rojas JJ: **Recombinant viruses delivering the necroptosis mediator MLKL induce a potent antitumor immunity in mice**. *Oncoimmunology* 2020, **9**(1):1802968.

247. Diaconu I, Cerullo V, Hirvinen ML, Escutenaire S, Ugolini M, Pesonen SK, Bramante S, Parviainen S, Kanerva A, Loskog AS *et al*: **Immune response is an important aspect of the antitumor effect produced by a CD40L-encoding oncolytic adenovirus**. *Cancer research* 2012, **72**(9):2327-2338.

248. Wei W, Chen X, Ma X, Wang D, Guo Z: **The efficacy and safety of various dose-dense regimens of temozolomide for recurrent high-grade glioma: a systematic review with meta-analysis**. *J Neurooncol* 2015, **125**(2):339-349.

249. Liikanen I, Ahtiainen L, Hirvinen ML, Bramante S, Cerullo V, Nokisalmi P, Hemminki O, Diaconu I, Pesonen S, Koski A *et al*: **Oncolytic adenovirus with temozolomide induces autophagy and antitumor immune responses in cancer patients**. *Mol Ther* 2013, **21**(6):1212-1223.

APPENDIX I

LIST OF SELECTED PUBLICATIONS

Publications

1. **Liu CH**, Wong SH, Tai CJ, Tai CJ, Pan YC, Hsu HY, Richardson CD, and Lin LT. *Ursolic Acid and its Nanoparticles are Potentiators of Oncolytic Measles Virotherapy against Breast Cancer Cells*. **Cancers (Basel). 2021 Jan 4;13(1):136. **[1st Author]**

2. Tai CJ[1], **Liu CH[1]**, Pan YC, Wong SH, Tai CJ, Richardson CD, Lin LT. *Chemovirotherapeutic Treatment Using Camptothecin Enhances Oncolytic Measles Virus-Mediated Killing of Breast Cancer Cells.* **Sci Rep. 2019 May 1;9(1):6767. **[Co-1st Author]**

3. Kuo YT[1], **Liu CH[1]**, Li JW, Lin CJ, Jassey A, Wu HN, Perng GC, Yen MH, Lin LT. *Identification of the phytobioactive Polygonum cuspidatum as an antiviral source for restricting dengue virus entry*. **Sci Rep. 2020 Oct 2;10(1):16378. **[Co-1st Author]**

4. **Liu CH**, Jassey A, Hsu HY, Lin LT. *Antiviral Activities of Silymarin and Derivatives*. **Molecules. 2019 Apr 19;24(8). pii: E1552. **[1st Author]**

5. **Liu CH**, Lin CC, Hsu WC, Chung CY, Lin CC, Jassey A, Chang SP, Tai CJ, Tai CJ, Shields J, Richardson CD, Yen MH, Tyrrell DL, Lin LT. *Highly bioavailable silibinin nanoparticles inhibit HCV infection.* **Gut. 2017 Oct;66(10):1853-1861. **[1st Author]**

Book Chapter

1. Burnouf T, **Liu CH**, Lin LT. *Strategies to Preclude Hepatitis C Virus Entry*, in "Advances in Treatment of Hepatitis C and B". Naglaa Allam (Ed). **InTech. 2017 Mar; DOI: 10.5772/65470; ISBN: 978-953-51-2994-3.**

Conference Abstracts

1. **Liu CH**, Pan YC, Richardson CD, and Lin LT. *The use of oncolytic measles-based vectors for targeted treatment of HCV-induced liver cancer.* **Canadian Liver Journal Winter 2020, Vol. 3, No. 1, pp. 15-157.**

2. **Liu CH**, Pan YC, Richardson CD, and Lin LT. *The use of oncolytic measles-based vectors for targeted treatment of HCV-induced liver cancer.* **Canadian Liver Journal February 2018, Vol. 1, No. 1, pp. 21-118.**

APPENDIX II

COPYRIGHT PERMISSIONS

1. **Liu CH**, Wong SH, Tai CJ, Tai CJ, Pan YC, Hsu HY, Richardson CD, and Lin LT. *Ursolic Acid and its Nanoparticles are Potentiators of Oncolytic Measles Virotherapy against Breast Cancer Cells*. **Cancers (Basel). 2021 Jan 4;13(1):136.**
   [Open Access License]

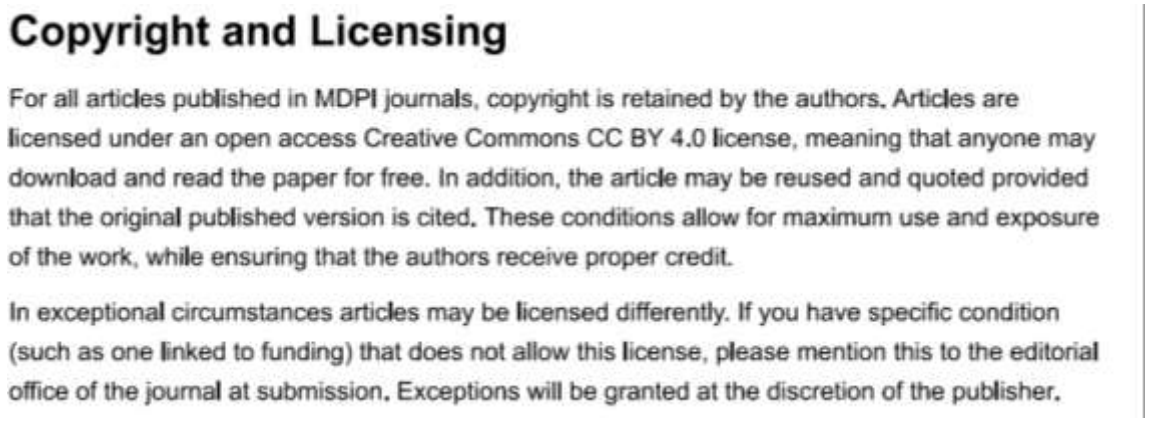

Copyright and Licensing

For all articles published in MDPI journals, copyright is retained by the authors. Articles are licensed under an open access Creative Commons CC BY 4.0 license, meaning that anyone may download and read the paper for free. In addition, the article may be reused and quoted provided that the original published version is cited. These conditions allow for maximum use and exposure of the work, while ensuring that the authors receive proper credit.

In exceptional circumstances articles may be licensed differently. If you have specific condition (such as one linked to funding) that does not allow this license, please mention this to the editorial office of the journal at submission. Exceptions will be granted at the discretion of the publisher.

https://www.mdpi.com/authors/rights

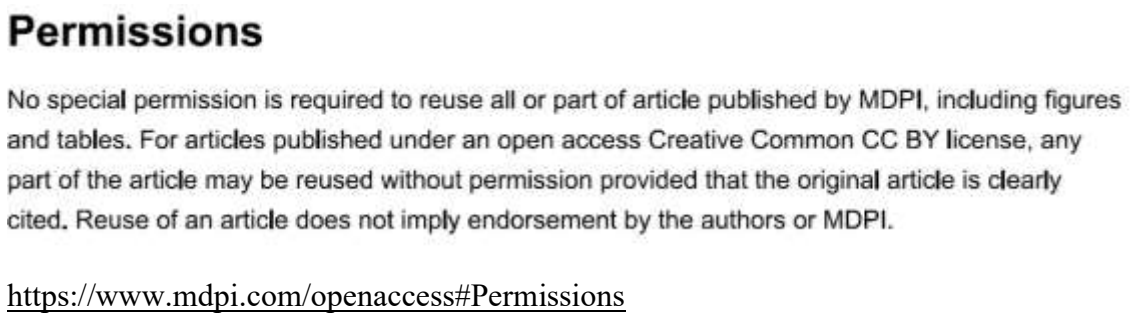

Permissions

No special permission is required to reuse all or part of article published by MDPI, including figures and tables. For articles published under an open access Creative Common CC BY license, any part of the article may be reused without permission provided that the original article is clearly cited. Reuse of an article does not imply endorsement by the authors or MDPI.

https://www.mdpi.com/openaccess#Permissions

2. Tai CJ[1], **Liu CH[1]**, Pan YC, Wong SH, Tai CJ, Richardson CD, Lin LT. *Chemovirotherapeutic Treatment Using Camptothecin Enhances Oncolytic Measles Virus-Mediated Killing of Breast Cancer Cells.* **Sci Rep. 2019 May 1;9(1):6767. [Open Access License]**

Copyright Clearance Center RightsLink®

Help | Email Support

SPRINGER NATURE

Chemovirotherapeutic Treatment Using Camptothecin Enhances Oncolytic Measles Virus-Mediated Killing of Breast Cancer Cells

Author: Chen-Jei Tai et al
Publication: Scientific Reports
Publisher: Springer Nature
Date: May 1, 2019

Copyright © 2019, The Author(s)

Creative Commons

This is an open access article distributed under the terms of the Creative Commons CC BY license, which permits unrestricted use, distribution, and reproduction in any medium, provided the original work is properly cited.

You are not required to obtain permission to reuse this article.
To request permission for a type of use not listed, please contact Springer Nature

© 2021 Copyright - All Rights Reserved | Copyright Clearance Center, Inc. | Privacy statement | Terms and Conditions
Comments? We would like to hear from you. E-mail us at customercare@copyright.com